Energy Metabolism Regulates Retinoic Acid Synthesis and Homeostasis in Physiological Contexts

by

Kristin Marie Obrochta

A dissertation submitted in partial satisfaction of the requirements for the degree of

Doctor of Philosophy

in

Comparative Biochemistry

in the

Graduate Division

of the

University of California, Berkeley

Committee in charge:

Professor Joseph L. Napoli, Chair
Professor Gregory W. Aponte
Associate Professor Jen-Chywan (Wally) Wang

Fall 2014

Abstract

Energy Metabolism Regulates Retinoic Acid Synthesis and Homeostasis in Physiological Contexts

by

Kristin Marie Obrochta

Doctor of Philosophy in Comparative Biochemistry

University of California, Berkeley

Professor Joseph L. Napoli, Chair

Mounting evidence supports a regulated and reciprocal relationship between retinoid homeostasis and energy metabolism, with a physiologically relevant consequence of disrupted energy balance. This research was motivated by an observation that all-*trans*-retinoic acid (atRA), and biosynthetic precursors, were responsive to acute shifts in energy status, in wild type animals with normal body weight and glucose tolerance, i.e. not consequent to metabolic syndrome. My dissertation was designed to characterize associations of retinoid changes under different metabolic conditions by targeting synthesis of retinoic acid, identifying underlying mechanism(s), and describing consequent function(s) in four contexts.

A model that compared fasted versus re-fed ad-libitum animals was used to evaluate the impact of an acute shift in whole body metabolism on retinoid status. In liver, atRA was elevated in fasted mice, and reduced by 50% in re-fed counterparts. Consistent with synthesis driving the atRA concentration in liver, expression of retinol dehydrogenase (Rdh) genes, *Rdh10* and *Rdh1*, were elevated by fasting, and reduced 50% in re-fed as well as glucose and insulin treated mice, which preceded the reduction in atRA. Subsequent characterization of *Rdh10* and *Rdh16* (human orthologue of mouse *Rdh1*) regulation in a human hepatoma (HepG2) cell line identified transcriptional repression by insulin that required PI3K, Akt (PKB) and suppression of the transcription factor FoxO1, which was required for optimal expression of *Rdh*s. Conversely, expressions of *Rdh*s were elevated and stabilized in serum free medium conditions. This study illustrated that liver atRA, and specifically its synthesis, is regulated by acute changes in feeding status. This controlled fluctuation in atRA concentration enables transcriptional regulation by atRA in a physiological context, and reinforces an established link between atRA and liver glucose metabolism via phospho*enol*pyruvate carboxy kinase.

In pancreas tissue, the 9-*cis*-retinoic acid (9cRA) concentration was reduced in animals that were fed ad-libitum, versus a fasted state, and also decreased rapidly and transiently in response to a glucose bolus versus a fasted state. 9cRA functions in pancreas to attenuate insulin secretion and synthesis, with the physiological impact of preventing hypoglycemia. In a fed, or glucose treated state, reduced 9cRA sensitizes

pancreas for optimum insulin secretion. To understand metabolic regulation of 9cRA, synthesis was characterized with focus on *Rdh5* expression in a beta cell model (832/13 rat insulinoma cells). *Rdh5* expression and activity were reduced by glucose and cAMP, and overexpression of *Rdh5* was sufficient to increase 9c-retinal and 9cRA synthesis. This work identified *Rdh5* as a physiologically relevant regulator of 9cRA synthesis in beta cells.

A third project aimed to characterize a regulatory function of atRA in central nervous system (CNS) mediated energy balance. The hypothalamus brain region is an integrative center for peripheral signals, and regulates a range of functions including reproduction, autonomic nervous system, immune response, sleep, thermoregulation, fluid homeostasis, food intake and energy expenditure. Research established active atRA metabolism by regionally distinct concentrations of atRA, expression of genes for synthesis and response to atRA, and *in situ* synthesis of atRA in hypothalamus tissue explants. However, the atRA concentration did not change during dietary interventions of acute fasting and feeding, high fat diet feeding, or to cold exposure. Nuclear receptor PPARδ localized to nuclei and axon structures of neurons in hypothalamus and other brain regions, as demonstrated by immuno-histochemistry and confocal microscopy. This work set a foundation for study of atRA activity, and non-genomic function of PPARδ in hypothalamus, but was unsuccessful in establishing a regulatory function of atRA on CNS mediated energy balance.

The impact of dietary vitamin A on retinoid levels was evaluated in multiple tissues of five mouse strains, over three generations. The model transitioned mice from chow diet, containing copious vitamin A, to a semi-purified, vitamin A sufficient (VAS) diet. Three generations of VAS feeding decreased atRA in most tissues of most strains, in some cases more than 50%, and maintained an order of liver ≈ testis > kidney > white adipose tissue ≈ serum. Neither serum retinol nor atRA reflected tissue atRA concentrations. Strain and tissue-specific differences in retinol and atRA that reflect different amounts of dietary vitamin A could have profound effects on retinoid action, and are predictive of strain dependent differences in enzymes regulating atRA synthesis and catabolism. Consequently, the lab has continued to provide semi-purified VAS diet in mouse studies that evaluate retinoid homeostasis.

In total, this collection of work provides original and novel insights into metabolic regulation of atRA biosynthesis. The controlled fluctuation in atRA concentrations, as demonstrated in multiple contexts of physiologically relevant shifts in energy status, enables dynamic regulation of downstream transcriptional targets of atRA.

To Luke Gaetano

Table of Contents

List of Figures

Chapter 1: Insulin Regulates Retinol Dehydrogenase Expression and all-*trans*-Retinoic Acid Biosynthesis through FoxO1

Chapter 2: Glucose and cAMP Regulate Retinol Dehydrogenase 5 Expression and 9-*cis*-Retinoic Acid Biosynthesis in Pancreas Beta Cells

Chapter 3: Retinoid Metabolism and PPARδ Expression in Hypothalamus

Chapter 4: Effects of diet and strain on mouse serum and tissue retinoid concentrations

Acknowledgements

First and foremost I thank Professor Joseph Napoli for providing the opportunity to earn my PhD in his laboratory. I believe that Dr. Napoli saw my potential at times when I could not. His steadfast optimism motivated me to persevere through experimental set-backs and project changes. His mentorship allowed me to develop independently, with confidence to work through challenges and own my achievements.

My dissertation committee members, Jen-Chywan (Wally) Wang and Greg Aponte, as well as the Head Graduate Advisor of the Comparative Biochemistry Graduate Group, Andreas Stahl, were essential to my completion of the degree. Wally's expert advice, and provision of critical reagents, moved my research project forward in time and depth mechanistically. His career oriented mentorship was welcomed and appreciated. Greg's thoughtful discussions encouraged me to think outside-the-box. His holistic support was exemplified by calling me Super Woman, which was a confidence boost. Andreas's stern delivery and enforcement of guidelines created order.

I am fortunate to have shared my graduate school experience with many accomplished and inspiring colleagues. Chuck Krois is one of the most intelligent and considerate scientists I know. I have been fortunate to work with him for longer than either of us care to admit. He has generously shared countless discussions, offering thoughtful opinions on data, experiment design, presentations, posters, and some non-science topics as well. Marta Vuckovic is a motivated and conscientious researcher with excellent mentorship skills. She has taught me, directly and by example, valuable lessons about navigating a research career. I thank Maureen Kane and Sunny Wang for their analytical expertise as they enabled were integral to my projects.

I acknowledge the Nutritional Sciences and Toxicology Department for adopting me as a graduate student, despite belonging to the Comp Bio graduate group. I appreciate the collegial support and sense of community in NST. I am specifically grateful for tangible assistance over the years from Graduate Student Affairs Officers Olga and Nikki, and from Department Managers Janna and Holli.

Elements of my research were made possible with assistance from related services. I would like to thank Animal Technician Jay Seville, for his attentive care of my mice, and maintaining open communication when issues arose. Veterinarian Lindsey Jennings enthusiastically approached learning new surgical procedures, and facilitated animal transfers. At the Biological Imaging Facility (College of Natural Resources), Denise Schichnes and Steve Ruzin provided training and troubleshooting for sectioning and imaging experiments. At the UCSF Islet Production Core, Greg Szot provided islets,

and Vinh Nguyen trained me to isolate islets. I am generally grateful for the available resources and the relationships I developed along the way.

I am blessed with an amazing husband, Jesse Obrochta, who is loving, respectful, and makes me laugh. He is my rock. His support, in so many ways, has made this achievement possible. Our son, Luke, has brought indescribable joy and purpose to my life, and also forced me to maintain a healthy balance. My mom, Lisa, and grandmother, Louana, are my cheerleaders, and among other ways, have demonstrated their support by embracing weekly care for Luke.

I will forever be indebted to my Nana and Papa, Joyce and Joe Bruno, for their vision and priority to provide me with an education. I appreciate my Aunt Gina's influence and success in carrying forward the mission to create options in my life through education. I credit my Dad, Mark, with instilling my self-respect and building courage. Most of my family and friends, despite their best of intentions, cannot relate to my experience of earning a PhD, or understand the language in this dissertation. It's okay. Thank you all for the love and support along the way.

Introduction

Vitamin A

Vitamin A is a lipid soluble micronutrient, essential for vertebrate life. It was identified in 1913 as lipid soluble A, but its therapeutic value was appreciated as far back as 1500 BC, when ancient Egyptians used liver extract to treat night blindness (1–3). Vitamin A and its derivatives support a wide range of biological functions essential for development, cell differentiation and proliferation, reproduction, immune response, nervous system function, and energy metabolism. Both extreme excess and deficiency of all-*trans*-retinoic acid (atRA) can be deadly, while moderate fluctuations in atRA have toxicological effects, such as abnormal fetal development, disrupted energy balance regulation and cancer (4–6). Vitamin A deficiency is a public health concern in developing countries, and is responsible for over 1 million deaths and cases of blindness per year, affecting primarily young children and pregnant women (7). A weakened immune system precedes clinical manifestations of xerophthalmia, night blindness, and further morbidity (8). In contrast, excessive vitamin A intake causes abnormal morphological development, or teratogenicity (9). Consequently, the United States Department of Agriculture sets both dietary reference intakes (DRI), formerly recommended dietary allowances (RDA), and upper limit (UL) for human consumption of vitamin A.

Forms of dietary vitamin A include preformed retinyl esters (RE) from animal sources, and pro-vitamin A carotenoids from plant sources. Carotenoids are cleaved by carotenoid monooxygenase enzymes in intestinal enterocytes. β-carotene yields two molecules of all-*trans*-retinal. The bioavailability of carotenoids is low due to physical matrix entrapment and aggregation in crystalline structures, and is why vitamin A deficiency remains a problem in populations with primarily plant based dietary vitamin A intake (10). Retinal is reduced to retinol by retinal reductase, and then esterified by acyl-transferase enzymes. REs are packaged into chylomicrons for transport into the lyphatic sytem, and delivery to target tissues (11). The largest depot of RE storage is in hepatic stellate cells, accounting for 80% of total body vitamin A stores, with second highest in adipose tissues (12). Transport of vitamin A, such as in mobilization of liver storage, is primarily in the form of retinol. Retinol in blood is chaperoned by retinol binding protein 4 (RBP4) and transthyretin (TTR), to prevent renal clearance (13, 14). The stimulated by retinoic acid 6 (STRA6) receptor recognizes retinol-RBP, and transports retinol into extra hepatic tissues (15), and RBP4 receptor-2 (RBPR2) similarly mediates uptake of retinol in liver (16). Internalized retinol is bound by cellular retinol binding protein (CRBP), to regulate substrate delivery and flux through specific retinoid biosynthetic pathway (17).

Retinoid Homeostasis

Retinoids support biological functions differently in the eye and in the remainder of the body. In the vision cycle, 11-*cis*-retinal serves as the photo-active detector molecule. 11-*cis*-retinal is isomerized to all-*trans*-retinal upon light sensing. All-*trans*-

retinal is reduced to all-*trans*-retinol, esterified to retinyl ester, mobilized to 11-*cis*-retinol by a combination hydrolase-isomerase, retinal pigment epithelium 65 (RPE65), and finally is oxidized to regenerate 11-*cis*-retinal, by retinol dehydrogenase 5 (RDH5) (18). Outside of the eye, atRA synthesis is the only established function of retinol, and atRA is widely accepted as the active metabolite mediating biological functions. atRA is synthesized from retinol in tissues, *in situ*, to meet specific needs. Hence, quantification of atRA, retinol, and RE, as well as stabilized retinal, can be performed from animal tissues, by assays with sufficiently low detection limits. Biosynthesis of atRA is a highly regulated process that involves interaction of specific enzymes with chaperone binding proteins, to maintain retinoid homeostasis (17). atRA is synthesized from retinol by sequential dehydrogenation reactions. The first, reversible and rate limiting reaction, is catalyzed by retinol dehydrogenase (RDH) enzymes. RDHs are members of the short chain dehydrogenase/reductase (SDR) enzyme class, are membrane anchored in endoplasmic reticulum, and require pyridine nucleotide (NAD^+ or $NADP^+$) cofactor. The second reaction is catalyzed by cytosolic retinal dehydrogenase (RALDH) enzymes, to generate atRA. Expression of multiple isozymes of RDH and RALDH differ by temporal and spatial distribution, and specific activity with different isoform substrates limits functional overlap. Notably, cytoplasmic alcohol dehydrogenase (ADH) enzymes are capable of converting retinol to retinal *in vitro*, but do not recognize physiologically relevant form of intracellular retinol bound to CRBP (17). Excess retinol is esterified by lecithin retinol acyl-transferase (LRAT) for storage, and hydrolyzed by retinyl ester hydrolase (REH) enzymes. atRA is inactivated by cytochrome p450 (CYP) enzymes, which generate 4-hydroxy-RA, 4-oxo-RA and 18-hydroxy-RA as initial steps in the secretory path. Specifically, CYP26A1, 26B1, 26C1 and 2C39 (only in mice) are preferentially active toward atRA (19). Retinoids self-regulate their biosynthesis and catabolism to maintain appropriate levels. Retinol bound with CRBP1 (holo-CRBP) chaperones retinol toward esterification by LRAT, while unbound CRBP1 (apo-RBP1) stimulates hydrolysis of RE. Thus, the ratio of apo-CRBP to holo-CRBP influences flux of retinol into and out of storage, and modulates availability of substrate for atRA biosynthesis (5). atRA also drives storage of retinol as RE by increasing STRA6, CRBP1 and LRAT expression (20), and inhibiting ALDH1 expression (21). Conversely, atRA stimulates its catabolism through activation of CYP enzymes (22). Thus, atRA regulates its concentration by reducing synthetic substrate and enhancing its catabolism.

Retinoic acid Function(s)

Pleiotropic effects of atRA are achieved through modulation of gene expression (23). atRA functions as a ligand to regulate transcription via hormone nuclear receptors (NR). Retinoic acid receptors (RARs) are members of the type II class of endocrine nuclear receptors, which includes NRs for fat-soluble hormones and vitamins, such as thyroid receptor (TR) and vitamin D receptor (VDR) (24). This class of NRs heterodimerize with retinoid X receptors (RXRs) and bind a response element sequence in the promoter of target genes, to regulate ligand mediated transcriptional activity. Three isoforms of RAR (α, β, and γ) are encoded by different genes, and bind atRA with Kd in sub-nanomolar (nM) range (25–27). Heterodimerization with three isoforms of

RXR (α, β, and γ), enables multiple pairings that provide specificity of gene targets and variable biological consequence (28). RAR binds retinoic acid response element (RARE) sequence, defined by two direct repeats of a hexameric motif (A/G) G (G/T) TCA, separated by 1, 2, or 5 nucleotides (29). In the absence of ligand, RARs generally complex with co-repressor proteins to silence expression of target genes. Binding of atRA ligand causes dissociation of co-repressors and recruitment of co-activators, to initiate transcription of target genes (30). Ligand mediated activation of RXR is not sufficient to induce conformational changes leading to co-activator recruitment, but is synergistic with RAR activation, a phenomena named subordination (31). The isoform 9-*cis*-retinoic acid (9cRA) is described as the ligand for RXRs *in vitro*, however lack of its widespread detection *in vivo* reduces its physiological relevance in regulation of RXR activity (32). Similar to chaperone of retinol and retinal precursors by CRBP, binding of RA by cellular retinoic acid binding proteins (CRABP) guides the metabolite to appropriate intracellular fate. CRABPI leads atRA to CYPs for catabolism, while CRABPII delivers RA to nuclear RAR for transcriptional regulation (33). By an analogous mechanism, fatty acid binding protein 5 (FABP5) escorts RA into nucleus to bind peroxisome proliferator activated receptor delta (PPARδ). The relative expression of binding proteins CRABPII to FABP5 in a biological context determine atRA delivery to the cognate nuclear receptors, and account for contrasting transcriptional programing (34, 35). Outside of the nucleus and canonical transcriptional regulation, atRA has non-genomic effects, to activate two mitogen activated protein kinase (MAPK) signaling pathways. Activation of the p42/p44 extracellular signal-regulated kinases (ERK) MAPK pathway has been demonstrated in neurons, Sertoli, and embryonic stem cells, and activation of p38MAPK in fibroblasts, and various cancer cell models (29). It appears common that plasma membrane bound RARα facilitates non-genomic atRA activity, with location specificity according to cell type. Consequences of non-genomic atRA activity include translational regulation (36) and downstream phosphorylation of transcription factors, including NRs (37). This emerging area warrants additional investigation before broad generalizations may be drawn.

Retinoic Acid and Energy Metabolism

Energy metabolism and atRA are integrated through regulation of genes involved in cellular fuel utilization as well as formation and maintenance of metabolic tissues. The increased prevalence of metabolic syndrome and accompanying obese and diabetic phenotypes, demands improved understanding of mechanistic relationships between retinoids and energy balance. Multiple lines of evidence support that atRA protects against obesity and insulin resistance. In a dietary intervention study, diet induced obese (DIO) mice treated with atRA by slow release of implanted pellet (15 mg over 90 days) display reduced body weight and adiposity (38). One mechanism of atRA, identified in white adipose, is prevention of pre-adipocyte differentiation to moderate formation of new fat cells, through activation of *Pref-1* and other transcriptional targets (39). In another *in vivo* study, pharmacological doses of atRA (100 mg/kg) to mice fed standard diet or vitamin A deficient diet (VAD), reduced adiposity and body weight, possibly through increased thermogenic potential of brown adipose tissue (40). Follow up studies of atRA treated *in vivo* (10-100 mg/kg) measured reduced expression of

adipose-secreted hormones, leptin and resistin, both in adipose tissue (mRNA) and in circulation (protein) (41, 42). Conversely, mice fed VAD displayed increased adiposity and small increase in body weight (43). Identification of atRA as a PPARδ ligand further expands possible mechanisms for atRA regulation of energy metabolism, because of the central role of PPARδ in determining fuel utilization according to energy status (34, 44). In the reciprocal relationship, retinoid metabolism is disrupted in response to energy status, as evident by RBP4 alteration. Circulating RBP4, synthesized and secreted from adipose, is elevated in insulin-resistant and obese mice and humans, is sufficient to cause insulin resistance in normal mice, and ablation of RBP4 genetically or pharmacologically improves insulin sensitivity (45). Association of RBP4 expression with insulin sensitivity, including shifts in liver and muscle metabolism, indicate that retinoid mobilization is affected by energy status, and involved in progression of energy imbalance.

Identification of specific transcriptional target genes provides a mechanistic link between atRA and glucose and lipid metabolism. Gluconeogenesis was identified as responsive to atRA from the observation that whole-animals fed a VAD diet were glycogen deficient (46). Phospho*enol*pyruvate carboxykinase 1 (PCK1), the rate-limiting enzyme and committed step in gluconeogenesis (47), is a direct transcriptional target of atRA (48). Subsequent characterization of PCK1 has detected reduced expression in liver of VAD fed mice, and identified three RAREs in the promoter with corresponding RAR isoforms mediating transcriptional response to atRA (49). Thus, atRA regulation of PCK1 has become a prototype of transcriptional response to atRA, and a solid foundation integrating atRA and glucose metabolism. atRA influence on lipid metabolism is evidenced by transcriptional regulation of uncoupling proteins 1-3 (UCP 1-3). UCP1 is expressed in brown adipose and functions to uncouple oxidative phosphorylation from ATP synthesis, which defines the unique ability of brown adipose tissue to generate heat by thermogenesis. UCP2 and UCP3 are expressed in brown adipose and other tissues. Expression of UCP genes are elevated with atRA treatment and reduced by VAD (40, 50). atRA activates UCP1 expression by a non-canonical RARE and PPARE, UCP3 by a canonical RARE, and UCP2 by an undefined mechanism (38, 51, 52). Together, regulation of UCPs link atRA to lipid metabolism, and specifically energy expenditure via thermogenesis.

Ablation of genes involved in atRA homeostasis display phenotypes with disrupted energy balance. The retinol dehydrogenase 1 (RDH1) null mouse has increased adiposity due to impaired brown adipose tissue function (53). The cellular retinol binding protein I (RBP1) null mouse has dis-regulated glucose metabolism, with increased gluconeogenesis and fatty acid oxidation (54). Raldh1 (*Aldh1a1*) null mouse shows no apparent phenotype in the absence of metabolic stress (55). When challenged with a high fat diet (HFD), this mouse resists diet induced obesity, insulin resistance, and displays increased energy dissipation (56). Together, these examples illustrate that energy imbalance results from disruption of retinoid homeostasis. Specifically, reduced retinoic acid signal is associated with impaired energy expenditure and increased energy storage.

Rationale for Dissertation

This dissertation addresses the relationship between retinoid homeostasis and energy metabolism. It is motivated by an observation that atRA, and synthetic precursors, are responsive to acute shifts in energy status, in wild type and metabolically normal mice. The approach focuses on atRA synthesis by metabolic regulation of the rate limiting step of RDH enzymes. Chapters are divided by metabolic tissues of interest, including liver, pancreas, hypothalamus, and systemic endogenous retinoids in response to dietary vitamin A.

Chapter 1

Insulin Regulates Retinol Dehydrogenase Expression and all-*trans*-Retinoic Acid Biosynthesis through FoxO1

INTRODUCTION

A wide scope of biological processes, including embryonic development, cell differentiation/proliferation, immune function, neurogenesis and energy metabolism, depend on the vitamin A (retinol) metabolite all-*trans*-retinoic acid (atRA) (57–61). atRA controls energy balance by inhibiting differentiation of pre-adipocytes into mature white adipose, regulating function of white adipose cells, and by regulating whole body lipid and carbohydrate metabolism (49, 62–64). Dosing atRA to mice fed a chow diet, which contains ample vitamin A, produces resistance to diet-induced obesity (38, 65). Impairing atRA homeostasis causes abnormalities in intermediary metabolism. Mice with ablated cellular retinol binding-protein 1 (encoded by *Rbp1*), which regulates retinol homeostasis, experience glucose intolerance from enhanced gluconeogenesis, resulting from hyperglucagonemia, and also undergo increased adipocyte differentiation (54, 66). atRA functions through the nuclear hormone receptors RARα, β and γ and PPARδ, which affect transcription and translation (31, 34). Genes regulated by atRA through nuclear receptors include: *Pck1,* which expresses phospho*enol*pyruvate carboxykinase, the enzyme that catalyzes the committed step in gluconeogenesis (67); *Ucp1*, which expresses uncoupling protein 1, a mediator of adaptive thermogenesis (68); and inhibitors of adipogenesis, including *Pref1*, *Klf2* and *Sox9* (69). Despite the impact of atRA on energy balance, little is known about whether energy balance might regulate atRA homeostasis.

Two successive dehydrogenations produce atRA from retinol (5). During limited or normal vitamin A nutriture, retinol dehydrogenases (RDH) of the short-chain dehydrogenase/reductase gene family catalyze the first and rate-limiting reaction to produce all-*trans*-retinal. Retinal dehydrogenases, of the aldehyde dehydrogenase gene family, catalyze the second reaction to produce atRA. Multiple isoforms of retinoid-metabolizing enzymes occur in both families, often in the same cell types, but these enzymes differ in subcellular expression loci, and can show differential cell expression patterns. RDH1 and RDH10 are the most thoroughly characterized RDH in the path of atRA biosynthesis: both are expressed early in embryogenesis and throughout multiple tissues, and both contribute to atRA biosynthesis from retinol in intact cells in the presence of retinal dehydrogenases (70–72). Dehydrogenase reductase 3 (DHRS3) functions as a retinal reductase, which interacts with RDH10 to control retinoid homeostasis (73). *Rdh1*-null mice are born in Mendelian frequency, but experience increased weight and adiposity, which is prevented by feeding copious vitamin A (53). In contrast, most *Rdh10*-null mice die by embryonic day 12.5, but can be rescued by maternal administration of retinoids (74). Notably, like *Rdh1*-null mice, *Rdh10*-null mice

do not exhibit total atRA deficiency, suggesting complementary actions of the two and/or occurrence of additional RDH.

Liver has a central function in maintaining whole body metabolic homeostasis (75). During feeding, liver catalyzes increased energy storage by generating glycogen and triacylglycerol. During fasting, liver generates glucose and ketone bodies, from gluconeogenesis, glycogenolysis and fatty acid oxidation. Glucose, insulin, and glucagon control the balance between energy storage during feeding and production of fuels during fasting. The combination of portal vein glucose, insulin, and neuronal signals cause the liver to transition from catabolic to anabolic metabolism (76). Insulin binding to its cell surface receptors activates two canonical pathways in hepatocytes: the mitogen-activated protein kinase (MAPK) and phosphoinositide-3-kinase (PI3K). The MAPK pathway includes extracellular-signal regulated kinase (ERK) signaling and regulates transcription involved in differentiation, growth and survival (77). The PI3K pathway activates Akt (PKB) to mediate metabolic transitions, including promotion of glycogen and lipid synthesis, and suppression of gluconeogenesis. Effectors downstream of PI3K/Akt include: glycogen synthase kinase-3 (GSK-3), which regulates glycogen synthesis; mammalian target of rapamycin complex 1 (mTORC1), which regulates protein synthesis; BCL2-associated agonist of cell death (BAD), which regulates cell survival; and forkhead box Other (FoxO), which regulates transcription of genes required for gluconeogenesis (78).

This report compares *Rdh1* and *Rdh10* expression in tissues of fasted vs re-fed mice, and focuses on atRA in liver. Liver served as the focus of this study because of its central contributions to both energy and retinoid homeostasis. We found that insulin, via inactivating FoxO1, represses *Rdh1* and *Rdh10* expression, with an associated decrease in atRA biosynthesis. These observations are consistent with the recent conclusion that FoxO1 may link gluconeogenesis to retinoid homeostasis (79). These results provide direct evidence showing that energy status regulates atRA biosynthesis, and provides new insight into the relationship between atRA biosynthesis and its regulation of energy balance.

MATERIALS AND METHODS

Animals

C57Bl/6J male mice, age 2-3 months, bred in-house were housed up to 5 per cage with litter mates, and fed AIN93G semi-purified diet with 4 IU vitamin A/g (Dyets, catalog# 110700), unless noted otherwise. The exceptions were: mice in the 12 hr re-fed experiment were both male and female (no significant difference in atRA values was detected by sex); mice used for fasting and insulin or exendin-4 treatments were purchased from Jackson laboratories (Cat# 000664) and were fed laboratory chow. Experimental groups were normalized to controls consisting of fasted mice of the same age, diet, and sex. Tissues were harvested immediately after euthanasia, frozen in liquid nitrogen, and stored at -80 until atRA quantification. Fasted groups were deprived of food for 16 hr, beginning ~2 hr prior to initiation of the dark cycle. Re-fed groups were provided diet ad-libitum. An oral gavage glucose dose of 2 g/kg body weight was delivered as 10 µl/g body weight of a 20% glucose solution in PBS. Intraperitoneal (i.p.) glucose was delivered in two injections of 2 g/kg body weight each at 0 and 45 min following a 16 hr fast. Insulin (0.375 and 0.5 IU/kg, Humulin, Eli Lily #8715) and exendin-4 (10 µg/kg, Sigma E7144) were delivered in two i.p. injections of 1.8 µl/g and 2 µl/g body weight, respectively. Animal experiments were approved by Office of Laboratory and Animal Care at University of California Berkeley.

Cell culture

HepG2 cells (ATCC, HB-8065) were maintained in EMEM medium (ATCC 30-2003) supplemented with 10% fetal bovine serum (Life Technologies 10082), and incubated at 37°C with 5% CO_2. Medium containing serum is referred to as growth, and without serum as serum-free. Cells were treated with the following, delivered in medium or DMSO: 25 µg/mL (20 µM) actinomycin D (Life Technologies A7592), 10 µg/mL cycloheximide (Sigma C4859), 10 nM human insulin (Sigma I9278), 100 nM glucagon (CalBiochem 05-23-2700), 50 µM LY294002 (Cell Signaling Technologies #9901), 1 µM Triciribine (a.k.a. API-2, Cayman #10010237), 200 nM Rapamycin (Cayman #13346), 20 µM PD98059 (CalBiochem #513000). Adenovirus constructs dnFoxO1 (FoxO1Δ256) or lacZ were infected into 70% confluent Hep2 cells and collected for analysis after 48 hr.

Retinoid quantification

Liver atRA was quantified in 6 to 9 mice per group. Tissues were collected under yellow light and frozen immediately in liquid nitrogen. On the day of analysis, tissues were weighed, thawed on ice, and hand homogenized in 0.9% saline. HepG2 cells were collected under yellow light in 1x reporter lysis buffer (Promega E3971), and stored at -80°C. Cell protein was quantified with the Pierce BCA Protein Assay Kit (Thermo Scientific #23227). For atRA biosynthesis in HepG2 cells, 50 nM (100 pmol) all-*trans*-retinol (Sigma R7632) was delivered in DMSO 4 hr before cell harvest. Cells were homogenized by pipetting and vortexing. Retinoids were recovered by a two-step acid and base extraction (80). All materials in contact with samples were glass or stainless

steel. Internal standards were used to calculate extraction efficiency of retinoids. atRA was extracted and quantified by LC/MS/MS, with 4,4-dimethyl retinoic acid as internal standard (81). Retinol was extracted and quantified by HPLC/UV, with 3,4-didehydro retinol as internal standard (82).

RNA isolation and qPCR

Isolation of RNA from liver and cells was by the Trizol reagent (Invitrogen) method. Liver was homogenized using a Qiagen Tissue Lyser II set at 30 Hz for 1 min. cDNA was prepared using iScript reagent kit (BioRad 170-8891). Real-time qPCR was prepared with 2x TaqMan master mix (Life Technologies 4369016), and Taqman Gene Expression Assays: mouse ACTB Mm00607939_s1, Rdh10 Mm00467150_m1, Rdh1 Mm00650636_m1, Dhrs3 Mm00488080_m1; human ACTB Hs01060665_g1, RDH10 Hs00416907_m1, G6PC Hs00609179_m1, Rdh16 Hs00559712_m1, Dhrs3 Hs00191073_m1 (Life Technologies), and run on an ABI 7900 thermocycler. Gene expression was analyzed by the ΔΔ-Ct method, normalized to β-actin, and expressed as fold change relative to expression in fasted liver or the reference condition described in cells.

Protein expression

Western blots were done with the Mini PROTEAN system (Biorad), 10% TGX gels (Biorad #456-1033), and semi-dry transfer (Biorad Trans-blot SD) to nitrocellulose membranes (Whatman). Western blots were visualized with the Licor Odyssey system, and quantified by densitometry in reference to actin expression. Primary antibodies: actin (ProSci #3779), HA (12CA5) (Roche #11583816001). Secondary antibodies: LI-COR IR Dye (680LT #926-68020, 800CW #926-32211).

Immunofluorescence

HepG2 cells were fixed in ice-cold acetone for 10 min, then stained with FoxO1 primary antibody (Santa Cruz #11350) for 2 hr at 37°C, and incubated with Alexa Fluor 488 secondary antibody (Life Technologies #A11034) 1 hr at 37°C. Cover slips were mounted onto glass slides with Vectashield mounting medium containing DAPI (Vector Labs #H-1200) and imaged by fluorescence microscopy (Zeiss AxioImager).

Statistics

Data are presented as mean ± standard errors (SE) and were analyzed using two-tailed, unpaired Student's *t* tests or linear regression analysis.

RESULTS

Re-feeding decreased *Rdh* mRNA in multiple mouse tissues and atRA in liver

To address regulation of atRA biosynthesis by energy status, we measured expression of *Rdh1* and *Rdh10* in tissues of mice that had been fasted 16 hr or re-fed ad libitum 6 hr after a 16 hr fast. In liver, *Rdh1* and *Rdh10* mRNA decreased in re-fed animals 86 and 57%, respectfully, relative to expression in fasted animals (Figure 1A, B). In brown adipose tissue (BAT) of re-fed mice, *Rdh1* decreased 77%, whereas *Rdh10* expression was unchanged. In pancreata of re-fed mice, *Rdh10* mRNA decreased 43%, and *Rdh1* expression was below the limit of detection. In epididymal white adipose tissue (eWAT) of re-fed mice, *Rdh10* expression was unchanged and *Rdh1* expression was below the limit of detection. In kidney of re-fed mice, *Rdh10* expression decreased 62%. Focusing on liver, the atRA concentration was reduced 9 and 12 hr after re-feeding, but not after 6 hr (Figure 1C). Thus, reduced *Rdh* mRNA preceded reduced atRA concentrations in re-fed animals.

Insulin and oral glucose decrease liver *Rdh10* mRNA

We next measured *Rdh10* and *Rdh1* expression in liver of fasted mice vs. mice fasted and dosed with glucose by oral gavage (Fig. 2A). Oral glucose repressed *Rdh10* and *Rdh1* expression similar to re-feeding. We elected to focus on *Rdh10* because its expression levels exceed those of *Rdh1* by ~100-fold (Fig. 2B). An independent experiment verified that re-feeding reduced *Rdh10* expression at 6 hr, with partial recovery at 12 hr (Fig. 2C). We tested expression of *Dhrs3,* because during these studies a report concluded that RDH10 and DHRS3 form a heterodimer, which modulates the activities of both enzymes (73). *Dhrs3* mRNA decreased 50% in liver of mice re-fed 12 hr, relative to expression in fasted mice. To determine whether the route of glucose dosing affected *Rdh10* expression, we compared the impact of oral gavage and i.p. injection. Glucose injected i.p. had no effect on *Rdh10* expression (Fig. 2D). Insulin, however, caused a dose-dependent decrease in liver *Rdh10* expression that reached statistical significance at 0.5 IU/kg (Fig. 2E), a dose recommended for the insulin tolerance test (83). Because nutrients trigger incretin secretion, we tested the impact of glucagon-like-peptide 1 (GLP-1). GLP-1 is short lived in circulation from inactivation by dipeptidyl peptidase-4 (84). Therefore, we used the stable GLP-1 receptor agonist, exendin-4 (85). Treatment with exendin-4 had no impact on *Rdh10* expression. These data demonstrate that re-feeding, oral gavage with glucose and i.p. insulin each are sufficient to reduce liver *Rdh10* expression from relatively high fasted levels.

In HepG2 cells, *RDH10* mRNA transcription increases with serum removal, and is attenuated by insulin

We used the human hepatoma cell line, HepG2, to study mechanisms of *RDH10* regulation. The presence or absence of serum in the medium can model the impact of growth factors, including insulin (86, 87). Therefore, serum was removed from the medium, which prompted a 2-3 fold increase in *RDH10* mRNA 4 hr after the change of

medium (Fig. 3A). *RDH10* mRNA remained elevated at least 16 hr. The increase in *RDH10* mRNA correlated with that of glucose-6-phosphatase (*G6PC*), which is induced transcriptionally in liver during fasting (88). Expression of *DHRS3* increased 1.5 fold in 4 hr of serum-free medium, and insulin prevented the increase (Fig. 3B). Although insulin prevented the increase in *RDH10* mRNA prompted by serum-free medium, neither high nor low glucose affected *RDH10* expression (Fig. 3C). Glucagon had no effect on *RDH10* expression in either growth (10% serum) or serum-free medium. These data validate HepG2 cells as a model for insulin regulation of *RDH10* expression in liver.

The transcription inhibitor actinomycin D (ActD) inhibited the increase in *RDH10* mRNA prompted by removing serum (Fig. 3D). ActD effects were neither additive nor synergistic with those of insulin, indicating that both serum and insulin repress *RDH10* transcription. Cycloheximide (CHX) prevented the increase in *RDH10* expression upon serum exclusion, consistent with a requirement for protein synthesis for an increase in, or stabilization of, the mRNA. The actions of CHX and insulin were additive, suggesting insulin regulates *RDH10* independently of translation.

Insulin inhibits *RDH10* transcription via PI3K, Akt and suppression of FoxO1

PI3K or Akt inhibitors had no impact on *RDH10* expression in serum-free medium, but prevented repression by insulin (Fig. 4A). Inhibition of mTORC1 or MEK/ERK did not prevent the increase in *RDH10* expression induced by serum-free medium and did not ameliorate insulin inhibition. These data demonstrate that PI3K and Akt are required for suppression of *RDH10* transcription by insulin and suggest that FoxO1, which insulin suppresses, induces *RDH10* transcription. To test need for FoxO1, we infected HepG2 cells with an adenovirus expressing a dominant negative FoxO1 construct (dnFoxO1), which produces a truncated mutant that binds DNA, but lacks the transcription activation domain (89). Cells infected with dnFoxO1 did not increase *RDH10* expression when exposed to serum-free medium. Insulin had no further effect on *RDH10* expression in these cells. In contrast, adenovirus expressing lacZ responded to serum-free medium with an increase in *RDH10* mRNA that was inhibited by insulin (Fig. 4B). Western blot confirmed expression of HA-tagged dnFoxO1 (Fig. 4C). Insulin signaling induces phosphorylation and nuclear export of FoxO1 (90). Cells in serum-free medium had FoxO1 located in puncta within the nucleus. Cells treated with insulin had FoxO1 expressed in a diffuse pattern within the cytoplasm, consistent with nuclear export (Fig. 4D).

Serum-free medium increase and insulin decreases *RDH10* mRNA stability

We determined the elimination half-life ($t_{½}$) of *RDH10* mRNA in cells cultured 16 hr in serum-free medium, or maintained in growth medium, and then exposed to ActD for 24 hr (Fig. 5A). *RDH10* mRNA had a $t_{½}$ of 35 hr in the absence of serum and insulin. In the absence of serum, but in the presence of insulin, the $t_{½}$ decreased to 19 hr. In the presence of serum and absence of insulin (growth medium), *RDH10* mRNA had a biphasic $t_{½}$. The mRNA decreased 50% by 8 hr; after 8 hr the mRNA stabilized with a $t_{½}$ of 118 hr. Adding serum for 8 hr to cells that had been exposed to serum-free medium for 16 hr also decreased the amount of *RDH10* mRNA by 50%. Because *RDH10*

expression is elevated 2-3 fold in serum-free medium, the amounts of message in cells with serum-free medium, with or without insulin, continued to exceed those of cells maintained in growth medium. In absence of ActD, *RDH10* expression in cells exposed to serum-free medium 16 hr, then treated 4 hr with insulin, was unchanged (Fig. 5B). In contrast, treatment with serum, or serum and insulin, reduced *RDH10* mRNA to the amount in growth medium. Even though *RDH10* mRNA is relatively stable in the absence of insulin, translation was required to maintain stability, demonstrated by reduced mRNA in cells exposed to serum-free medium 16 hr, then treated 8 hr with CHX and ActD vs ActD alone (Fig. 5C).

RDH16 is regulated similarly to *RDH10*

Because mouse *Rdh1* expression also was reduced in liver of re-fed vs fasted mice, we examined its human ortholog *RDH16* in HepG2 cells. Removing serum from the medium increased in *RDH16* expression within 2 hr, rising to 4-fold by 16 hr (Fig. 6A). Insulin prevented the increase in *RDH16* mRNA prompted by serum-free medium, but neither glucagon nor glucose had an effect (Fig. 6B). The increase in *RDH16* mRNA that occurs in serum-free medium depended on transcription, as shown by ActD treatment (Fig. 6C). Interestingly, ActD treatment reduced *RDH16* expression more than that of growth medium or insulin. FoxO1 was required for *RDH16* transcription. Insulin had no effect in the presence of dnFoxO1, which reduced *RDH16* mRNA to a greater extent than insulin treatment in serum-free medium (Fig. 6D).

FoxO1 is required for elevated atRA biosynthesis in serum-free medium

To test impact of reduced *RDH* mRNA expression on atRA biosynthesis from retinol, HepG2 cells infected with dnFoxO1 or lacZ control were maintained 16 hr in growth or serum-free medium, and then were incubated 4 hr with all-*trans*-retinol. atRA increased ~4-fold in cells incubated in serum-free relative to growth medium (Fig. 7). The increase was prevented by dnFoxO1. Quantification of retinol recovered in cells revealed greater uptake in cells maintained in serum-free relative to growth medium. Thus, despite the increased intracellular retinol concentration, atRA biosynthesis was decreased by dnFoxO1, relative to the rate observed in serum-free medium.

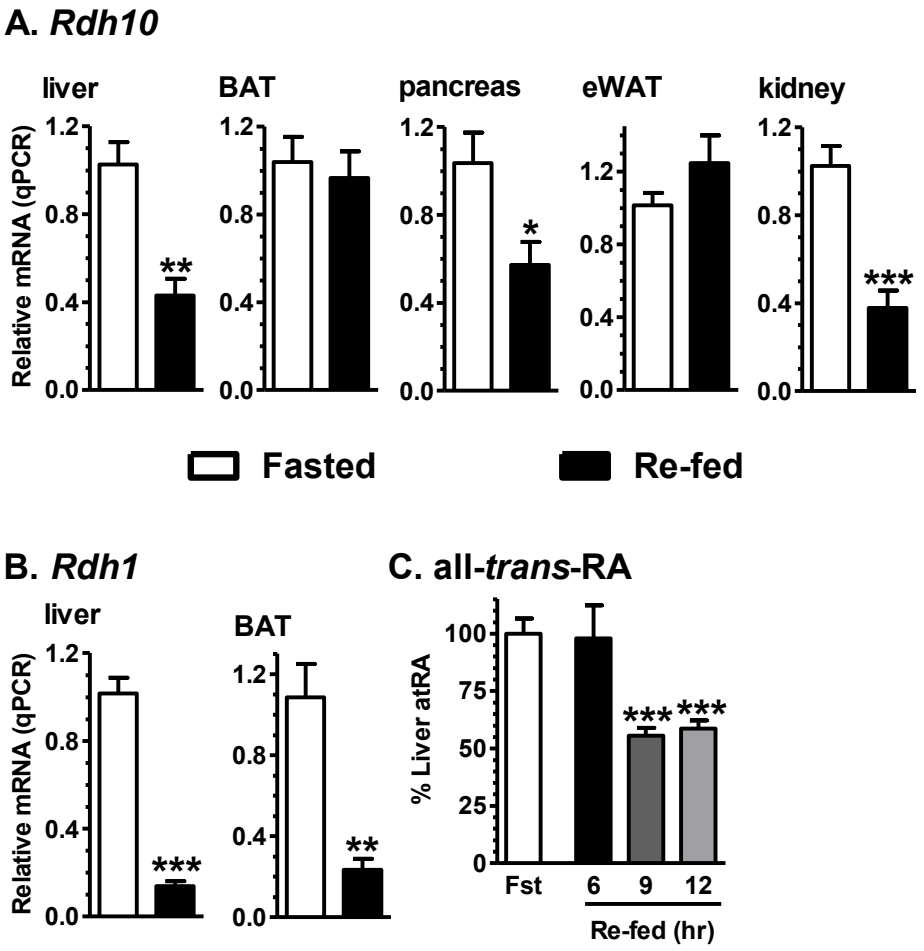

Figure 1. Regulation of *Rdh* expression and atRA concentrations by fasting and re-feeding. mRNA expression of (A) *Rdh10* and (B) *Rdh1* in tissues of mice fasted 16 hr, or fasted and re-fed ad libitum 6 hr. Data show a representative experiment of 2-5 experiments, each with 4-8 mice per group/experiment. (C) Liver atRA in mice fasted 16 hr, or fasted and re-fed ad libitum. Each re-fed group was normalized to its fasted group. Data show a representative experiment of 3 experiments, each with 6-9 mice per group/experiment: **P* < 0.05, ***P* < 0.005, ****P* < 0.0005, relative to fasted values.

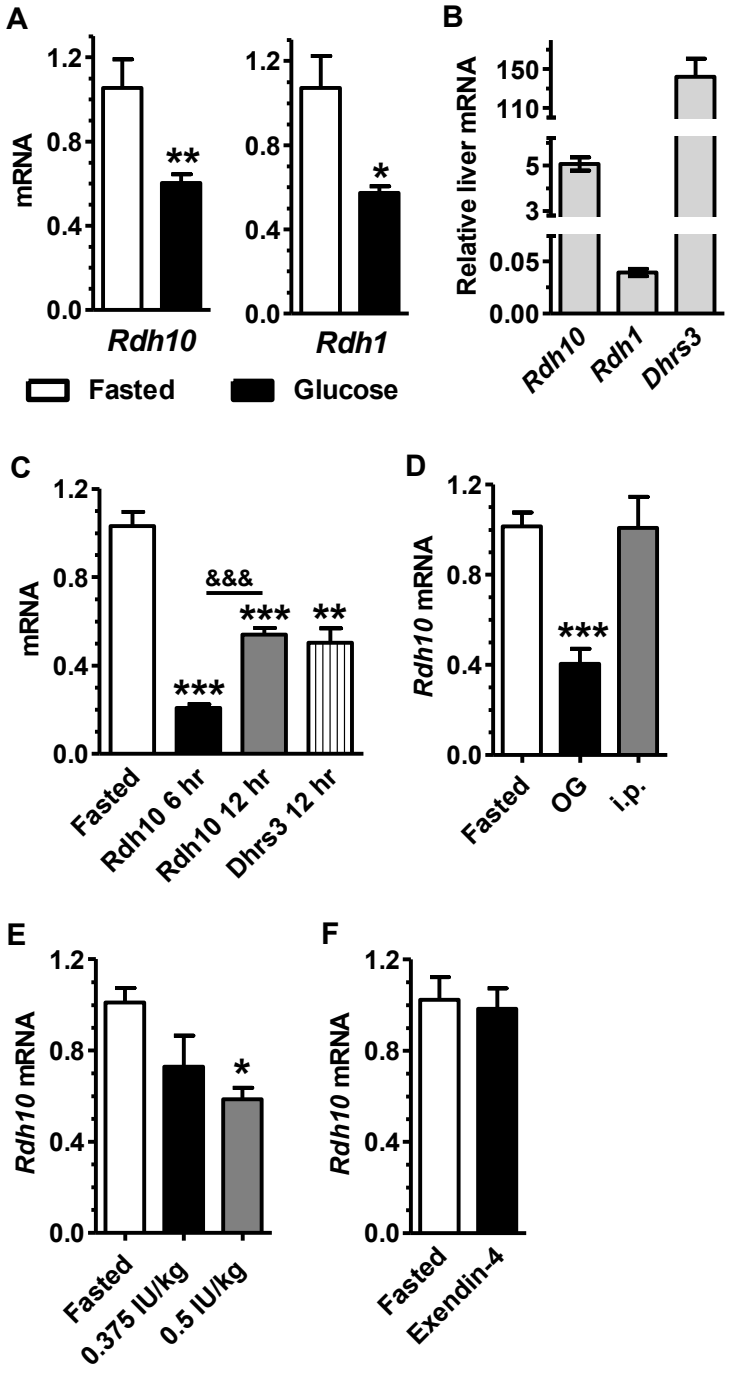
A
mRNA
1.2
0.8
0.4
0.0
**
*
Rdh10
Rdh1
Fasted
Glucose
B
Relative liver mRNA
150
110
5
3
0.05
0.00
Rdh10
Rdh1
Dhrs3
C
mRNA
&&&
***
***
**
Fasted
Rdh10 6 hr
Rdh10 12 hr
Dhrs3 12 hr
D
Rdh10 mRNA
***
Fasted
OG
i.p.
E
Rdh10 mRNA
*
Fasted
0.375 IU/kg
0.5 IU/kg
F
Rdh10 mRNA
Fasted
Exendin-4

Figure 2. Regulation of liver *Rdh* expression by energy balance. (A) Liver expression of *Rdh1* and *Rdh10* are relatively high in fasted mice and decrease in mice dosed with glucose by oral gavage. Samples were collected after a 16 hr fast or 6 hr after glucose dosing following a 16 hr fast. (B) Relative expression levels of *Rdh* and *Dhrs* mRNA in liver of fasted mice. (C) Effects of re-feeding on liver *Rdh10* and *Dhrs3* mRNA in mice fasted 16 hr and re-fed for the times indicated. (D) Glucose dosed by oral gavage (OG), but not i.p. injection, decreased *Rdh10* mRNA in liver of mice fasted 16 hr. (E) Insulin dosing repressed *Rdh10* mRNA in liver of mice fasted 16 hr. (F) The Glp-1 receptor agonist, exendin-4, did not repress *Rdh10* mRNA expression. Treated groups were collected after 6 hr, with the exception of the 12 hr re-fed group. qPCR data were normalized to their respective fasted groups: $^{*}P < 0.05$, $^{**}P < 0.005$, $^{***}P < 0.001$, relative to fasted values; $^{\&\&\&}P < 0.001$.

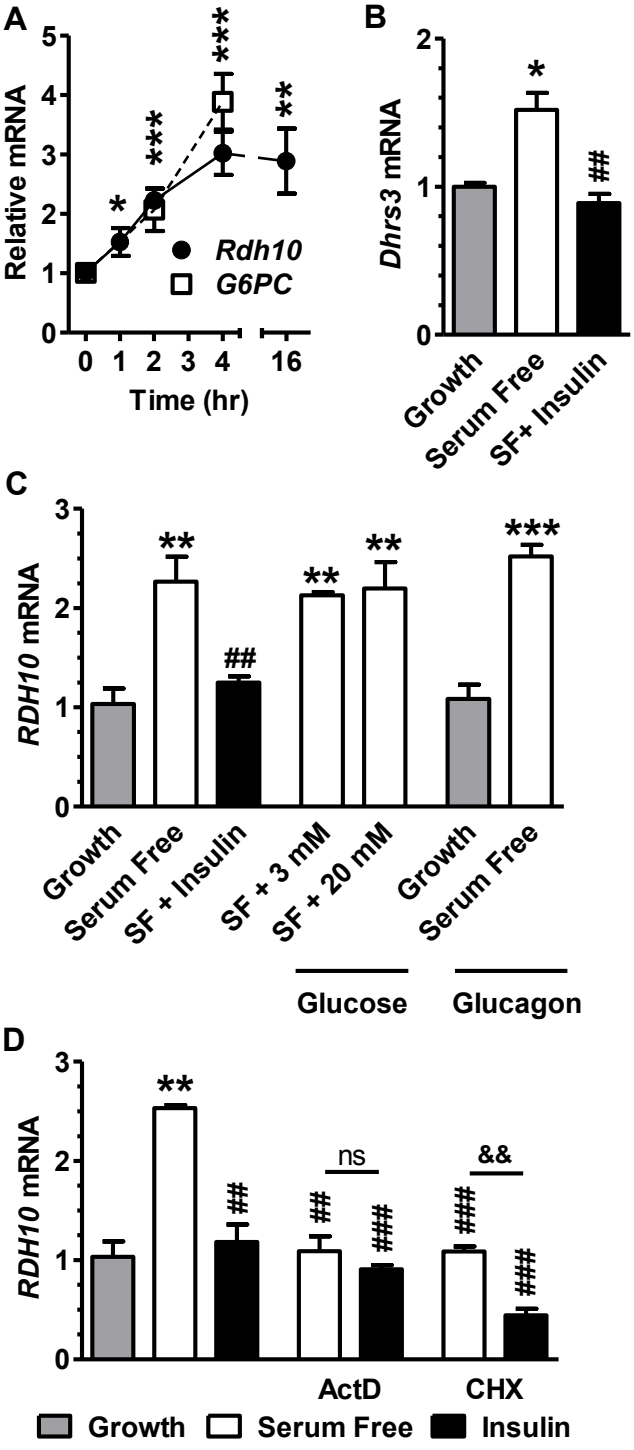
A
Relative mRNA
Time (hr)
Rdh10
G6PC
B
Dhrs3 mRNA
Growth
Serum Free
SF+ Insulin
C
RDH10 mRNA
Growth
Serum Free
SF + Insulin
SF + 3 mM
SF + 20 mM
Growth
Serum Free
Glucose
Glucagon
D
RDH10 mRNA
ns
&&
ActD
CHX
Growth
Serum Free
Insulin

Figure 3. Insulin inhibits *RDH10* and *DHRS3* transcription. (A) HepG2 cells were transitioned from serum-containing (growth) to serum-free (SF) medium at 0 hr, and the mRNA of *RDH10* and glucose-6-phosphatase (*G6PC*) were monitored. (B) Cells were exposed to growth or serum-free medium and treated with 10 nM insulin for 4 hr. (C) Cells were exposed to growth or serum-free medium and treated for 6 hr with 10 nM insulin, 3 or 20 mM glucose, or 100 nM glucagon. (D) Cells were exposed to growth or serum-free medium and treated 4 hr with 10 nM Insulin, 25 μg/mL ActD, or 10 μg/mL CHX: $^{*}P < 0.05$, $^{**}P < 0.005$, $^{***}P < 0.0005$ relative to growth values; $^{\#\#}P < 0.005$, $^{\#\#\#}P < 0.001$ relative to serum-free values; $^{\&\&}P < 0.005$.

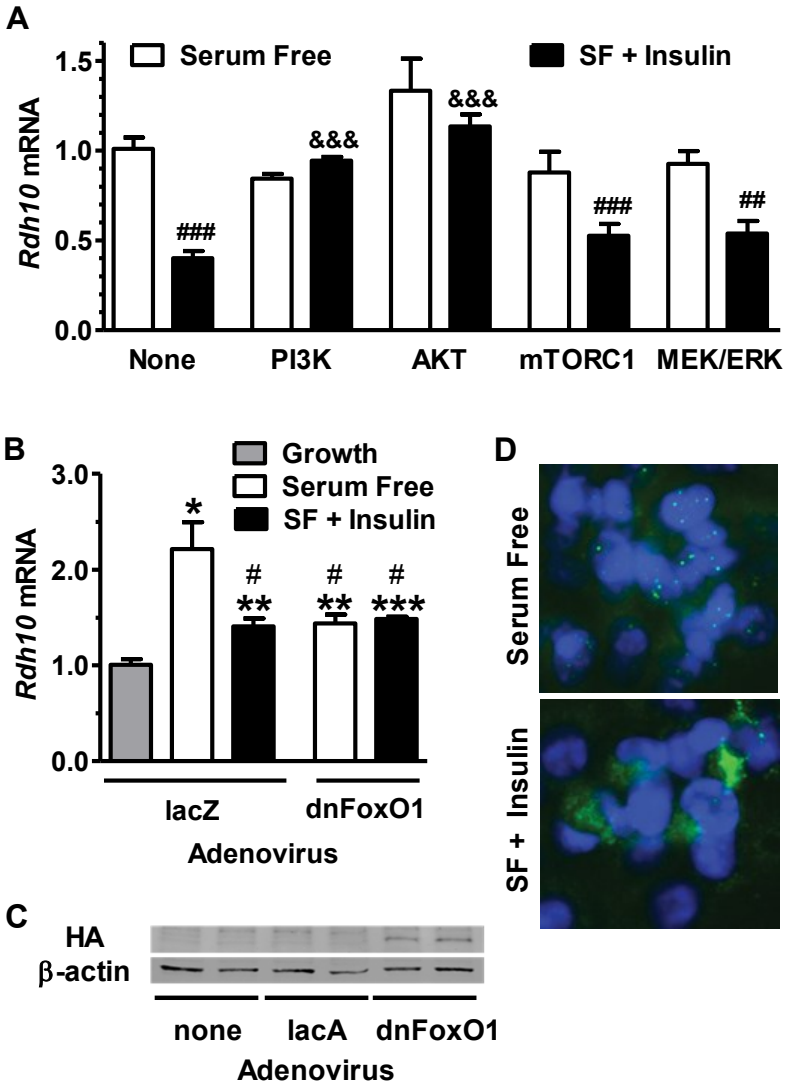
A
Serum Free
SF + Insulin
Rdh10 mRNA
1.5
1.0
0.5
0.0
###
&&&
&&&
###
##
None
PI3K
AKT
mTORC1
MEK/ERK
B
Growth
Serum Free
SF + Insulin
Rdh10 mRNA
3.0
2.0
1.0
0.0
*
#
**
#
**
#
***
lacZ
dnFoxO1
Adenovirus
C
HA
β-actin
none
lacA
dnFoxO1
Adenovirus
D
Serum Free
SF + Insulin

Figure 4. Transcriptional regulation of *RDH10* expression by insulin requires FoxO1. (A) *RDH10* mRNA expression in HepG2 cells pre-treated with inhibitors or DMSO vehicle for 1 hr, then 4 hr with fresh inhibitors in serum-free medium, with or without 10 nM insulin. PI3K was inhibited with 50 μM LY294002; Akt was inhibited with 1 μM Triciribine; mTORC1 was inhibited with 200 nM rapamycin; MEK/ERK was inhibited with 20 μM PD98059. (B) *RDH10* mRNA expression in cells infected with adenovirus expressing dominant negative FoxO1 (dnFoxO1) or lacZ control for a total of 48 hr, and treated with growth or serum-free medium ± 10 nM insulin during the final 4 hr. qPCR data were combined from two independent experiments with n = 3-4 each. (C) Western blotting verified expression of HA tagged dnFoxO1 in cells infected with adenovirus dnFoxO1, and not in untreated or adenovirus lacZ cells. (D) Immunohistochemistry detection of FoxO1 (green) and DAPI (blue) in HepG2 cells treated 4 hr with serum-free medium ± 10 nM insulin. Image data represent one of two experiments. qPCR: $^{\#}P < 0.05$, $^{\#\#}P < 0.005$, $^{\#\#\#}P < 0.001$ vs serum-free control, $^{\&\&\&}P < 0.0005$ vs insulin-treated control (no inhibitor), $^{*}P < 0.05$,$^{**}P < 0.005$, $^{***}P < 0.001$ vs growth medium control.

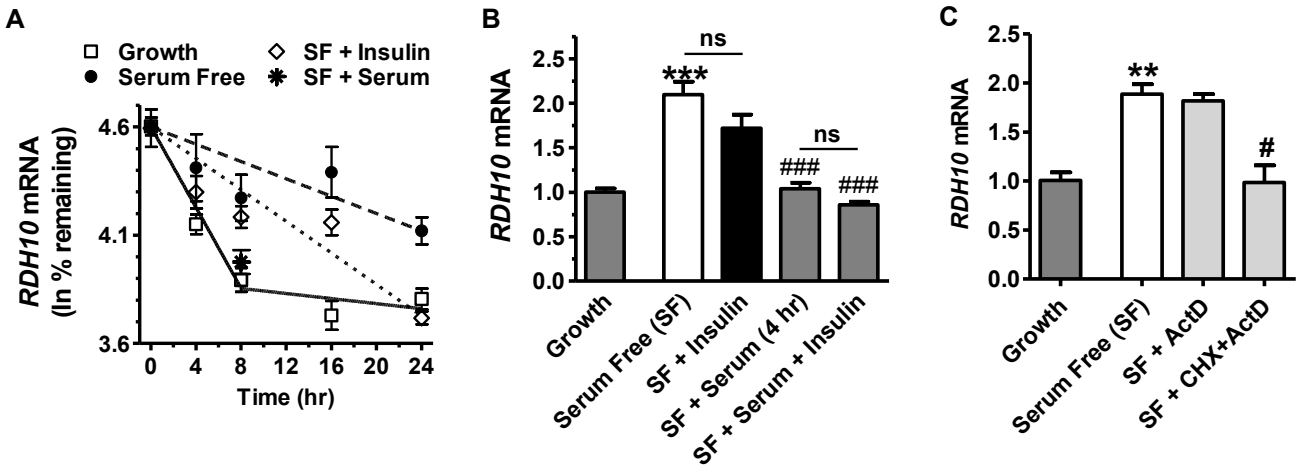

Figure 5. Insulin and serum effects on the elimination half-life of *RDH10* mRNA. (A) HepG2 cells were maintained in growth medium, or pre-incubated in serum-free medium for 16 hr before time 0. At time 0, cells were treated with 25 µg/mL ActD, with or without 10 nM insulin, or 10% serum. qPCR data were normalized to 100% relative expression at time 0 for each condition and plotted as ln % remaining. Half-lives ($t_{½}$) were calculated as 0.693/slope, with the slope determined by linear regression analysis. (B) Cells were maintained in growth medium, or pre-incubated in serum-free medium for 16 hr, then treated with 10 nM insulin and/or 10% serum for 4 hr. (C) Cells were maintained in growth medium or pre-incubated in serum-free medium for 16 hr, then treated 8 hr with DMSO (vehicle control), 25 µg/mL ActD, or ActD and 10 µg/mL cycloheximide (CHX): $^{**}P < 0.005$, $^{***}P < 0.001$ vs growth values, $^{\#}P < 0.05$, $^{\#\#\#}P < 0.001$ vs serum-free values.

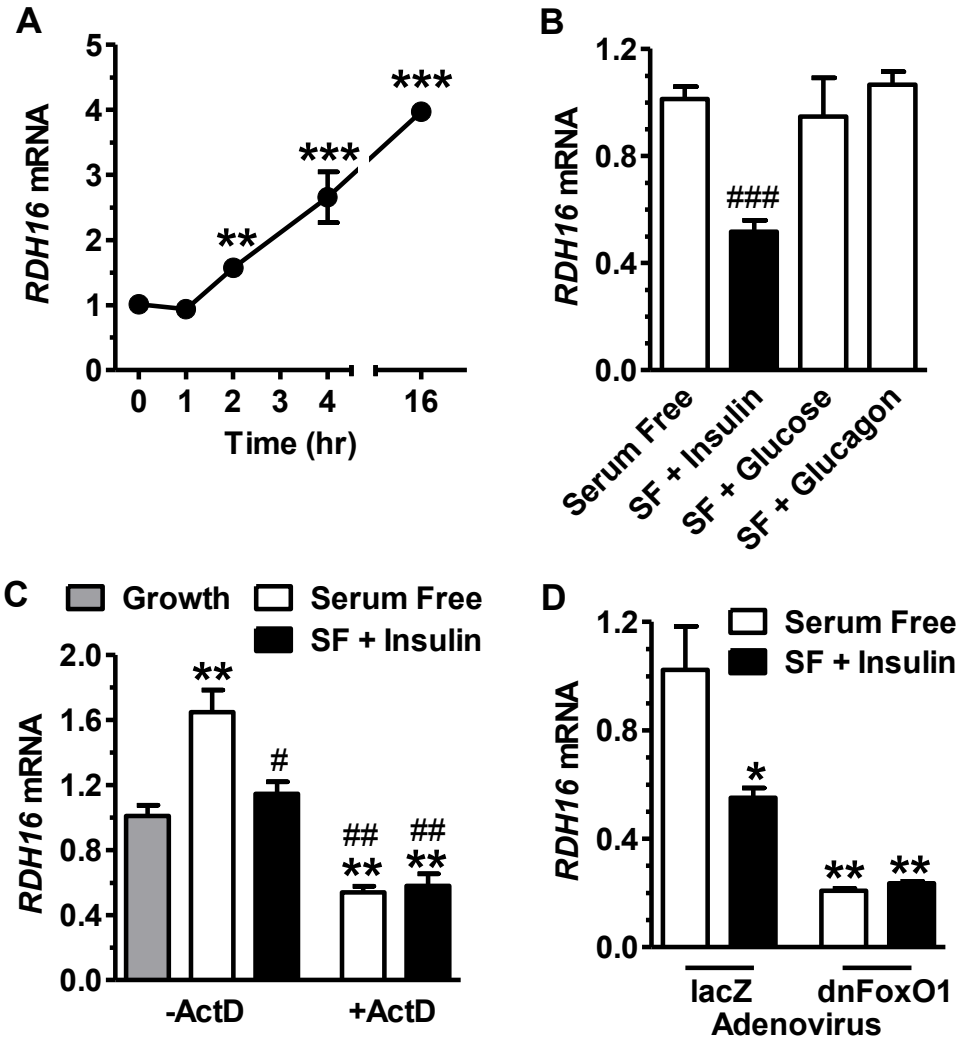

Figure 6. Serum and insulin repress *RDH16* expression in HepG2 Cells. (A) Cells were transitioned from growth (serum-containing) medium to serum-free medium at time 0 and assayed by qPCR for *RDH16* mRNA. (B) Cells were exposed to serum-free medium and treated with 10 nM insulin, 20 mM glucose, or 100 nM glucagon, for 6 hr. (C) Cells were exposed to growth or serum-free medium and treated 4 hr with 10 nM insulin and/or 25 µg/mL ActD. (D) Cells were infected with adenovirus expressing dnFoxO1 or lacZ for 48 hr, and treated with serum free-medium ± 10 nM insulin during the final 4 hr: **P* < 0.05, ***P* < 0.005, ****P* < 0.0005 vs growth values; $^{\#}$p<0.05, $^{\#\#}$p<0.005, $^{\#\#\#}$p<0.0005 vs serum-free values.

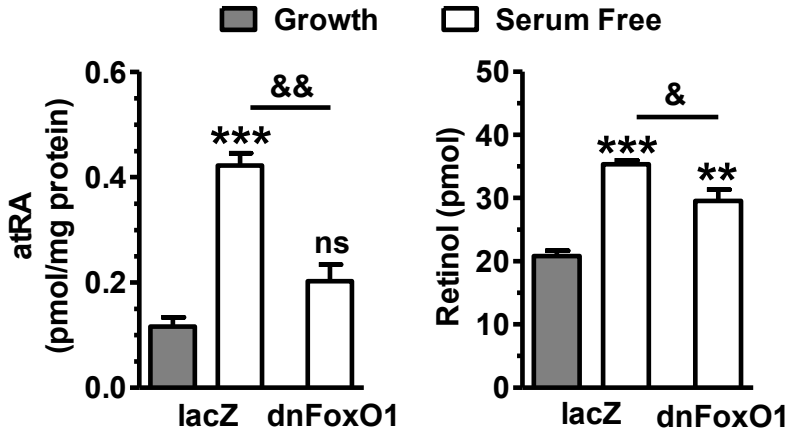

Figure 7. FoxO1 promotes atRA biosynthesis. HepG2 cells were infected with adenovirus 48 hr prior to harvesting, incubated in growth or serum-free medium for 16 hr, then treated with 50 nM (100 pmol) retinol in the final 4 hr. Left: atRA synthesis is elevated in cells in serum-free medium. Dominant negative FoxO1 (dnFoxO1) prevents the increase. Right: the amount of retinol recovered in cells is elevated in cells incubated in serum-free medium: $^{**}P < 0.005$, $^{***}P < 0.0001$ vs growth values, $^{\&}P < 0.05$, $^{\&\&}P < 0.005$ as labeled; ns, not significantly different from growth medium.

DISCUSSION

This report reveals a reciprocal interaction in which energy status regulation of atRA biosynthesis through insulin would attenuate regulation of energy balance by atRA. Serum contains factor(s) other than insulin that control *Rdh* expression and mRNA stability. We focused on insulin because of its importance to regulating metabolism in liver, including suppressing gluconeogenesis, a process stimulated by atRA (49, 91). Another motive was the observation that animals fed a vitamin A-deficient diet were glycogen deficient owing to a defect in gluconeogenesis, caused by low expression of *Pck1* (46–48).

Increased expression of *Rdh10* and *Rdh1* in liver during fasting emphasizes the importance of increasing atRA synthesis to regulate metabolic genes, such as *Pck1*. In contrast to liver, *Rdh1* may have a unique function in BAT of integrating energy status with retinoid signaling, because *Rdh10* does not change in BAT with changes in energy status. eWAT and pancreata do not express *Rdh1* (data not shown), but express *Rdh10*. The non-responsiveness of *Rdh10* in eWAT to changes in energy balance allows several interpretations, including presence of another *Rdh* that responds to changes in energy status, or feeding vs. fasting does not modify atRA concentrations in adult mice. These possibilities are the subjects of ongoing studies. The decrease in *Rdh10* expression in pancreas during re-feeding is consistent with the requirement for retinoids in pancreatic development (92, 93) and function (94, 95), and also is a subject of ongoing studies. Suppression of *Rdh1* in liver by re-feeding, and *Rdh10* in liver and kidney, relate insulin action with atRA signaling in two gluconeogenic tissues. Decreased expression of *Dhrs3* in liver of re-fed versus fasted mice is consistent with a mutually activating interaction of *Rdh10* and *Dhrs3* (73), and the reduction in atRA biosynthesis. Evidently, energy metabolism affects *Rdh* expression in multiple tissues to regulate retinoid signaling effects.

Oral dosing has a singular effect on glucose uptake and insulin action in liver (76). Glucose delivery by the portal vein combined with insulin, and an as yet unidentified neuronal signal, increases net hepatic glucose uptake compared to peripheral delivery, with a concomitant impact on insulin-regulated processes (96, 97). Comparison of oral glucose dosing and infusion via the portal vein revealed similar enhancement in hepatic glucose uptake relative to peripheral presentation, which excludes a need for a gut-secreted factor, such as Glp-1 (98). Yet, secretion of Glp-1 upon feeding contributes to reduced glucose production in liver by augmenting glucose-stimulated insulin secretion from pancreas (99). Our data are consistent with these observations, supporting physiologically significant regulation of *Rdh* expression in liver during glucose uptake.

Reduced *Rdh* expression preceded the reduction in liver atRA, and associated with a lower rate of atRA biosynthesis in HepG2 cells, consistent with a cause and effect relationship. atRA homeostasis, however, auto regulates via induction of both catabolic cytochromes P-450 and the retinyl ester-forming lecithin:retinol acyltransferase (LRAT) (100–102). The former decreases atRA itself, whereas the latter decreases the amount of retinol available to support atRA biosynthesis. These factors

likely attenuated the extent of atRA differences in the fasted vs the re-fed liver. Overall effects would depend on a combination of the change in *Rdh* expression, and the activities of other enzymes involved in retinoid homeostasis, including retinyl ester biosynthesis and atRA degradation. The two-fold decrease in liver atRA resulting from insulin action seems remarkable in context of this impetus to sustain atRA homeostasis.

Inhibitor studies excluded *Rdh10* regulation through MAPK kinase, and mTORC1, suggesting FoxO1 as a candidate for the insulin effect. FoxO (forkhead box 'Other') proteins constitute a subgroup of a family of evolutionarily conserved transcription factors that mediate insulin signaling in mammals, but also mediate metabolism and longevity in primitive organisms such as *C. elegans* and drosophila (103, 104). FoxO proteins contribute to metabolic regulation through effects in liver, muscle, adipose tissue and pancreas. Of these, FoxO1 stimulates a committed step in hepatic gluconeogenesis, catalyzed by phospho*enol*pyruvate carboxykinase (*PCK1*), and also of the last step catalyzed by glucose-6-phosphatase (*G6PC*) (89, 105–107). Haploinsufficiency of *FoxO1* restores insulin sensitivity in insulin-resistant mice (108). A constitutively active gain-of-function *FoxO1* mutant targeted to liver and pancreas manifests a diabetic phenotype (108). Liver-specific inactivation results in decreased serum glucose at birth and upon fasting in adult mice, from impaired glycogenolysis and gluconeogenesis (107). A liver-specific *FoxO1*-null mouse crossed with an insulin receptor-null mouse has reduced glucose production and lacks the neonatal diabetes and hepatosteatosis that occur in insulin receptor-null mice (107). Liver-specific *FoxO1*-null mice treated with the β-cell toxin streptozotocin, have elevated VLDL secretion, cholesterol, and plasma free fatty acids (109).

Insulin-stimulated phosphorylation of FoxO1 by Akt causes nuclear export, resulting in ubiquitination-mediated proteasomal degradation (110), and down-regulation of target gene transcription (90). Indeed, we confirmed ability of insulin to cause nuclear export of FoxO1 in HepG2 cells (Fig. 4D). FoxO1 activity also is stimulated by deacetylation, catalyzed by sirtuin1 (111). Inhibition of sirtuin1 in HepG2 cells with Ex-527 incubated in serum-free medium did not affect *RDH10* expression (data not shown), indicating that acetylation is not involved in regulation of *RDH10*, at least under the conditions tested.

Recent insight into the functions of the insulin receptor substrates IRS1 and IRS2 indicate that both coordinate responses to insulin via FoxO1 (112, 113). During the re-fed state, insulin activates IRS1 to suppress FoxO1 and allow an increase in glucokinase (*GCK*) and sterol regulatory element binding transcription factor 1 (*SREBF1*, a.k.a. *SREBP1*) expression that promotes glycolysis and lipid biosynthesis, respectfully. In contrast, insulin inhibits IRS2. Because IRS2 stimulates gluconeogenesis by inducing *PCK1* and *G6PC* in liver through FoxO1, the relatively low levels of insulin in the fasted state allow IRS2 to induce gluconeogenesis. Based on these insights, the higher insulin levels in the re-fed state would function through IRS1 to suppress *RDH* expression, whereas the lower insulin levels in the fasted state would allow IRS2 to induce *RDH* expression.

The actions of insulin and serum both prevented transcription and destabilized *RDH* mRNA. The effects differed in degree, and resulted in different levels of mRNA, but did not totally eliminate *RDH* mRNA. In both serum-free medium and insulin-containing serum-free medium, the amounts of *RDH* mRNA after 24 hr remained 2 to 3-fold higher compared to serum-containing medium, because the initial concentrations were 2 to 3-fold higher. The reduction but not elimination of *RDH* mRNA by insulin and serum is compatible with the continued presence and biosynthesis of atRA, and a need for *RDH* to modulate basal gluconeogenesis and/or its other multiple functions, whether related or unrelated to energy balance, such as regulating proliferation (114).

Translation was required for increase and stability of *Rdh10* mRNA in serum free medium (CHX results in Fig. 3D and 5C, respectively), and are subjects of ongoing studies. AU-rich elements (AREs) are regulatory sequences in the 3' untranslated region of short-lived mRNAs, and are recognized by RNA binding proteins to confer stability (115). *RDH10* mRNA has three pentamer AREs in AU rich regions, predicting stabilization by HuR or similar mRNA binding protein (http://arescore.dkfz.de/arescore.pl). Cellular retinoic acid-binding protein 2 interacts directly with HuR to increase its affinity toward target mRNAs and protect them against degradation (116). atRA does not destabilize *RDH10* mRNA, but it does increase its transcription (data not shown). Forward regulation of atRA synthesis via increased *RDH10* may reinforce elevated atRA in fasted state to increase gluconeogenesis.

FoxO1 binding sites have been identified in promoters of genes associated with retinoid metabolism, including dehydrogenase/reductase SDR family member 9 (*Dhrs9*), cellular retinol binding protein type 1 (encoded by *Rbp1)* and *Rdh8*, but not in *Rdh1* or *Rdh10* (79). To address the impact of FoxO1 regulated expression of retinoid genes, atRA target genes *Pck1* and *Pdk4* were measured in cells with *FoxO1* knocked down. Induction of both genes in response to atRA or to its precursor, retinol, were blunted. The dose (20 μM) of atRA used, however, exceeded those found in tissues by 400 to 4000-fold, and those used in vitro by 20-fold. Nevertheless, these results also are consistent with FoxO1 linking retinoid metabolism and hepatic gluconeogenesis. FoxO1 binding sites for *Rdh10* or *Rdh1/16* have not been reported in ChIP sequencing data (Encyclopedia of DNA Elements Consortium, ENCODE; UCSC genome browser). This could imply indirect regulation of these *Rdh* by FoxO1 or reflect a lapse in identifying the sites.

Regulation by insulin signaling prompts the question whether abnormal *RDH* expression associates with human disease. For example, impaired insulin secretion and insulin resistance during diabetes predicts elevated *RDH* expression and atRA synthesis (117). Conversely, enhancement of insulin signaling through PI3K/Akt from loss of PTEN in cancer implicates decreased *RDH* (118). Reduced *RDH* expression would decrease atRA biosynthesis, which could affect tumor differentiation and/or aggressiveness. Various cancers show alterations in the atRA signaling pathway, such as loss of atRA receptors (119, 120) and down-regulation of atRA chaperons (121, 122). atRA biosynthesis is impaired in breast cancer cell lines relative to normal cells (123). Reduced atRA synthesis in the *Rbp1*-null mouse is consistent with increased mammary tumors, and suggests consequences of the epigenetic silencing of *Rbp1* in

25% of human breast cancers (124). In contrast, overexpression of *RDH10* in HepG2 cells reduces proliferation (114).

In summary, this work demonstrates regulation of *Rdh* mRNA by energy status via insulin, with consequent changes in atRA synthesis. Coordinate induction of *Rdh* and *Pck1* by FoxO1 would increase atRA synthesis and gluconeogenesis during fasting and decrease *Rdh* in the fed state to establish an interactive relationship between energy balance and atRA (Fig. 8). These data predict altered atRA in human diseases characterized by dysfunctional insulin signaling, including diabetes and cancer.

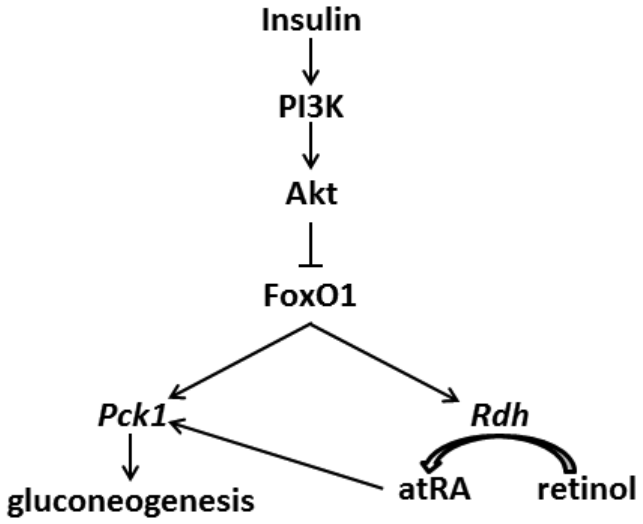

Figure 8. Regulation of *Rdh* expression by insulin signaling. Both atRA and FoxO1 induce *Pck1* transcription to increase gluconeogenesis. FoxO1 induces atRA biosynthesis via inducing *Rdh* mRNA. Insulin suppresses FoxO1 activity, thereby suppressing gluconeogenesis and atRA biosynthesis through decreasing *Rdh* transcription and mRNA stability. Activation of PI3K/Akt represents a molecular indicator of cancer, implicating decreased atRA.

Chapter 2

Glucose and cAMP Regulate Retinol Dehydrogenase 5 Expression and 9-*cis*-Retinoic Acid Biosynthesis in Pancreas Beta Cells

INTRODUCTION

The physiological role(s) of 9-*cis* retinoic acid (9cRA) were uncharacterized until identification of 9cRA exclusively in pancreas tissue, by liquid chromatography tandem mass spectrometry (32). 9cRA was reduced in pancreas of mice fed ad-libitum versus fasted for 12 hours, and decreased rapidly and transiently in response to glucose bolus. 9cRA dosed prior to a glucose tolerance test (GTT) elevated blood glucose and impaired insulin secretion. 9cRA attenuated glucose stimulated insulin secretion (GSIS) in 832/13 beta cell line and in primary isolated islets on a short time scale, indicative of a non-genomic mechanism. 9cRA was elevated in pancreas tissue of mice with metabolic conditions of obesity and diabetes, characterized by chronic hyperglycemia. Streptozotocin treatment demonstrated that depletion of beta cells decreased pancreas tissue 9cRA, and indicated 9cRA was primarily located in beta cells.

The enzymatic pathway regulating 9cRA metabolism is unknown. Activity of select RA biosynthesis enzymes with *cis*- isoforms of retinol and retinal *in vitro* predict a parallel synthetic pathway to that of all-*trans*-RA (atRA). Additionally, detection of 9-*cis*-retinol (9c-retinol) substrate in pancreas microsomes supports synthesis of 9cRA from 9c-retinol, rather than by isomerization of atRA. RA is synthesized from retinol by two sequential dehydrogenation reactions, to yield retinal, then RA (5). Rdh enzymes catalyze the first and rate limiting step in RA biosynthesis. *Rdh5* is active with *cis*-isoforms of retinol (125–128). Mutations in the *Rdh5* gene cause fundus albipunctatus in humans, which is characterized by night blindness (129). However, redundancy of *cis*-acting *Rdh*s in the eye made the *Rdh5* knock out mouse unable to recapitulate the human phenotype (130). Expression of *Rdh5* outside of the eye indicates it has additional function (131).

Pancreas tissue consists of multiple cell types, likely with different retinoid needs and pathway regulation. Endocrine pancreas cells are organized into islets, which make up 1-5% of the pancreas. Beta cells make up 70-80% of islets, and function to sense glucose and secrete insulin (132). The 832/13 beta cell line was selected from INS-1 rat insulinoma cells following stable transfection with human pro-insulin (133). These cells maintain ability to secrete insulin in response to physiological glucose exposures, i.e. GSIS. The MIN6 cell line is a mouse derived insulinoma cell line that also maintains glucose inducible insulin secretion (134). Both cell lines were evaluated for their ability to robustly model the regulation of *Rdh5* detected in pancreas and in accordance with synthesis of 9cRA.

Beta cells initiate a series of signaling events in response to glucose that secrete insulin in the short term, and modulate gene expression in the long term. After receptor

mediated uptake, metabolism of glucose increases the ratio of adenosine triphosphate (ATP) to adenosine diphosphate (ADP), which initiates closure of ATP-sensitive K+ channels, and causes influx of calcium. Elevated intracellular calcium triggers release of insulin containing vesicles, and also relieves suppression of transcription factor carbohydrate response element binding protein (ChREBP). Glucose is not typically sensed in isolation. Rather, in response to feeding, beta cells receive a combination of signals from nutrients, incretin hormones, adipokines, and neuronal factors, to influence secretory and transcriptional activity. Glucagon-like peptide 1 (GLP-1) is an incretin hormone that stimulates cyclic adenosine monophosphate (cAMP) production in beta cells after binding its G protein-coupled receptor. Coordinated elevation of intracellular calcium, as result of glucose, and cAMP, as result of GLP-1, maximize insulin secretion in beta cells by aligning pulsatile fluctuations (135). Transcriptional response to cAMP is mediated by cAMP response element binding protein (CREB) family, of which cAMP response element modulator (CREM) can repress transcription (136). A microarray study evaluated transcriptional response to glucose and cAMP in beta cells, and differentiated results as rapidly responding immediate-early genes, versus target genes, based on sensitivity to the protein synthesis inhibitor cycloheximide (137). Their results demonstrate the vast transcriptional response to metabolic fluctuation in beta cells. This work identifies *Rdh5* as a physiologically relevant regulator of 9cRA synthesis in beta cells, and begins to characterize transcriptional regulation of *Rdh5* by glucose and cAMP.

MATERIALS AND METHODS

Animals

Wild-type C57Bl/6J, or Rbp -/-, male mice, age 2-3 months were bred in-house and housed up to 5 per cage with litter mates, and fed AIN93G semi-purified diet with 4 IU vitamin A/g (Dyets, catalog# 110700). Wild-type Sprague Dawley rats (Charles River) were maintained on chow diet (Harlan Teklad #2018). Fasted groups were deprived of food for 16 hr, beginning ~2 hr prior to initiation of the dark cycle. Re-fed groups were provided diet ad-libitum for times indicated. An oral gavage glucose dose of 2 g/kg body weight was delivered as 10 µl/g body weight of a 20% glucose solution in PBS. Intraperitoneal (i.p.) glucose was delivered in one or two injections of 2 g/kg body weight following a 16 hr fast. Experimental groups were normalized to controls consisting of fasted animals of the same age, diet, and sex. Tissues were harvested immediately after euthanasia, frozen in liquid nitrogen, and stored at -80 until mRNA or retinoid quantification. Animal experiments were approved by Office of Laboratory and Animal Care at University of California Berkeley.

Cell culture

The pancreas beta cell line 832/13 was cultured in growth medium (RPMI 1640 containing 11mM glucose, 10% FBS, 2 mM L-glutamine, 1 mM sodium pyruvate, 50 µM 2-mercaptoethanol, and 10 mM Hepes), under 5% CO_2 in 75 cm^2 flasks or 6-well plates as described (133). The medium was refreshed every 2-3 days. Cells were subcultured at > 70% confluency. Experimental conditions were exposure to growth RPMI 1640 medium in absence of FBS, and containing 3 mM (low) or 15 mM (high) glucose, for times specified. Cells were treated with 400 ng insulin (Sigma I9278), 0.1 µg/mL actinomycin D (Life Technologies A7592), 100 µM IBMX (Sigma #I7018), 10 µM forskolin (Fisher Scientific BP2520-1), 1 µM U0126 (Cell Signaling Technology #9903S), or 20 µM PD98059 (CalBiochem #513000). 832/13 cells were transiently transfected with 10 ng of pSG5 vector, either empty or containing the coding region of human Rdh5 gene. 24 hr post-transfection, cells were collected for mRNA expression, or treated with 9-*cis*-retinol substrate for 9cRA synthesis assay.

MIN6 cells were cultured in growth medium (DMEM containing 4.5g/L = 25 mM glucose, 10% FBS, 40 mM sodium bicarbonate, 110,000 Units Penicillin, 36,000 I.U. Streptomycin, and 0.0005% β mercaptoethanol), under 5% CO_2 in 25 cm^2 flasks or 6 well plates as described (134). Experimental conditions were exposure to growth DMEM medium in absence of FBS, and containing low (3 mM) or high (25 mM) glucose.

GSIS assay

832/13 cells were pre-incubated in HBSS containing 3 mM glucose for 2 hr, then in HBSS containing 3 mM or 23 mM glucose ± IBMX for 2 hr to stimulate insulin secretion as described (133). Secretion assay buffer was collected for insulin measurement by ELISA (Alpco), and cells collected for protein quantification by Bradford assay (Sigma). In MIN6 cells GSIS was performed using HEPES-balanced Krebs Ringer Bicarbonate

Buffer (KRBB) containing 0.1% BSA as described in (138). Cells pre-starved for 30-60 min in 3 mM glucose, then stimulated with 3, 15, or 25 mM glucose for 1 hr at 37 °C, and 9cRA (100 uM) treatment or DMSO vehicle. Supernatent was collected for Insulin measurment by ELISA (ALPCO). Secreted insulin was normalized to cellular protein by bradford assay (Sigma).

9c-Retinal and 9cRA synthesis

832/13 cells were incubated 24 hr in experimental medium, or with transfected vector, then treated with 9-*cis*-retinol (TRC R252095) or DMSO vehicle for 4 hr. Retinoids were handled under yellow light and all materials in contact with samples were glass or stainless steel. Cell samples were rinsed with PBS, harvested in reporter lysis buffer (Promega E3971), and frozen -80 °C until extraction for retinoid quantification. Retinal was converted to retinal-oxime, extracted as described (80), and quantified by UPLC/MS method. Retinoic acid was extracted and quantified by LC/MS/MS using select reaction monitoring and 4,4- dimethyl atRA as internal standard, as described in detail (80, 81).

RNA isolation and qPCR

RNA was isolated from tissues and cells by the Trizol reagent (Invitrogen) method. Pancreas tissue was collected rapidly in small (5 mg) chunks and frozen directly in liquid nitrogen to prevent degradation by proteases, then homogenized with Trizol as a frozen powder using a chilled mortar and pestle. cDNA was prepared using iScript reagent kit (BioRad 170-8891). Real-time qPCR was prepared with 2x TaqMan master mix (Life Technologies 4369016), and Taqman Gene Expression Assays: mouse/rat Actb Mm00607939_s1, rat Rdh5 Rn01527179_g1, rat Rdh10 Rn00710727_m1, rat RoDH2 (Rdh16) Rn01505848_g1, rat Crem Rn01538528_m1, mouse Rdh5 Mm00506111_m1 (Life Technologies), and run on an ABI 7900 thermocycler. Gene expression was analyzed by the ΔΔ-Ct method, normalized to β-actin, and expressed as fold change relative to expression in reference condition as described.

Islets

Islets were isolated by the University of California, San Francisco Diabetes and Endocrinology Center. Fifty islets per well from wild-type mice fed chow diet ad libitum, were cultured overnight in RPMI 1640 containing 11 mM glucose, 10% FBS, 100 U/mL penicillin, 100 µg/mL streptomycin, 10 mM Hepes, 2 mM L-glutamine, 1 mM sodium pyruvate, 50 µM β-mercaptoethanol, in 12 well plates at 5% CO2 and 37°C. After overnight culture, islets were treated with serum free medium containing 3 mM or 15 mM glucose for 6 or 16 hr, then collected for mRNA quantification.

Statistics

Data are presented as means ± standard errors (SE) and were analyzed using two-tailed, unpaired Student's *t* tests.

RESULTS

Rdh5 mRNA is reduced in re-fed, versus fasted, pancreas tissue

Rdh5 expression varies with metabolic status in pancreas tissue, *in vivo*. Pancreas *Rdh5* mRNA expression was elevated in mice fasted for 16 hr, and decreased significantly in response to re-feeding. Expression was reduced temporally, with decreases of 40 and 67 percent in 4 and 6 hr, respectfully (Fig. 1A). Dosing animals with glucose by intraperitoneal (i.p.) injection, following an overnight fast, did not recapitulate the reduction in *Rdh5* mRNA in response to re-feeding (Fig. 1B). In mice re-fed for 6 hours, *Rdh5* mRNA decreased 43, 68 and 85% in liver, kidney, and brown adipose tissue (BAT), respectfully, increased 33% in epididymal white adipose tissue (eWAT), and increased 2.5-fold in retinal pigment epithelium (Fig. 2A-E). Glucose administered by i.p. injection reduced *Rdh5* by 38 percent in BAT, increased *Rdh5* by 1.4-fold in eWAT, and did not affect expression in liver or kidney. Glucose administered by oral gavage reduced *Rdh5* mRNA by 55, 62, 92, and 45 percent in liver, kidney, brown adipose, and eWAT, respectfully. *Rdh5* expression in pancreas was not measured from mice treated with glucose by oral gavage.

9cRA is reduced in pancreas of re-fed, versus fasted, rats

9cRA was measured in pancreas of wild type rats following experiments similar to those done with mice (32). 9cRA decreased 52 percent in pancreas of mice re-fed for 4 hr following an overnight fast, relative to fasted 16 hr (Fig. 3A). Retinol also decreased 20 percent, while retinyl esters trended down (Fig. 3B-C). Reduced 9cRA in rat pancreas demonstrates conservation among species. 9cRA did not decrease in pancreas of rats treated with glucose by oral gavage for 15 min following a 16 hr fast (Fig. 3D). Retinol increased 1.4-fold following glucose treatment, but retinyl esters were unchanged (Fig. 3E-F). Rapid changes in the 9cRA concentration are likely by mechanism(s) independent of synthesis, and remain undefined.

9cRA attenuates GSIS in beta cell culture model

Cell culture models were used to characterize regulation of 9cRA synthesis. GSIS assay confirmed that 832/13 cells in this project maintained the ability to secrete insulin when stimulated (Fig. 4A). A 6.7-fold increase was detected in response to high glucose (15 mM), and a 12.6-fold increase was detected in response to maximal stimulation with 3-Isobutyl-1-methylxanthine (IBMX), which elevates cyclic adenosine monophosphate (cAMP). GSIS in MIN6 cells maintained glucose response, with increases of 4.5 and 5.5-fold secretion of insulin, in response to 15 and 25 mM glucose in secretion buffer, respectfully (Fig. 4B). Notably, 9cRA treatment attenuated GSIS in MIN6 cells, as previously demonstrated in 832/13 cells (32).

9cRA synthesis is repressed by glucose and induced by *Rdh5* expression

9cRA concentration was measured in 832/13 cells using a model of glucose exposure conditions. The endogenous 9cRA concentration was reduced 22 percent in high (15 mM), relative to low (3 mM), glucose exposed cells for 28 hr (Fig. 5A). Synthesis of

9cRA from 9c-retinol substrate was reduced 46 percent in high, relative to low, glucose exposed cells, with both 20 nM and 250 nM 9c-retinol treatment. Synthetic ability in 832/13 cells was dose responsive to the retinol concentration, and was blunted by high glucose. To test the hypothesis that *Rdh5* catalyzes synthesis of 9cRA, *Rdh5* was overexpressed in 832/13 cells by transient transfection. Synthesis of 9c-retinal from 9c-retinol was increased 28% in cells transfected with *Rdh5* (Fig. 5B). Synthesis of 9cRA from 9c-retinol increased 16% in cells overexpressing *Rdh5* (Fig. 5C). *Rdh5* mRNA was elevated 20-fold in transfected cells after 28 hr (Fig. 5D).

Rdh5 expression is repressed by glucose and cAMP

In 832/13 cells, *Rdh5* mRNA expression is reduced 53% in high (15 mM), relative to low (3 mM), glucose exposure after 6 hr (Fig. 6A). Neither *Rdh10* nor *Rodh2* (rat orthologue of mouse *Rdh1*) were regulated by glucose in 832/13 cells under the same conditions. *Rdh5* expression was not responsive to insulin treatment in high or low glucose conditions after 16 hr (Fig. 6B). In MIN6 cells, *Rdh5* expression was reduced 23% in high (25 mM), relative to low (3 mM), glucose after 16 hours (Figure 6C). No change in *Rdh5* expression was detected in 6 hours (data not shown).

To address the mechanism regulating *Rdh5* mRNA expression, actinomycin D (ActD) was used to inhibit transcription. In cells pre-incubated in high glucose medium, to reduce *Rdh5* expression, ActD prevented the increase in *Rdh5* message observed in low glucose exposure (Fig. 7). This demonstrates that increased *Rdh5* mRNA in low glucose is result of new transcription. Treatment with ActD in high glucose medium did not affect *Rdh5* level within 6 hr, indicating that *Rdh5* mRNA is stable in high glucose condition.

Elevated cAMP potentiates GSIS in beta cells during re-feeding (135). Forced increase in cAMP, using phosphodiesterase inhibitor, IBMX, and adenylyl cyclase activator, Forskolin, reduced *Rdh5* expression in both low and high glucose conditions (Fig. 8A). Therefore, cAMP is sufficient to suppress *Rdh5* mRNA, and acts either downstream or in parallel with glucose regulation of *Rdh5* in 832/13 cells. The transcription factor *Crem* mRNA increased in conditions of high glucose and elevated cAMP, 3- and 15-fold, respectively, in 832/13 cells (Fig. 8B). Therefore, *Crem* is a candidate to mediate repression of *Rdh5* by glucose and cAMP.

The mitogen activated protein kinase (MAPK) pathway is activated downstream of glucose and cAMP in beta cells. Two inhibitors of MAPK pathway were used to block phosphorylation of ERK1/2 by MEK1/2, U0126 and PD98059. Both inhibitors blocked the increase in *Rdh5* message in low glucose condition, demonstrating that MEK/ERK signaling was required for transcription of *Rdh5* (Fig. 9). This finding is inconsistent with MAPK pathway activation by metabolic status; namely that MEK/ERK is activated in the fed state, in presence of glucose and growth factors, and inactive in the fasted state. While this data is reproducible in my hands, using two inhibitors, I cannot reconcile its meaning physiologically.

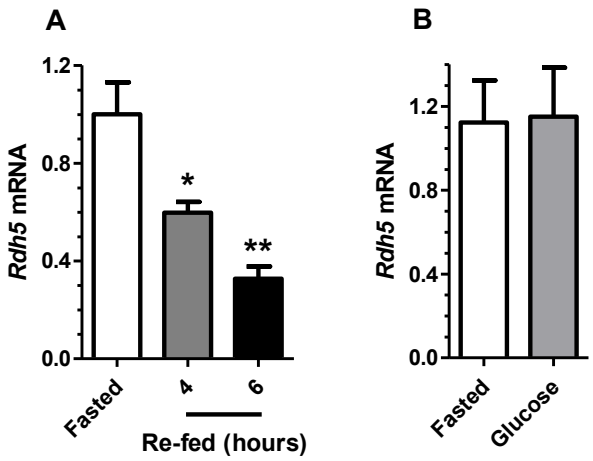

Figure 1. Pancreas *Rdh5* is reduced in re-fed vs fasted mice. (A) Mice were fasted 16 hr, or re-fed ad libitum for 4 and 6 hr following a 16 hr fast. Data includes two independent experiments with N = 5-7 mice per condition. (B) Mice were fasted 16 hr, or treated with i.p. glucose following a 16 hr fast, and collected 3 hr later. Data show a representative experiment of two experiments, N=7-9 per group. Data are means ± SE: **P* < 0.05, ***P* < 0.005

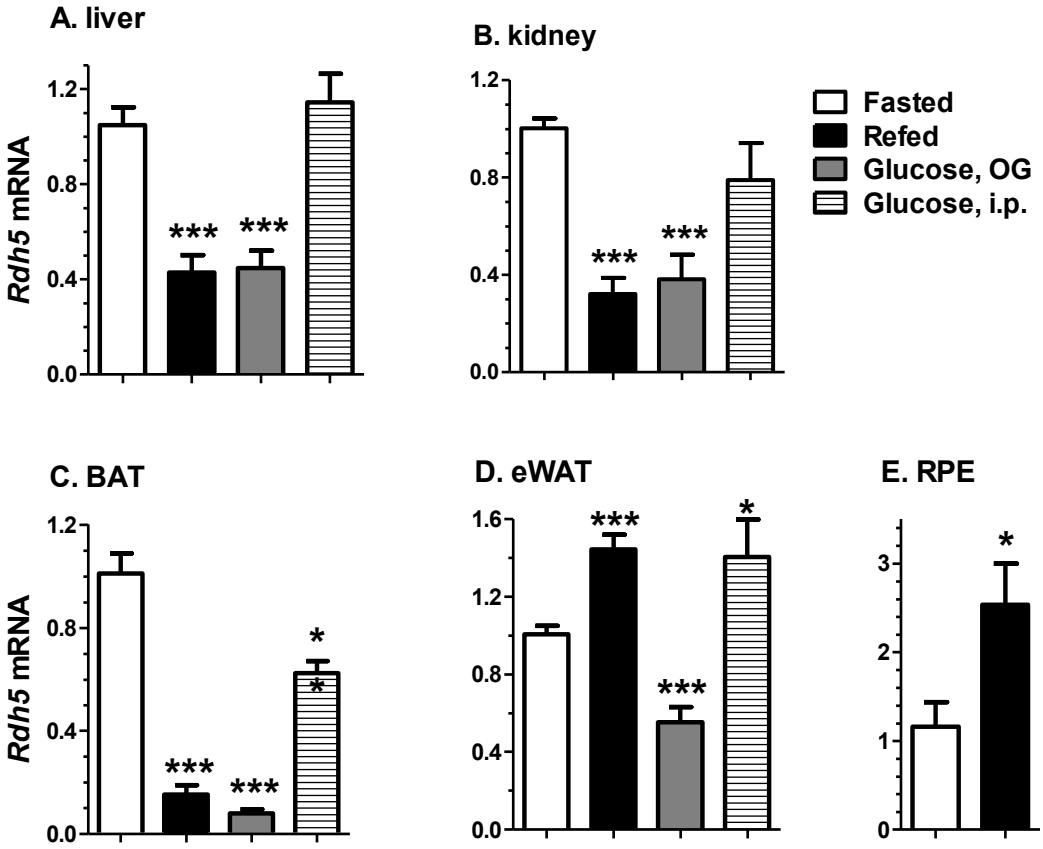

Figure 2. Metabolic regulation of *Rdh5* in multiple tissues. Mice were fasted 16 hr or treated for 6 hr following a 16 hr fast. Mice were re-fed ad libitum, treated with a single dose of 2 g/kg glucose by oral gavage, or treated with two i.p. injections of 2 g/kg glucose at times 0 and 45 min. Data show a representative experiment of 1-5 experiments, and are normalized to respective fasted group. Data are means ± SE: **P* < 0.05, ***P* < 0.005, ****P* < 0.001 vs fasted values.

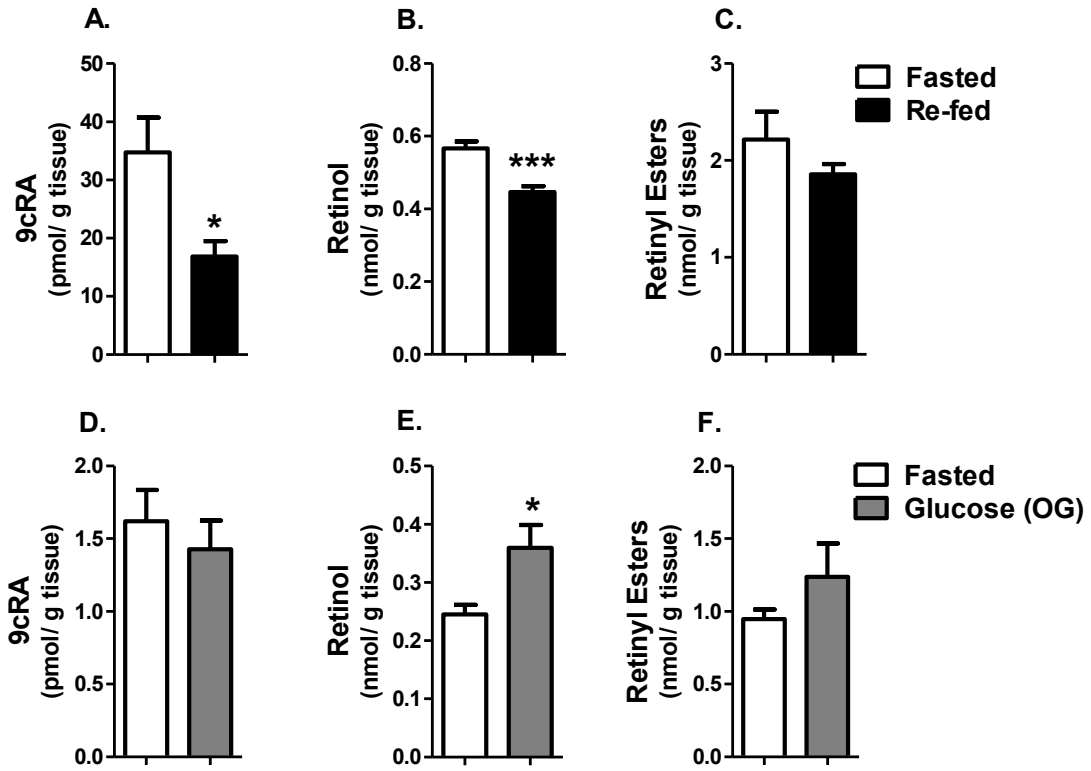

Figure 3. 9cRA in rat pancreas is reduced with re-feeding, but not by oral glucose. (A-C) Wild type Sprague Dawley rats were fasted 16 hr or fasted then re-fed 4 hr prior to tissue collection. 9cRA, retinol, and retinyl esters were quantified from pancreas tissue. (D-F) Rats were fasted 16 hr or fasted then treated with 2 g/kg glucose by oral gavage and collected after 15 min for quantification of 9cRA, retinol, and retinyl esters. N=6-7 animals per group. Data are means ± SE: **P* < 0.05, ****P* < 0.0005 vs fasted.

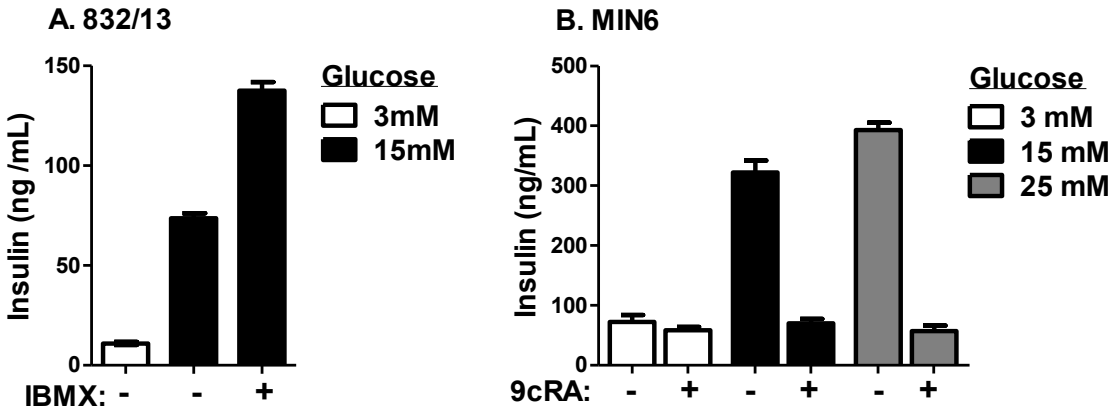

Figure 4. GSIS in beta cell models. (A) 832/13 cells were pre-incubated in HBSS containing 3 mM glucose for 2 hr, then treated with HBSS containing 3 mM or 15 mM glucose (-/+ 100 µM IBMX) for 2 hr. (B) MIN6 cells were pre-incubated in KRBB containing 3 mM glucose for 1 hr, then treated with 3, 15, or 25 mM glucose +/- 100 µM 9cRA for 1 hr. Insulin secreted into supernatent medium was quantified by ELISA assay.

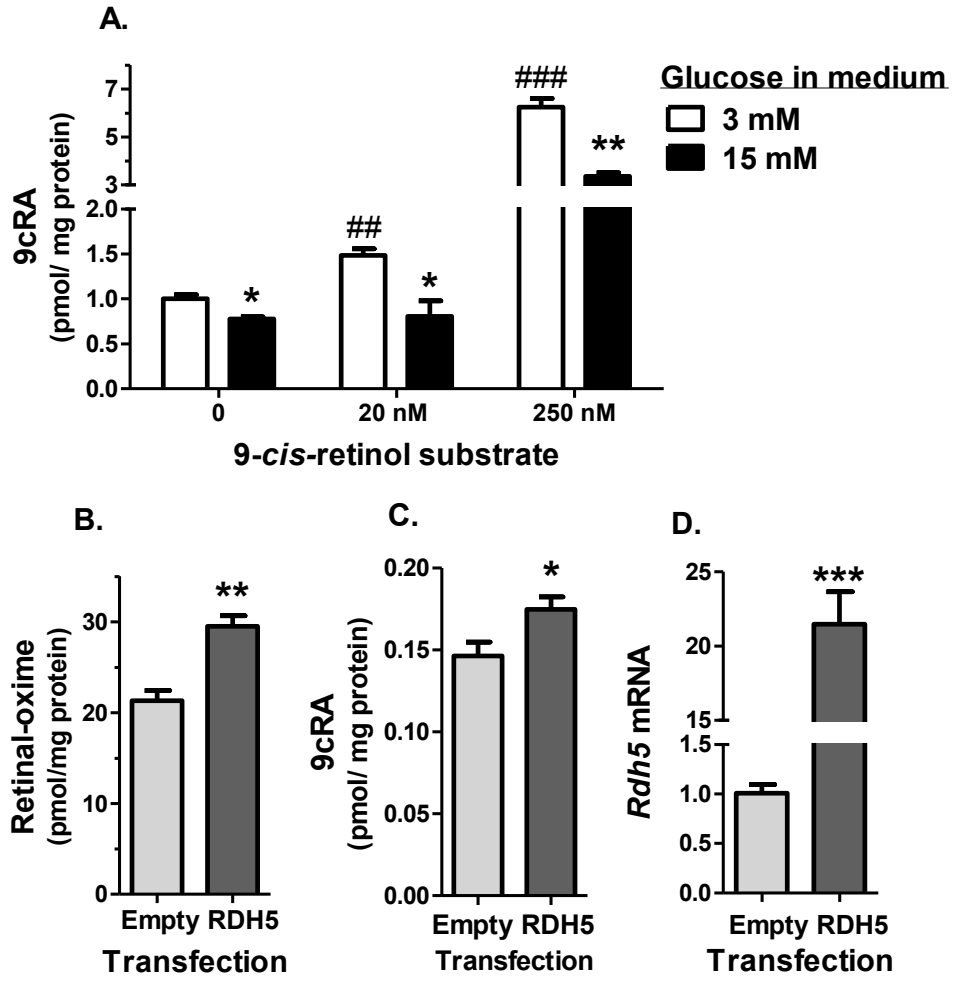

Figure 5. 9cRA biosynthesis is regulated by glucose and *Rdh5*. (A) 832/13 cells were treated for 24 hr with 3 mM or 15 mM glucose in medium containing no FBS, then 4 hr with fresh medium +/- 9-*cis*-retinol substrate. Data are combined from two experiments with n=3 each per group. (B) 832/13 cells were transfected with 10 ng pSG5 *Rdh5* vector, and treated for 24 hr in 3 mM glucose serum-free medium, then with 250 nM 9-*cis*-retinol in 3 mM serum-free medium for 4 hr. Retinal was quantified and normalized to cellular protein. (C) 832/13 cells were maintained in medium containing 11 mM glucose, and treated with 20 nM 9-*cis*-retinol for 4 hr. 9cRA was quantified and normalized to cell protein. (D) *Rdh5* expression in 832/13 cells transfected with 10 ng of pSG5 *Rdh5* vector after 28 hr in 3 mM serum-free medium. Data are means ± SE: **P* < 0.05, ***P* < 0.005 vs 3 mM glucose or empty transfection; $^{\#\#}P$ < 0.005, $^{\#\#\#}P$ < 0.0005 vs vehicle substrate.

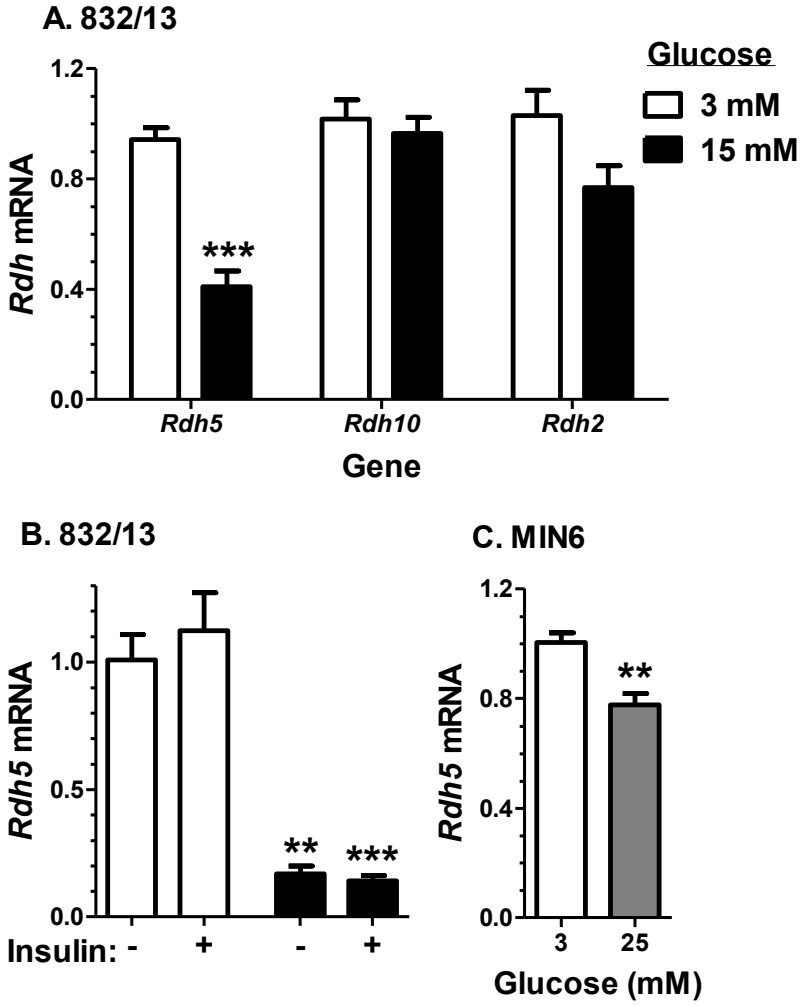

Figure 6. Glucose represses *Rdh5* mRNA in 832/13 and MIN6 cells. (A) 832/13 cells were treated in serum free medium containing 3 mM or 15 mM glucose for 6 hr. (B) Cells were treated in serum free medium containing 3 mM or 15 mM glucose, +/- 400 ng insulin for 16 hr. (C) MIN6 cells were treated in serum free medium containing 3 mM or 25 mM glucose for 16 hr. Data are means ± SE: $^{**}P < 0.005$, $^{***}P < 0.001$ vs 3 mM, untreated.

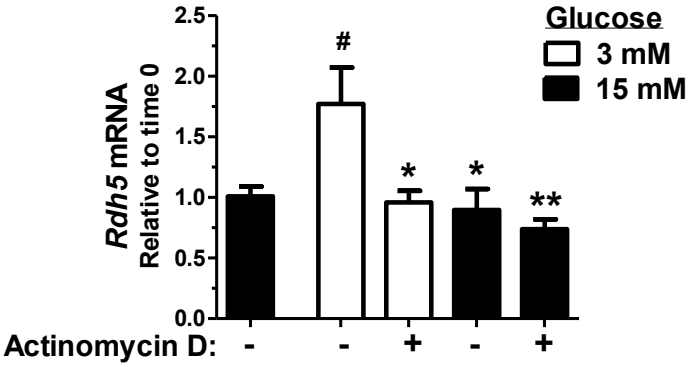

Figure 7. *Rdh5* transcription is activated in low glucose. Cells were pre-incubated overnight (16 hr) in 15 mM glucose medium (reference condition), then treated for 6 hr with 3 mM or 15 mM glucose medium, +/- 0.1 µg/mL ActD. Data shows one representative experiment of four experiments with n= 4-5 per condition. Data are mean ± SE: $^{\#}P < 0.05$ vs time 0; $^{*}P < 0.05$, $^{**}P < 0.005$ vs 3 mM, vehicle treated.

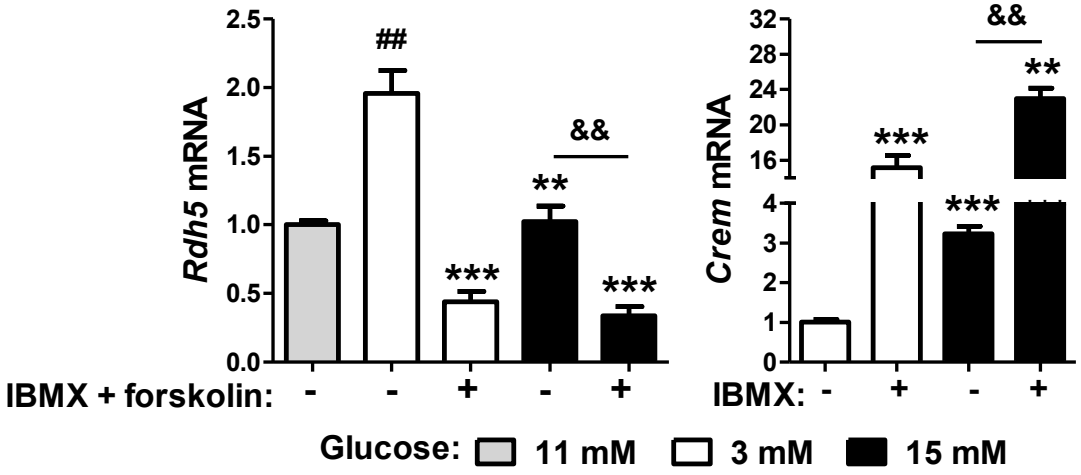

Figure 8. cAMP represses *Rdh5* expression. (A) Cells were treated for 6 hr with 11 mM, 3 mM, or 15 mM glucose in serum-free medium ± 100 μM IBMX and 10 μM forskolin. (B) Cells were treated for 6 hr with 3 mM or 15 mM glucose in serum free medium ± 100 μM IBMX. Data are means ± SE: $^{\#\#}P < 0.005$ vs 11 mM; $^{**}P < 0.005$, $^{***}P < 0.001$ vs 3 mM vehicle treated, $^{\&\&}P < 0.001$.

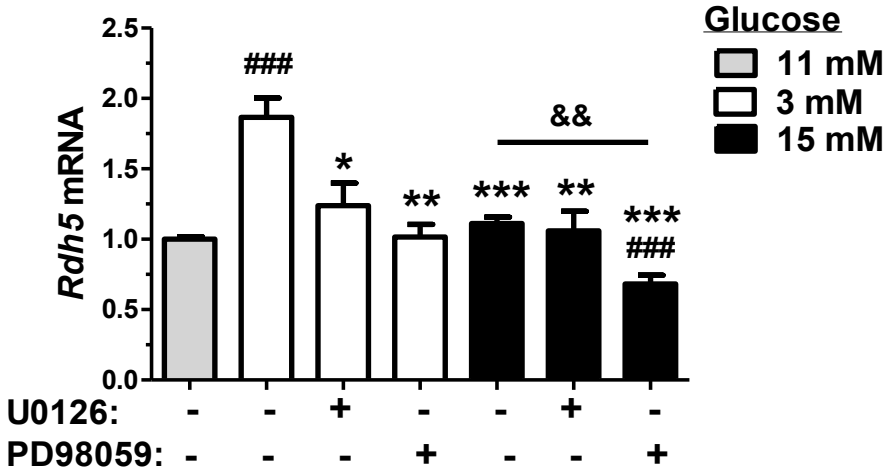

Figure 9. MAPK signaling is required for fasting induced increase in *Rdh5*. Cells were treated for 6 hr with 11 mM, 3 mM, or 15 mM glucose in serum-free medium ± 1 μM U0126 or 20 μM PD98059. Data is the average of 2 experiments, and is representative of three experiments. Data are means ± SE: $^{###}P < 0.001$ vs 11 mM, $^{*}P < 0.05$, $^{**}P < 0.005$, $^{***}P < 0.001$ vs 3 mM vehicle treated.

DISCUSSION

This project characterized regulated *Rdh5* expression in tissues and beta cells, and consequent 9c-retinal and 9cRA synthesis in beta cells. Reduced *Rdh5* mRNA in pancreas of re-fed versus fasted mice is consistent with reduced 9cRA in fed versus fasted mice (32) and rats (Fig. 3A), and focuses on reduced synthesis. Pancreas 9cRA reduced rapidly and transiently in oral gavage glucose treated mice (32), but not rats (Fig. 3B), and glucose treatment by i.p. injection did not affect pancreas *Rdh5* mRNA, while oral gavage glucose impact on pancreas was not tested. Related work on regulation of all-*trans Rdh*s identified glucose as relevant intermediate signal of feeding in *vivo* (Chapter 1, In review), and beta cells uniquely sense and respond to glucose during feeding (139). Differential regulation of *Rdh5* mRNA in most tissues (pancreas, liver, kidney, and brown adipose) versus retinal pigment epithelium supports alternate function to 11c-retinal production in the vision cycle. The function of regulated *Rdh5* expression in tissues lacking detectable 9cRA is intriguing and a subject of further investigation.

In 832/13 beta cells, glucose concentration in medium is sufficient to model 9cRA concentration and synthesis from 9c-retinol substrate. Furthermore, overexpression of *Rdh5* in 832/13 cells elevated 9c-retinal synthesis, independently of glucose. Retinal synthesis from retinol is a direct measure of *Rdh* activity, whereas RA synthesis may be impacted by activity of retinal dehydrogenases, retinal reductases and RA inactivating enzymes. The modest increase in 9c-retinal synthesis compared to 9cRA synthesis may be because retinal production is beyond the rate limiting step of RA synthesis and transient in RA production. Additionally, the modest impact of *Rdh5* overexpression on 9c-retinal synthesis may indicate that *Rdh5* is one of multiple enzymes that contribute to metabolically regulated 9cRA synthesis or stabilization.

Results for *Rdh5* mRNA expression implicate transcriptionally regulated repression downstream of glucose and/or cAMP. There are multiple possible mechanisms for how glucose may represses transcription of *Rdh5*. One hypothesis is based on chromatin immuno precipitation sequencing (ChIP-seq) data provided by the ENCyclopedia of DNA Elements (ENCODE) project, and available through UCSC Genome Browser (https://genome.ucsc.edu/). The transcription factor CCCTC-binding factor (CTCF) was identified to bind the *Rdh5* promoter region with a cluster score of 1000 out of 1000. This binding has been reported by a number of sources, using various model systems and three different antibodies. Intriguingly, a recent publication demonstrated that CTCF mediates glucose effects on beta cell survival, through repression of target gene *Pax6* (140). Regulation of *Pax6* expression by glucose is strikingly similar to that of *Rdh5*, and makes CTCF a candidate worth following up. Another hypothesis is that carbohydrate response element binding protein (ChREBP) may regulate transcriptional repression of *Rdh5*. ChREBP activity is regulated by cytoplasmic-nuclear shuttling in response to glucose environment. Binding proteins that sequester ChREBP in the cytoplasm are relieved by calcium influx that follows elevation in glucose uptake. In the nucleus, ChREBP binds to the carbohydrate response element in gene promoters to regulate transcription (141). In beta cells, ChREBP mediates

glucose activation of L-type pyruvate kinase (*L-pk*), acetyl-coA carboxylase (*Acc*) and fatty acid synthase (*Fas*), to regulate glycolysis and fatty acid synthesis (142). ChREBP represses *Pparα* and *Arnt/hif1b* expression to reduce fatty acid oxidation and insulin secretion, respectfully, during glucotoxicity (143, 144). A third hypothesis is that glucose may act through PI3K/AKT and FOXO1 pathway. This mechanism was reported to repress *Men1* expression in beta cells, in regulation of proliferation and tumor formation (145). The latter is intriguing since we have identified that all-*trans* Rdhs, *Rdh10* and *Rdh16* (human), are regulated by insulin via the PI3K-AKT-FOXO1 axis in hepatocytes. Of the three proposed transcription factor mediators, CTCF is a preferred mechanism to pursue since direct promoter binding has been established. Sufficiency, by overexpression, and necessity, by knock down, of this gene would be the next steps to demonstrate mechanism of transcriptional repression.

Elevation of cAMP independently reduces *Rdh5* expression in the 832/13 cell model. Furthermore, *Crem* expression is elevated by high glucose, and raised higher still by cAMP. *Crem* gene expresses multiple isoforms by differential promoter use and mRNA splicing, and the inducible cAMP early repressor (ICER) isoforms are transcriptionally activated by cAMP to repress expression of genes via the cAMP response element (CRE or C/EBP) (146). A transcription factor sequence prediction program, TFSearch (http://www.cbrc.jp/research/db/TFSEARCH.html) identified multiple CREs in the proximal promoter of *Rdh5*. Notably, the hypotheses of glucose and cAMP driving regulation are not mutually exclusive, and may act in coordination since both signals are elevated in beta cells during feeding. A microarray study designed to identify immediate early response and target genes actually designed the intervention with both elevated glucose and cAMP (137). Their results include *Rdh14* as a target gene, repressed 1.6 fold in beta cells 4 hr after glucose and cAMP stimulation. Interestingly, *Rdh14* is active with 9c-retinol substrate. Independent evidence of *Rdh* repression under similar conditions supports a general phenomenon of RA synthesis regulated by metabolism.

I addressed regulation of *Rdh5* by insulin in beta cells, since insulin self-regulates phase-one insulin secretion and impacts glucose tolerance (147). No change in *Rdh5* expression was measured after 16 hr of insulin treatment, while the magnitude of change in response to glucose increased with extended treatment. In 832/13 cells, the lack of detectable insulin regulation of *Rdh5* may be due to the duration of treatment. Clarification of insulin affect is interesting because of related findings that all-*trans*- Rdh gene expression is regulated by insulin in hepatocytes.

Beta cells are located in islets of the endocrine pancreas, and make up 70-80 percent of cells. *Rdh5* mRNA expression in islets was elevated in high (15 mM), relative to low (3 mM), glucose exposure (Fig. S1). Interpretation of these contrasting results from beta cells and pancreas tissue is perplexing, but may be due to the mixture of cell types in islets and pancreas. The specific cells expressing *Rdh5,* and relative expression levels are unknown. In *situ* hybridization or immuno-histochemistry would visualize cell-type specific localization of mRNA and protein, respectively, and validate a model of isolated beta cells or islets as more physiologically relevant to 9cRA synthesis. Additionally, islet results include 6 and 12-fold increases in *Rdh1* expression in high

glucose for 6 and 16 hr, respectively, whereas *Rdh2* (Rat ortholog of mouse *Rdh1*) expression was unchanged in 832/13 beta cell model with glucose exposure. *Rdh1* may be more highly expressed in other cell types, i.e. alpha- or delta- cells, of islets. RA synthesis assays would be an interesting follow up to evaluate if apparent conflict in mRNA expression between islets and beta cell associated with Rdh activity.

Cellular retinol binding protein I (RBP1) null mouse has dis-regulated glucose metabolism, with increased gluconeogenesis and fatty acid oxidation, and elevated 9cRA in pancreas tissue (54). RBP1 null mice do not have elevated *Rdh5* expression in pancreas, as would be expected for increased synthesis of 9cRA (Fig. S2). Rather, *Rdh5* is reduced in RBP1 null mice, relative to wild type, and maintains reduction in response to re-feeding relative to fasted expression. RBP1 null mice are hyperglycemic, and chronic elevated blood glucose seems to suppress *Rdh5* expression similarly to acute high glucose. *Rdh5* expression predicts that elevated pancreas 9cRA is consequence of reduced degradation or another mechanism independent of synthesis. Consistent with published data, *Rbp2* is elevated to compensate for loss of *Rbp1*, and furthermore, all retinol binding proteins (*Rbp1-3*) decrease in re-fed vs fasted pancreas.

Regulation of *Rdh5* presented here is first to identify metabolic impact on its expression and subsequent activity with 9-*cis*-retinol substrate. This work focuses on *Rdh5* regulation in the context of pancreas and beta cells to characterize synthesis of physiologically relevant 9cRA. Presentation of conserved regulation of *Rdh5* expression in tissues outside of pancreas draws attention to some outstanding questions: If 9cRA is only detected in pancreas, why is *Rdh5* expressed elsewhere? Does *Rdh5* act on substrates other than 9-*cis*- and 11-*cis*-retinol, in pancreas and retinal pigment epithelium, respectfully? These issues are larger than the scope of this work, but certainly influence the impact of findings in this chapter.

Supplemental data

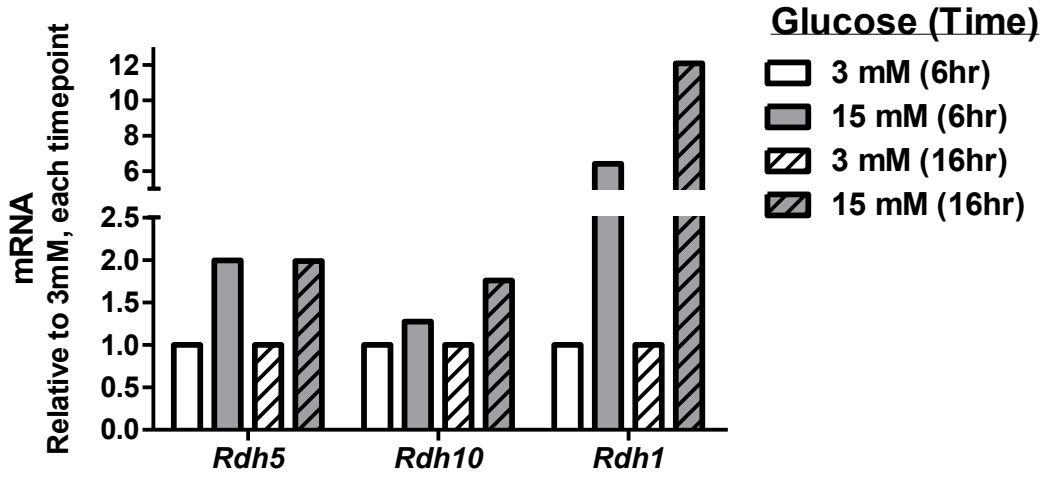

Figure S1. Glucose elevates *Rdh* mRNA in islets. Primary mouse islets were cultured overnight in 11 mM glucose medium, then treated for 6 hr or 16 hr with 3 mM or 15 mM glucose in serum free medium. Data show a representative experiment of two, n=1 well of approximately 50 islets per condition.

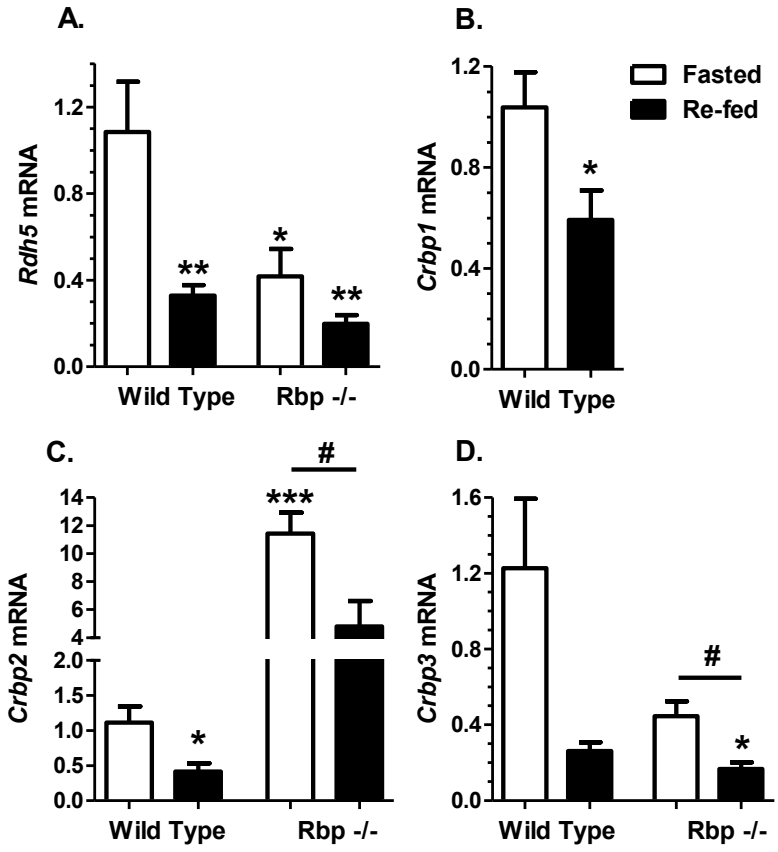

Figure S2. Pancreas gene expression in *Rbp -/-* mice. Mice were fasted 16 hr, or re-fed for 5.5 hr following a 16 hr fast. (A) *Rdh5* mRNA is reduced in fasted *Rbp-/-* vs WT mice, and decreased in re-fed vs fasted WT. (B) *Crbp1* mRNA is reduced in re-fed vs fasted WT mice, and undetectable in knock-out mice (data not shown). (C) *Crbp2* mRNA is elevated in *Rbp-/-*, and decreased in re-fed vs fasted for both genotypes. (D) *Crbp3* mRNA trends toward reduction in *Rbp-/-* vs WT mice and for re-fed vs fasted for both genotypes. Data are normalized to wild type fasted group for each gene, and expressed as fold change, n =3-5 per condition. Data are means ± SE: $^{*}P < 0.05$, $^{**}P < 0.005$, $^{***}P < 0.0005$ vs wild type fasted, $^{\#}P < 0.05$.

Chapter 3

Retinoid Metabolism and PPARδ Expression in Hypothalamus

INTRODUCTION

Retinoid metabolism is integral to energy balance regulation, and all-*trans*-retinoic acid (atRA) is protective against obesity and insulin resistance. Characterization of retinoid metabolism in hypothalamus addresses the possibility that atRA is involved in central nervous system (CNS) mediated energy balance regulation. atRA has been shown to inhibit proliferation of neural progenitor cells in hypothalamus (148). Photoperiodic regulation of genes in retinoid signaling implicate atRA in seasonal fluctuation of energy balance, including that of body weight in Syrian hamsters (149–151). Gene expression supports atRA biosynthesis and functionality in hypothalamus tissue. Mouse and rat hypothalamus express mRNA of retinoic acid receptors (*Rarα* and *Rarβ*), retinol binding protein (*Rbp1*), retinoic acid binding protein (*Crabp1*), and retinal dehydrogenases (*Raldh 1, 2,* and *3*) (152, 153).

The hypothalamus is a region located at the base of the brain, surrounding the third ventricle. It is a complex, integrative center for peripheral signals, and regulates a range of functions including reproduction, autonomic nervous system, immune response, sleep, thermoregulation, fluid homeostasis, food intake and energy expenditure. This brain region responds to peripheral signals including nutrients, hormones, and nervous system cues that are altered with feeding and energy status. The hypothalamus communicates with neighboring regions of the brain through synaptic connections and humoral signals to effect behavior and physiology. Within the hypothalamus, the arcuate nuclei region is at the base of the brain, and neurons have access to humoral signals in circulation that are restricted from other brain regions by the blood-brain barrier (154). Two neuronal populations in the arcuate nuclei respond to peripheral adiposity and satiety signals and act cooperatively to regulate energy balance. The orexigenic neuronal population is characterized by expression of neuropeptides agouti related peptide (AgRP) and neuropeptide Y (NPY), and express the inhibitory neurotransmitter γ-amino-butyric acid (GABA) (155). Orexigenic neurons are active in the absence of satiety signals, and function to increase food intake, reduce energy expenditure and increase body fat. A second population is anorexigenic neurons, which are characterized by expression of neuropeptide pro-opio melanocortin (POMC), and secrete the post translationally processed form, α-melanocyte-stimulating hormone (α-MSH) to regulate feeding behavior, and express excitatory neurotransmitter glutamate. Anorexigenic neurons are active in the presence of satiety signals, and

cause reduced food intake, increased energy expenditure, and reduced body fat. Anorexigenic neuron activity is inhibited by GABA and NPY secreted from active orexigenic neurons in the fasted state (156). Melanocortin receptors 3 and 4 (MC3R and MC4R) on neurons in the paraventricular nuclei and dorsomedial nuclei respond to ligand α-MSH in the fed state, and to endogenous antagonist, AgRP, in the fasted state.

Brain tissue consists of multiple cell types, including neurons and glia. Glial cells provide nutrients and support to neurons. Astrocytes are one type of glial cell, that biosynthesizes atRA in culture after addition of exogenous retinol (157). AtRA is secreted into the media, rather than accumulating in astrocytes, consistent with function of glial cells to nurture neurons. Additionally, pretreatment with atRA causes astrocytes to accumulate retinyl esters, the storage form of vitamin A, after retinol treatment. Thus, atRA auto-regulates its metabolism in astrocytes to maintain function in adult brain.

atRA regulates transcription of target genes by binding RARs and peroxisome proliferator-activated receptor delta (PPARδ) (34, 158). Both RARs and PPARs heterodimerize with retinoid X receptors (RXRs), to generate an array of combinatorial receptor mediated transcriptional response that differs spatially and temporally by recruitment of co-activators and co-repressors (159). Retinoid binding proteins control retinoid metabolism by chaperoning, and thus limiting access, to specific enzymes and receptors (17). atRA is escorted by CRABP2 and fatty acid binding protein 5 (FABP5) to RARα and PPARδ, respectfully, to elicit ligand mediated transcriptional regulation. The relative abundance of CRABP2 and FABP5 determines binding to atRA for nuclear delivery to cognate receptors, as exemplified by opposing functions on cell growth and survival (35).

Recent developments elucidate non-genomic effects of atRA via RARs to rapidly activate mitogen-activated protein kinase (MAPK) pathways and initiate translation (29, 160). Consistent with non-genomic functions, RARs are reportedly located in cytosol and plasma membranes. In hippocampal neurons, membrane-associated RARα is internalized by atRA ligand, rapidly activates mitogen activated protein kinase (MAPK) and mammalian target of rapamycin (mTOR) signaling, and relieves suppression of targeted mRNAs (36, 161). Subsequent translation of glutamate receptor 1 (*GluR1*) facilitates spine formation and synaptic plasticity, leading to enhanced memory formation in hippocampus. Non-genomic function of PPARδ has been reported in non-nucleated platelets, to rapidly and acutely inhibit platelet aggregation via binding PCKα (162, 163). Together, these examples illustrate non-genomic functions of RARs and PPARδ.

PPAR isoforms (α, γ, and δ) function primarily as lipid sensors, to regulate transcriptional response for storage and metabolism of dietary lipid intake (164). The

roles of PPARδ in metabolic regulation, and its activation by atRA ligand, make it an intriguing candidate to mediate atRA function in hypothalamus. Genetic models of manipulated PPARδ expression conclude that it increases fatty acid oxidation in white adipose and thermogenesis in brown adipose, increases energy expenditure in muscle, and improves insulin sensitivity (165–167). PPARδ is a key metabolic regulator of energy expenditure in peripheral tissues, and its expression is enriched in brain (168). Expression of PPARδ in brain has been evaluated by a few groups. Quantitative western blot of whole brain fractions detected PPARδ in nuclear, but not in cytoplasmic fractions (169). Immuno-localization in adult rat CNS detected PPARδ at moderate levels in multiple nuclei of hypothalamus region (170). By tissue microarray based immunohistochemistry, PPARδ was detected at moderate level in the nucleus, cytoplasm, and neurites of mouse hypothalamus neurons (171). At the time of this research project, little was published about PPARδ function in brain. Consistent with its role in lipid metabolism, acyl-CoA synthetase 2 was identified as a transcriptional target in rat brain cell cultures, utilizing a synthetic agonist (172), and PPARδ in brain reportedly contributed to inflammatory and oxidative damage responses (168). To date, nothing is known about function of PPARδ specifically in hypothalamus.

Leptin is a 16 kDa protein synthesized and secreted from adipose tissue in proportion to adiposity and in response to food intake or insulin. Extensive work on ob/ob (leptin deficient) mice, and db/db (leptin receptor deficient) mice, has established leptin as a satiety signal that contributes to energy balance. Circulating leptin levels vary diurnally in rodents, and are highest during the night after the largest food intake (173). Fasting prevents cyclic variation of leptin, and ob mRNA is restored in adipose tissue within four hr after re-feeding a fasted animal. Functional response to leptin requires activity of phosphoinositide 3-kinase (PI3K) and mTOR (174, 175). Neurons in arcuate nuclei of hypothalamus express long chain leptin receptors (LRbs), and respond sensitively to circulating leptin because of contact with blood circulation through the median eminence (154). Leptin imposes opposite regulation on anorexigenic and orexigenic neuron function to centrally influence energy balance. Leptin activates anorexigenic neurons by increasing transcription of POMC (176), depolarizing neurons causing them to fire, reducing GABA mediated inhibition, releasing the excitatory neurotransmitter glutamate, and causing secretion of neuropeptide α-MSH (156). Leptin inhibits orexigenic neuron activity by inhibiting transcription of NPY (176), hyperpolarizing neurons, and preventing secretion of neuropeptides (177) and neurotransmitters (174). In the absence of leptin, orexigenic neurons are active, and secrete the inhibitory neurotransmitter GABA and neuropeptides AgRP and NPY. GABA and NPY are received by receptors on neighboring anorexigenic neurons to inhibit their activity, while AgRP is received by MC3R and MC4R to repress signals of satiety. Activity of AgRP and NPY expressing neurons respond more than POMC expressing

neurons to acute changes in energy status (178). This is consistent with regulation of food intake by the central nervous system protecting from starvation rather than obesity. Behavioral and protein expression data in rats identified that anorectic effects of leptin in arcuate neurons require active signaling through mTOR. Administration of mTOR inhibitor, rapamycin, attenuates food intake and body weight changes induced by leptin treatment (175).

mTOR is a well conserved serine/threonine protein kinase. It is a component of two differentially regulated protein complexes, mTORC1 and mTORC2. TORC1 has been studied more extensively, and is uniquely inhibited by rapamycin. As a component of the heteromeric TORC1 complex, mTOR is activated by signals of nutritional and energy sufficiency. Activators include hormones such as leptin and insulin, and amino acids, specifically the branched chain amino acid leucine. mTOR activity is inhibited by low energy status, communicated by AMP-kinase (AMPK). Pathways of signal activation upstream of mTOR include PI3K through protein kinase B (Akt/PKB), and extracellular-regulated kinase (ERK1/2). Active mTOR signaling regulates general mRNA translation through phosphorylation of target proteins eukaryotic initiation factor 4E binding protein (eIF4E-BP) and ribosomal protein S6 kinase (p70S6K). Local dendritic translation in neurons occurs independently of general cellular translation, and is regulated by mTOR kinase and ERK1/2 (36, 179). mTOR is ubiquitously expressed in brain, but phosphorylated mTOR decreases in response to fasting, specifically in arcuate nuclei (175).

This project aimed to identify a function of atRA in hypothalamus neurons related to central regulation of energy balance. Identification of translational regulation by atRA via mTOR in hippocampus neurons, together with leptin signal requiring mTOR in hypothalamus, prompted a hypothesis of intersected activity between atRA and leptin, to regulate local protein translation or secretion of neuropeptides in feeding behavior. I further hypothesized that such a non-genomic function of atRA would be mediated by extra-nuclear expression of an atRA receptor, and focused on PPARδ because of its extensive role in energy regulation.

MATERIALS and METHODS

Animals

Wild type C57Bl/6 mice (Jackson lab, or bred in house) or Sprague Dawley rats (Charles River), age 2-3 mos unless otherwise noted, were used. Mice were fed semi-purified AIN93G diet (Dyets #110700), or High Fat diet containing 50% FDC (Dyets #180614), with the exception of pregnant dams for primary neuron culture, which were fed standard rodent chow diet (Harlan Teklad #2018). Rats were fed standard rodent chow (Harlan Teklad #2018). Animals were fed ad-libitum, unless noted for fasting and re-feeding experiments. The cold tolerance test was done during the final 6 hr of a 16 hr fast, and mice were either kept at normal housing temperature (21° C), or exposed to 4°C. Core body temperatures were measured rectally using a probe (Physitemp RET-3) attached to a digital thermometer (Physitemp BAT-12). Institutional guidelines required mice to be removed from study if body temperature fell below 28°C.

Hypothalamus tissue explant

Dissection of hypothalamus tissue was performed as two coronal cuts, anteriorly at the optic chiasma and posteriorly at the mammillary bodies, then parasagital cuts along the hypothalamic sulci and a dorsal cut at a depth of 2 mm from the ventral surface of the brain (180). Fresh hypothalamus tissue explants were used directly for gene expression and retinoid quantification, or cultured for neuropeptide secretion assay. For neuropeptide secretion assay, explants were equilibrated (1 hr) in artificial cerebral spinal fluid (aCSF), incubated for basal period (45 min) in fresh aCSF, treated (45 min) with atRA (Sigma R2625), recombinant mouse leptin (R&D Systems #498-OB), or vehicle DMSO, then depolarized (45 min) with 56 mM KCl, and supernatant was collected for analysis. aCSF was made of 126 mM NaCl, 6 mM KCl, 1.4 mM CaCl, 20 mM $NaHCO_3$, 5 mM glucose, 0.09 mM Na_2HPO_4, 0.09 mM $MgSO_4$, and 0.6 TIU/mL aprotinin. AgRP secreted from rat hypothalamus was detected by ELISA (Phoenix Pharmaceuticals #EK-003-57), and normalized to protein in tissue explant.

Primary neuron culture

Neurons were dissected from E17–18 C57/Bl6 mouse embryos. Hypothalamus was dissected in HBSS with 10 mM HEPES, 1 mM Na Pyruvate and 1% Pen/Strep (Invitrogen). Tissues were pooled and mechanically dispersed with flamed glass pipette tip, then seeded on plates or glass cover slips pre-coated with poly-D-Lysine (BD BioCoat). Neurons were plated in 24-well (1×10^5 cells/well) or 6-well (5×10^5 cells/well) plates, in Neurobasal medium with 25 µM glutamic acid, 0.5 mM glutamine and 2% B-27 (Invitrogen). Four hr after plating, 80% volume of medium was replaced with Neurobasal medium (Invitrogen) with 2% B27 supplement (Invitrogen). After 48 hr in

culture, 2 μM cytosine β-D arabinofuranoside (AraC) (Sigma) was added to prevent glial cell proliferation. Half of the medium volume was replenished every four days. Primary neurons were considered mature and used after 11 days in culture (DIC) (181). Neurons were treated with 1 μM atRA or GW501516 (Sigma).

Tissue fractionation

Sub cellular fractionation of total brain tissue was done as described (182), and outlined in schematic (Figure 11A). Western blot performed with primary antibody PPARδ (Pierce PA1-823A), and secondary antibody LI-COR IR Dye (800CW #926-32211).

RNA isolation and RT-PCR

RNA was isolated by Trizol protocol (Life Technologies), or RNAqueous Micro kit (Ambion #1931). cDNA synthesis with Superscript II reverse transcriptase (Invitrogen). PCR with thermocycler program 94°C 2 min (pre-denature), cycles: 94°C 30 sec (denature), 61°C 30 sec (annealing), 72°C 1 min (extension), 72°C 5 min (extension/stability). PCR primers were designed using primer-BLAST (http://www.ncbi.nlm.nih.gov/tools/primer-blast).

Retinoid quantification and atRA synthesis

Retinoids were extracted from hypothalamus tissue, with 2-3 pooled per sample from mice, or single tissues from rats. Tissues were collected under yellow light and frozen immediately in liquid nitrogen. On the day of analysis, tissues were weighed, thawed on ice, and hand homogenized in cold 0.9% saline. Protein was quantified by Bradford assay (Sigma). Retinoids were recovered by a two-step acid and base extraction (80). All materials in contact with samples were glass or stainless steel. Internal standards were used to calculate extraction efficiency of retinoids. Retinol and retinyl esters were extracted and quantified by HPLC/UV, with 3,4-didehydro retinol as internal standard (82). atRA was extracted and quantified by LC/MS/MS, with 4,4-dimethyl retinoic acid as internal standard (81). For atRA synthesis assay, hypothalamus tissue explants were treated with 0.5 μM all-*trans*-retinol (Sigma) for 2 hr. atRA and RE were normalized to mg tissue protein and expressed as rate of synthesis.

Immunofluorescent staining

Brains were cut coronally, and immediately frozen in isopentane (2-methyl butane) chilled over dry ice, then stored in -80 until sectioning. 10 μm cryosections were mounted on glass slides (Fisher Superfrost Plus), fixed in 4% PFA + 4% sucrose for 1 hr at 4°C. Sections were then washed in PBS, permeabilized in PBS with 0.2% Triton-x-100 for 10 min, then blocked in 10% serum, either overnight at 4°C or for 2 hr at room temperature. Primary antibodies were incubated overnight in 5% serum at 4°C: PPARδ

(Affinity Bioreagents PA1-823A), RARα (Abcam 28767), FABP5 (Santa Cruz 16060), NeuN (Abcam 104225), Smi-312 (Abcam 24574), MAP2 (Abcam 5392), GFAP (Millipore 3402). Secondary fluorescent antibodies Alexa 488 and Alexa 555 (Invitrogen) were incubated in 5% serum for 1 hr at room temperature. Coverslips were mounted with Vectashield medium containing DAPI (Vector Labs). Immunofluorescence of primary neurons was done similarly, except fresh neurons were directly fixed, and never frozen. Slides were kept in a moist chamber during immunofluorescence protocol. Confocal microscope images were obtained with a LSM510 Meta confocal microscope in the College of Natural Resources BioImaging facility.

Statistics

Data are presented as means ± standard errors (SE) and were analyzed using two-tailed, unpaired Student's *t* tests.

RESULTS

Retinoids in hypothalamus tissue

Retinoid concentrations were quantified in the hypothalamus of ad-libitum fed mice, and compared to those in olfactory bulb, cerebellum, cortex and hippocampus. atRA in hypothalamus tissue is higher than other regions tested (Fig. 1A). Retinol in hypothalamus is higher than cerebellum and cortex, and similar to olfactory bulb and hippocampus (Fig. 1B). Retinyl esters in hypothalamus are significantly higher than all other brain regions tested (Fig. 1C). These data are consistent with regionally distinct concentrations of atRA in adult mouse brain, as was previously reported, in absence of hypothalamus tissue (81). Ability to detect and quantify atRA from hypothalamus tissue was critical to pursue a functional study.

Hypothalamus atRA was quantified in response to energy status interventions by three models. In an acute model of altered feeding, mice were fasted overnight, or fasted then re-fed for 2 hr ad-libitum, or fed continuously ad-libitum. Hypothalamus atRA concentration was not different between the three feeding conditions (Fig. 2A). Retinol and retinyl esters were also unaffected (Fig. 2B, C). In a chronic model of altered feeding, mice were fed control diet (semi-purified, low fat: LFD), or high fat diet (HFD) for 6 weeks. Hypothalamus atRA, retinol and retinyl esters were unchanged between LFD and HFD fed mice (Fig. 2D-F). In a third adaptation to energy status, we performed a cold tolerance test on wild type mice. Mice were fasted for 16 hr, and exposed to cold temperature (4°C), or room temperature control (21°C) during the final six hr. Hypothalamus atRA and retinol trended down, insignificantly, in cold exposed mice, and retinyl esters were reduced by 40 percent (Fig. 3A-C). Retinyl ester values may be interpreted as mobilization of stores to maintain retinol and atRA levels from dropping significantly during cold challenge. Together, unchanged atRA values in acutely altered feeding and cold exposure, support highly regulated and consistently maintained concentration in hypothalamus tissue.

atRA synthesis in hypothalamus

Expression of genes regulating atRA synthesis, binding proteins and receptors were measured in hypothalamus tissue explants and mature primary cultured neurons from embryonic hypothalamus. Multiple isoforms of retinol dehydrogenase (*Rdh)* genes were expressed (Fig. 4A). Both tissue and primary neurons expressed *Rdh10* and *RetSDR8* (*Dhrs9*), only tissue expressed *17βHSD9*, and neither expressed *Rdh1* at detectable levels. *17βHSD9* expression in tissue, but not in primary neurons, suggests it may be expressed in other cell types such as glial cells. *Raldh1*, *2*, and *3* genes are

expressed in tissue, and were not measured in neurons (Fig. 4B). Expression of both *Rdh* and *Raldh* genes supports that local synthesis of atRA from retinol is possible in hypothalamus tissue, and specifically in neurons. Retinoic acid receptors *Rarα*, *Rarβ*, and *Rarγ*, as well as *Pparδ* are expressed in tissue and primary neurons (Fig. 4C). Receptor expression indicates that local response to atRA is functional in hypothalamus. Retinoid binding proteins, cellular retinol binding protein 1 (*Rbp1*), *Crabp2*, and *Fabp5* are all expressed in tissue and primary neurons (Fig. 4D). Expression of beta actin (*Actb*), as loading control, and neuropeptides *Agrp* and *Pomc*, are included as positive controls for hypothalamus neurons. Expression of *Fapb5* and *Pparδ* are higher than *Crabp2* and *Rarα*, respectfully, and predict that atRA may preferentially function through *Pparδ* in hypothalamus.

atRA synthesis *in situ*-, was confirmed in tissue explants of isolated hypothalamus, free from surrounding brain tissue. The rate of atRA synthesis was increased 17-fold in response to 0.5 μM retinol substrate (Fig. 5A). Elevated retinol in treated explant tissue confirms successful uptake (Fig. 5B). Retinyl ester synthesis trends toward an increase in retinol treated samples, but is insignificant (Fig. 5C). Thus, hypothalamus efficiently and preferentially synthesizes atRA from retinol.

PPARδ localization

Imaging of PPARδ and marker proteins in brain sections focused on the arcuate nuclei of hypothalamus. PPARδ is visible in neuronal cell nuclei as demonstrated by overlay with the Neuronal Nuclei (NeuN) marker protein and DAPI (Fig. 6) (183). There is additional PPARδ signal outside of nuclei, which appears as fibrous structures. Visualization of PPARδ with axon marker, Smi312, identified co-localization of PPARδ in neuronal axons (Fig. 7). An axon is the elongated nerve fiber that transmits impulses away from the neuron soma, to be released from a synapse at the axon terminal. PPARδ does not co-localize with dendrite marker, MAP2 (Fig. 8). This image provides contrast of signals, and offers a clear view of PPARδ location in neurons and axons, but not in dendrites. Finally, visualization of PPARδ with astrocyte marker, GFAP, shows no co-localization (Fig. 9A). Notably, PPARδ location in axons was observed in multiple regions of coronal brain sections, including hippocampus (Fig. 9B). Together, imaging data identifies PPARδ location in both neuronal nuclei, consistent with transcriptional activity, and in neuronal axons, which is indicative of non-genomic function.

Immunofluorescent imaging of RARα with neuronal nuclei marker, NeuN, shows co-localization in hypothalamus neurons (Fig. 10). RARα signal is most intense in nucleus and soma, but also visible in a few fibrous structures. Extensive co-localization with other cell markers was not performed for RARα to identify location of signals.

An alternate approach to measure localization of protein is by sub-cellular fractionation and western blot detection. The schematic of brain tissue fractionation protocol was adapted from Current Protocols in Neuroscience (Fig. 11A) (182). PPARδ expression was detectable in the crude synaptosomal membrane fraction (P2), and enriched in synaptosomal membranes (LP1) after further fractionation (Fig. 11B). Majority of PPARδ was detected in cytoplasm (S2), while none is detected in nucleus (P1). This contradicts immunofluorescent detection of PPARδ co-localized with NeuN and DAPI markers. However, detection in synaptosomal membrane fraction is consistent with axon localization by immunofluorescence imaging.

A change in PPARδ receptor localization or intensity may mediate a functional response to shifted energy status in hypothalamus. Immunofluoresence of PPARδ in hypothalamus from mice that were fed ad-libitum, fasted overnight, or re-fed for 4 hr following an overnight fast, shows a qualitative change. Based on visual evaluation, there appears to be a decrease in PPARδ in axons of fasted, relative to both fed (ad-libidum and re-fed) conditions (Fig. 12). Additional experiments are required to conclude differential expression of PPARδ according to energy status, including immunofluorescence with axon marker, Smi312, and quantitative measure of PPARδ protein in cell fractions by western blot.

Transcriptional activity of atRA in hypothalamus

Transcriptional activation was evaluated by expression of RARα and PPARδ target genes in response to treatment with atRA and PPARδ agonist, GW501516 (GW), in primary cultured neurons. atRA increased expression of RARα target genes, *Cyp26a1* and *Cyp26b1*, as shown in gel images (Fig. 13A) and quantified by densitometry (Fig. 13B). In contrast, none of the three PPARδ target genes measured were changed in response to atRA treatment. GW treatment increased expression of PPARδ target gene, angiopoietin-like 4 (*Angptl4)*, and none of the RAR target genes, as expected.

PPARδ and FABP5 were visualized in primary cultured neurons by immunofluorescence after 30 minute treatment with vehicle or atRA. Confocal microscope z-stack “slices” through the neuron allowed discrimination of views inside and outside of the nucleus. PPARδ was visible inside the nucleus of atRA treated cells, but FABP5 was not (Figure 14). Notably, PPARδ was observed in processes of primary cultured neurons.

Neuropeptide secretion

In a hypothalamus explant model, AgRP secretion was reduced in a dose responsive manner to leptin treatment (Fig. 15). Physiologically, leptin reduces the

orexigenic signal and feeding behavior during an energy sufficient state. Treatment with atRA alone had no effect on AgRP secretion, but attenuated the effect of leptin. Efforts to measure secretion of POMC and αMSH from functionally opposing neurons were unsuccessful, due to detection limits of radio-immuno assays and viability of the explant model.

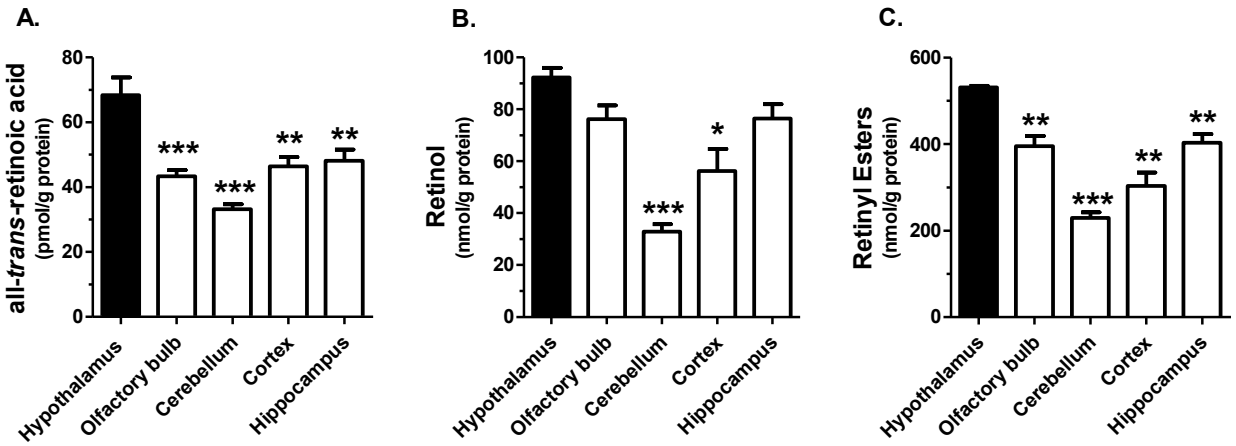

Figure 1. Retinoids in hypothalamus and brain regions. (A) atRA, (B) retinol, and (C) retinyl esters were quantified from brain regions of mice fed AIN93G diet, ad-libitum. N=12 mice, hypothalamus tissues pooled 3 per sample for n=4. Data are means ± SE: **P* < 0.05, ***P* < 0.005, ****P* < 0.0005 vs hypothalamus.

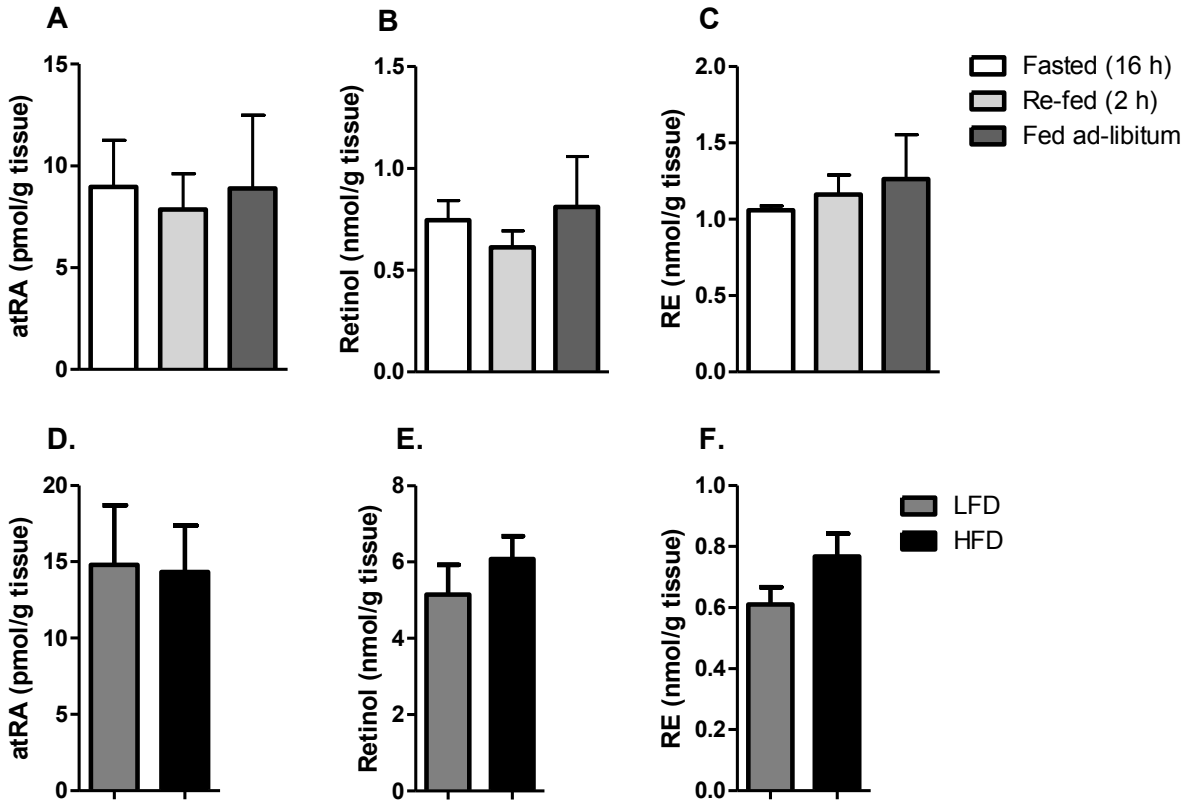

Figure 2. Hypothalamus retinoids are unchanged with dietary alteration. (A-C) Mice were fasted overnight, fasted then re-fed for 2 hr, or fed ad-libitum, and hypothalamus tissue collected for quantification of atRA, retinol, and retinyl esters. Mice were wild type males, age 2 months, fed AIN93G diet. N=4, 4, and 3 for fasted, re-fed, and fed ad-libitum groups, respectfully, with 2 hypothalamus tissues pooled per sample. (D-F) Mice were fed LFD (continued AIN93G) or HFD for 6 weeks, ad-libitum, and hypothalamus tissue collected for quantification of atRA, retinol, and retinyl esters. Mice were wild type males, age 6 months. N=10 per condition, with 2 hypothalamus tissues pooled per sample. Data are representative of three independent experiments.

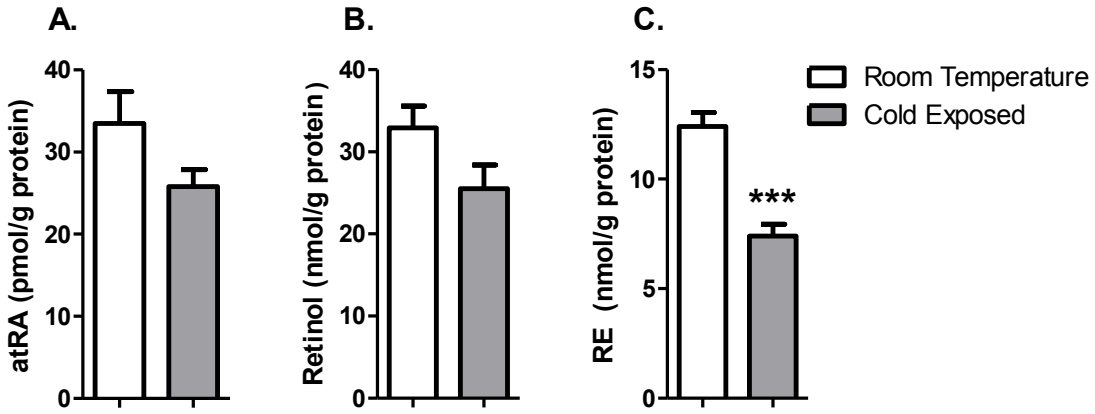

Figure 3. Hypothalamus retinoids during a cold tolerance test. Mice were fasted a total of 16 hr, and during the final 6 hr kept either at ambient temperature (21° C), or exposed to 4° C. Mice were wild type males, age 2-2.5 months, fed AIN93G diet. N=14 mice per condition with 2 hypothalamus tissues pooled per sample. Data are means ± SE: *** $P < 0.0001$

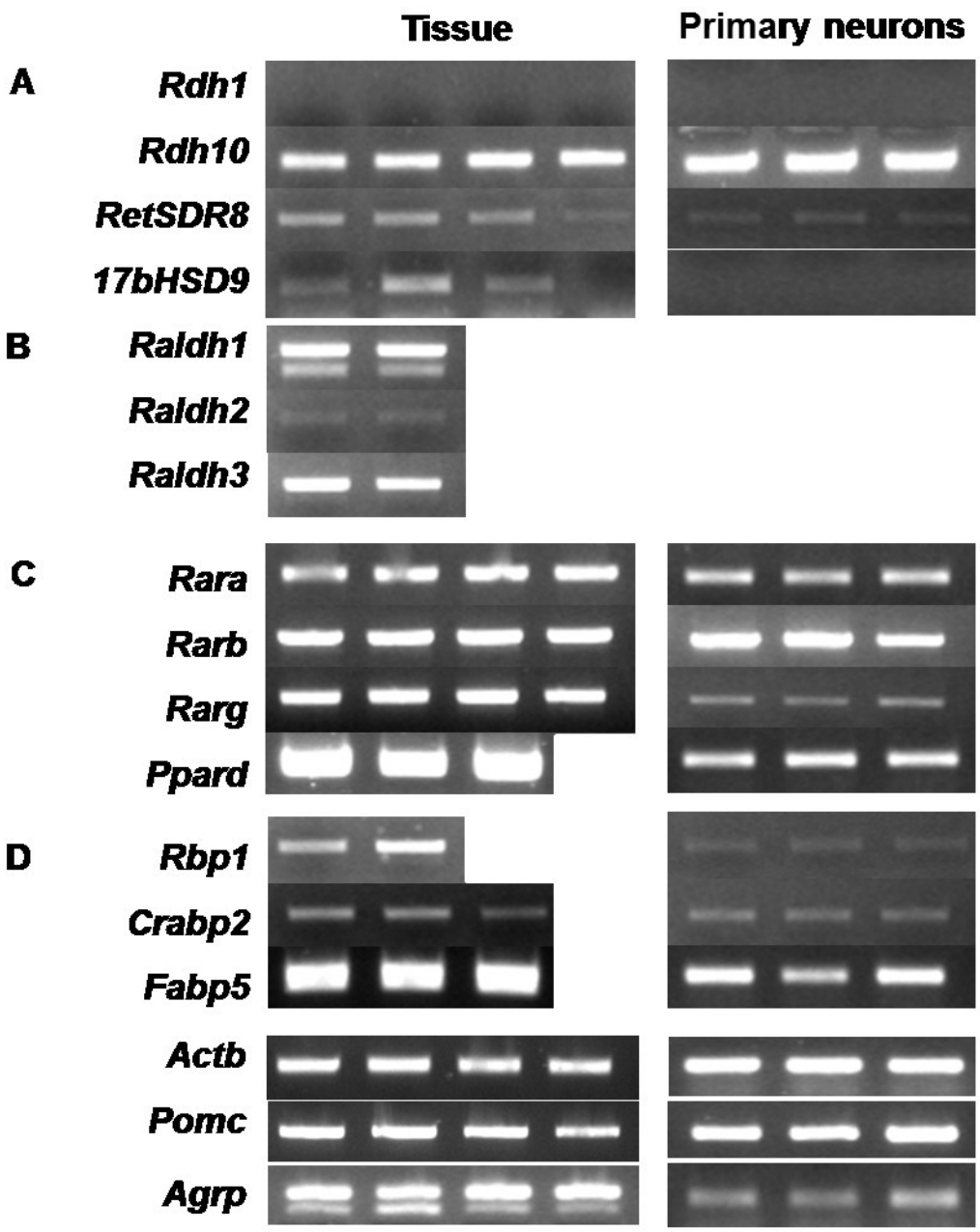

Figure 4. Expression of retinoid metabolism genes in hypothalamus. Gene expression was measured by RT-PCR from adult mouse hypothalamus tissue (left column) and mature primary hypothalamus neurons in culture (right column). Relative expression of genes (A) *Rdh*, (B) *Raldh*, (C) *Rar*, and (D) retinoid binding proteins (*Rbps*), are shown as bands on gels. PCR reactions were run for 35 cycles, with the following exceptions: from tissue samples *Actb*, *Pomc* (25); from primary neurons *Actb* (25), *Rdh10*, *Rbp1*, *Rarα*, *Pparδ*, *Fabp5* (30). Note *RetSDR8* is *Drhs9*.

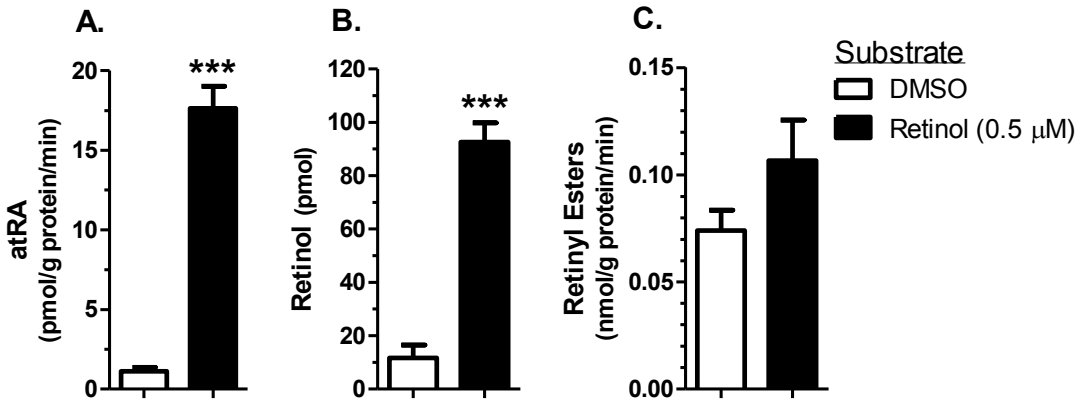

Figure 5. In *situ* atRA synthesis. Hypothalamus tissue explants were collected and treated with 0.5 μM retinol for 2 hr. (A) Rate of atRA synthesis. (B) Retinol recovered in tissue explants. (C) Rate of retinyl esters synthesis. N=8 explants per condition, treated in independent wells. Data are means ± SE: ***p<.0001

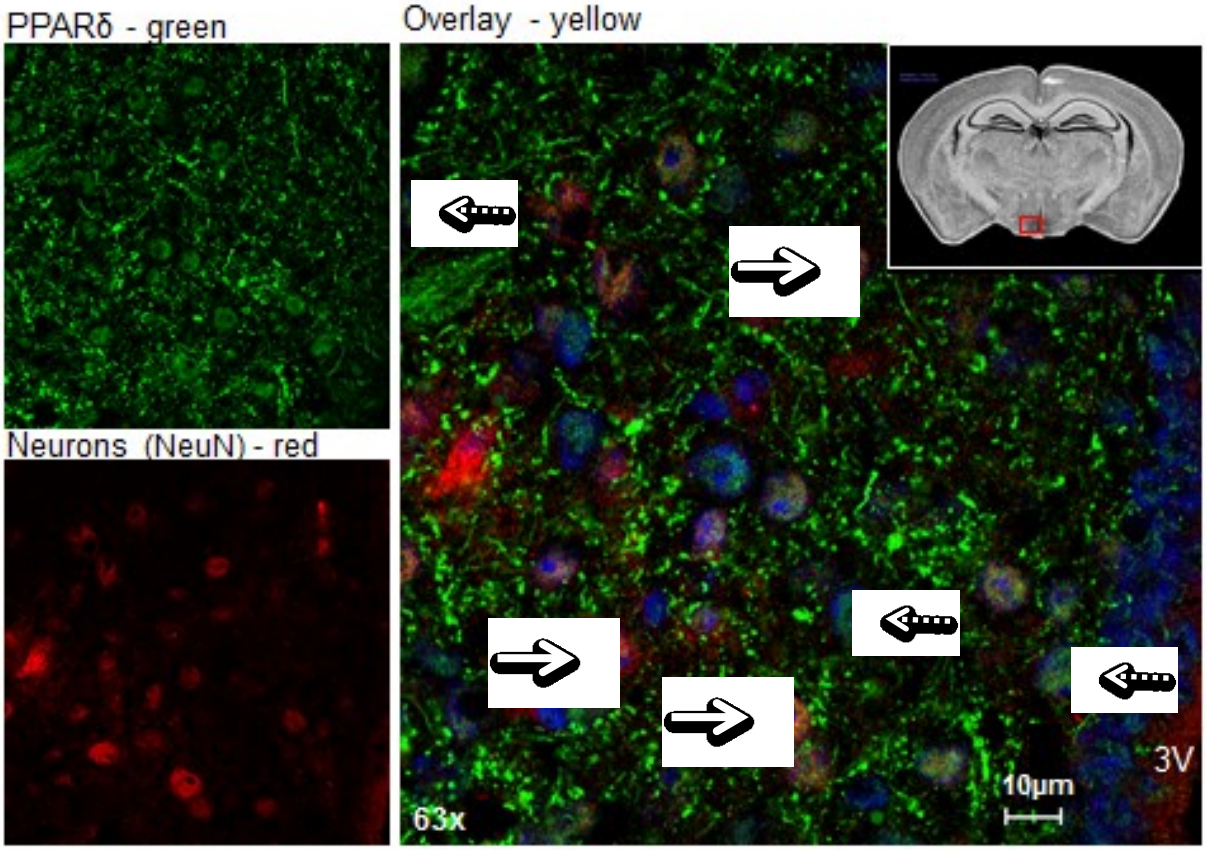

Figure 6. Immunofluorescence of PPARδ and neurons (NeuN) in hypothalamus. Coronal section of mouse brain immuno stained for PPARδ (green), neuronal nuclei with NeuN (red), and nuclei with DAPI (blue) shows co-localization of PPARδ in neuronal (orange-yellow, solid arrows), and other nuclei (green and blue, dashed arrows). Image was acquired with confocal microscope at 63x magnification and represents at least 3 repetitions.

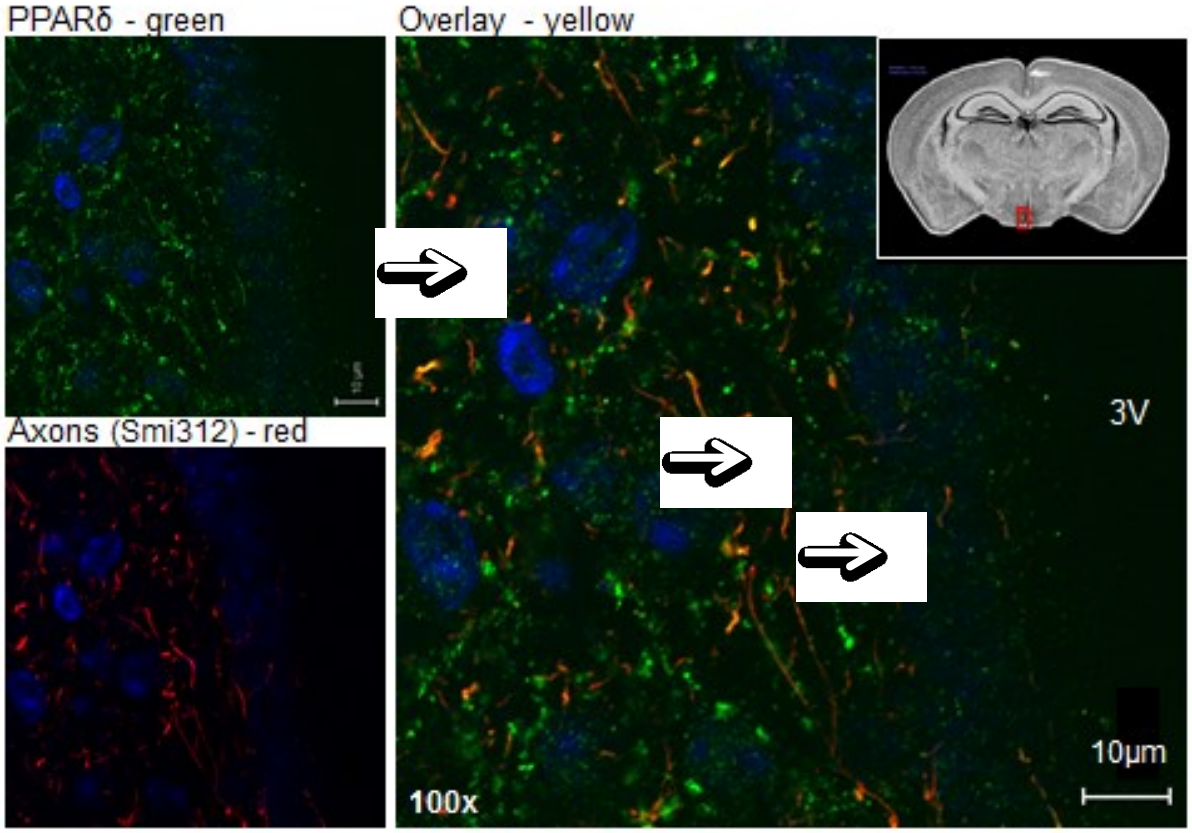

Figure 7. Immunofluorescence of PPARδ and axons (Smi312) in hypothalamus. Coronal section of mouse brain immuno stained for PPARδ (green), neuron axons with Smi312 (red), and nuclei with DAPI (blue), shows co-localization of PPARδ in axons (orange-yellow, solid arrows). Image was acquired with confocal microscope at 100x magnification and represents at least 3 repetitions.

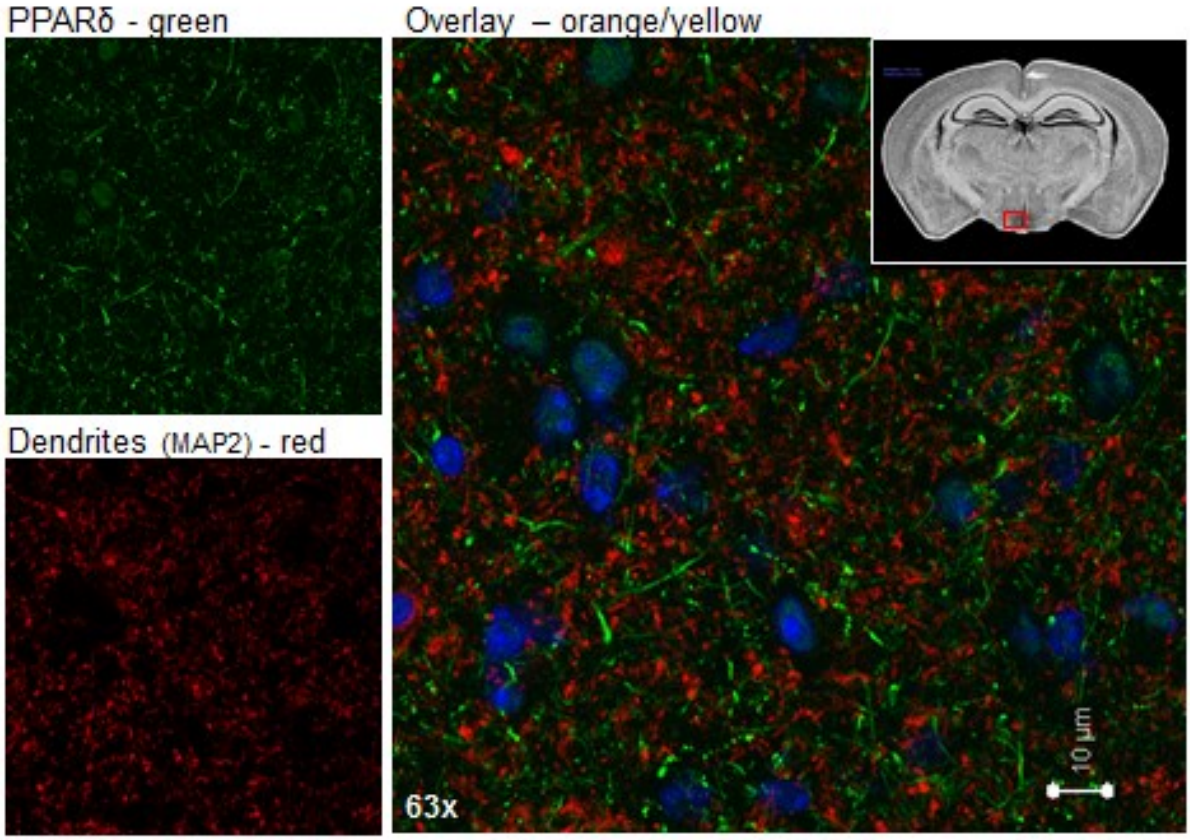

Figure 8. Immunofluorescence of PPARδ and dendrites (MAP2) in hypothalamus. Coronal section of mouse brain immuno stained for PPARδ (green), neuron dendrites with MAP2 (red), and nuclei with DAPI (blue), shows no co-localization of PPARδ in dendrites. Image was acquired with confocal microscope at 63x magnification and represents at least 2 repetitions.

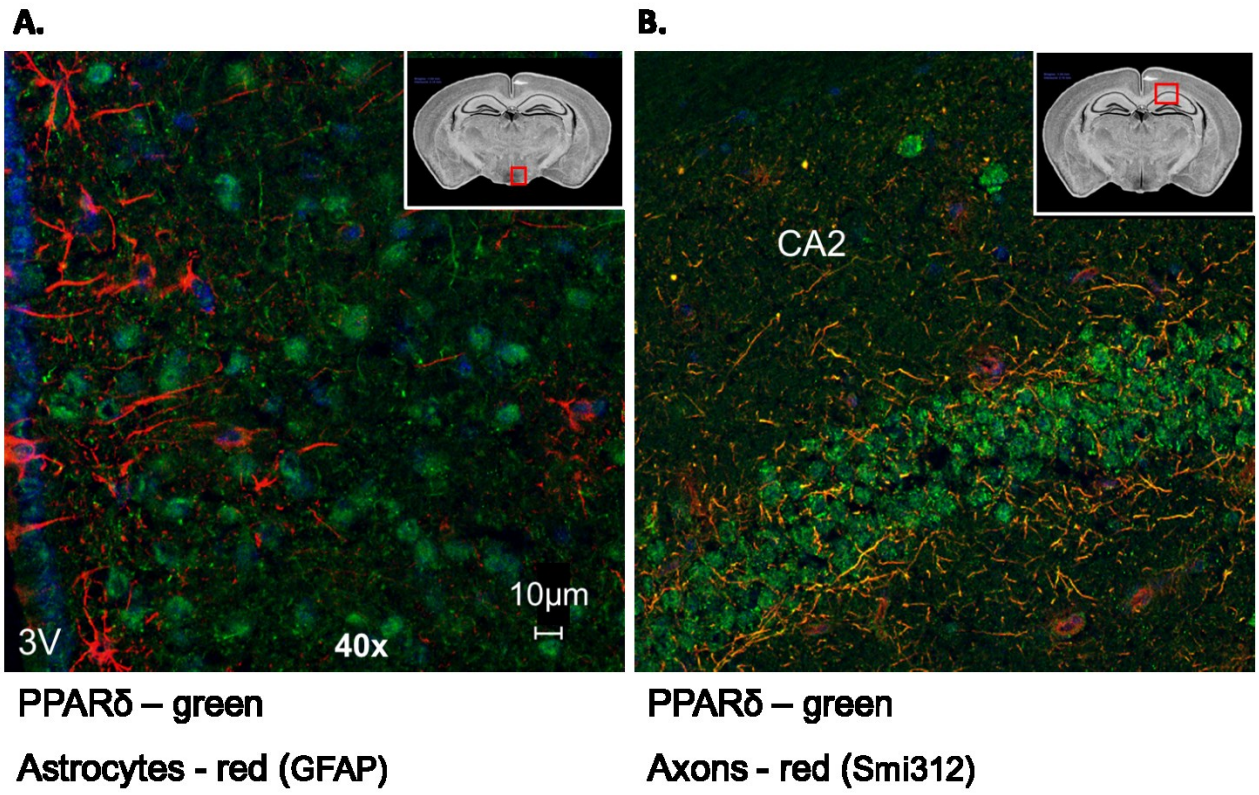

Figure 9. Immunofluorescence of PPARδ in hypothalamus and hippocampus. (A) Coronal section of mouse brain immuno stained for PPARδ (green), astrocytes with GFAP (red), and nuclei with DAPI (blue), shows no co-localization of PPARδ in astrocytes. (B) Coronal section of mouse brain immuno stained for PPARδ (green), neuron axons with Smi312 (red), and nuclei with DAPI (blue), shows co-localization of PPARδ in axons (orange-yellow), in hippocampus. Images were acquired with confocal microscope at 40x (A) and 25x (B) magnification and and represents at least 2 repetitions.

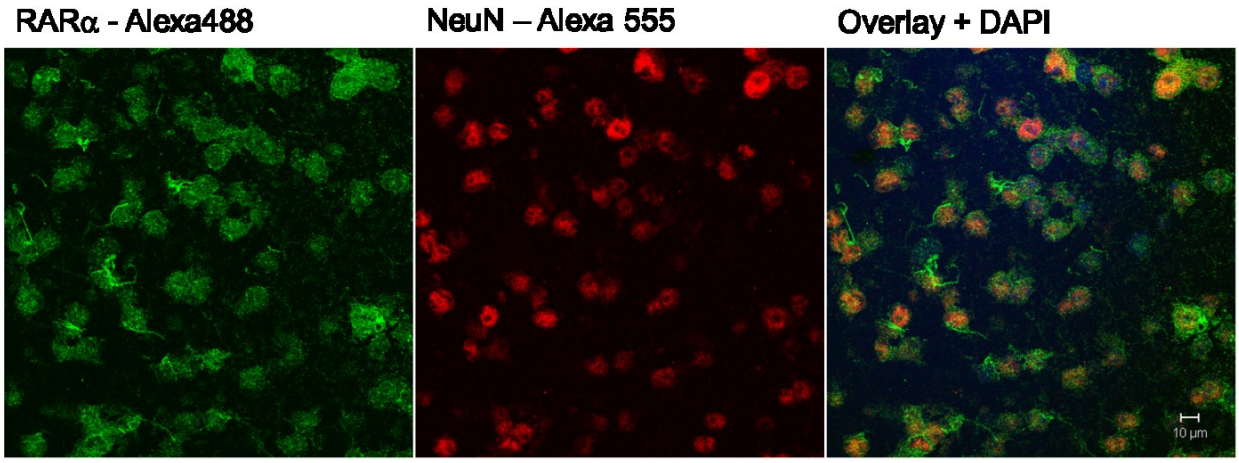

Figure 10. Immunofluorescence of RARα and neurons (NeuN) in hypothalamus. Coronal section of mouse brain immuno stained for RARα (green), neuronal nuclei with NeuN (red), and nuclei with DAPI (blue) shows co-localization of RARα in neuronal nuclei (orange-yellow), and some surrounding structures. Image was acquired with confocal microscope at 40x magnification and represents at least 2 repetitions.

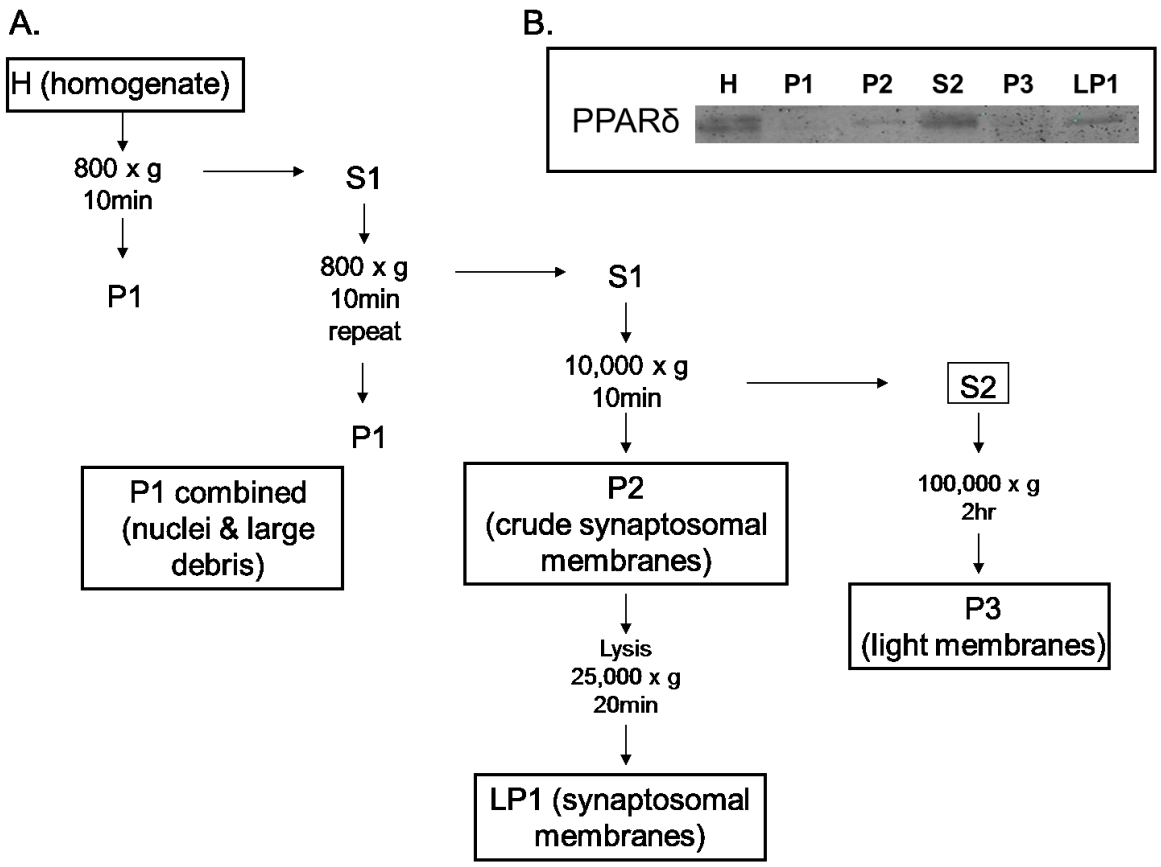

Figure 11. PPARδ protein expression in brain fractions. (A) Schematic of fractionation protocol adapted from Current Protocols in Neuroscience. (B) Western blot detection of PPARδ in brain fractions. Experiment performed once.

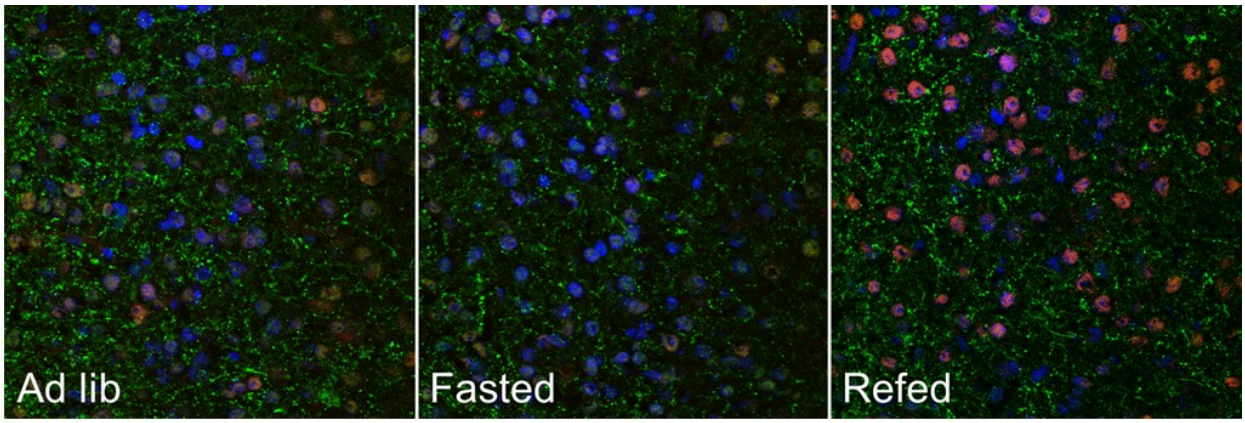

Figure 12. Immunofluorescence of PPARδ in fed and fasted states. Coronal section of mouse brain immuno stained for PPARδ (green), neuron nuclei with NeuN (red), and nuclei with DAPI (blue), shows reduced PPARδ signal in axons in fasted state. Images were acquired with confocal microscope at 25x magnification and are representative of many images. Experiment performed 2 times.

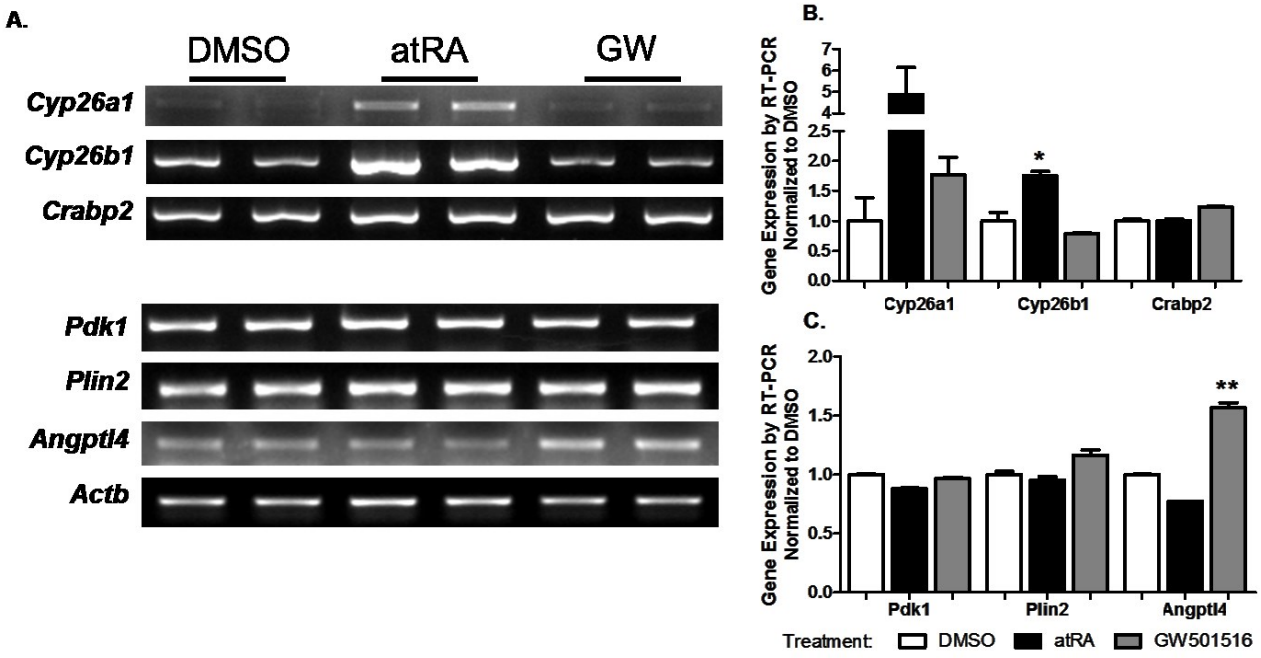

Figure 13. atRA activates transcription of RAR, not PPARδ target genes. Mature primary hypothalamus neurons, DIV 16, were treated with DMSO vehicle, or 1 μM atRA, or 1μM GW501516 for 17 hr. Expression of RAR and PPARδ target genes were measured by RT-PCR, visualized on gels (A), and quantified by densitometry (B). Pyruvate dehydrogenase kinase 1 (*Pdk1*); perilipin 2 (*Plin2*); angiopoietin-like 4 (*Angptl4*). N=2 wells of cells, data is representative of 2 repetitions. Densitometry data are means ± SE: * $P < 0.05$, ** $P < 0.005$.

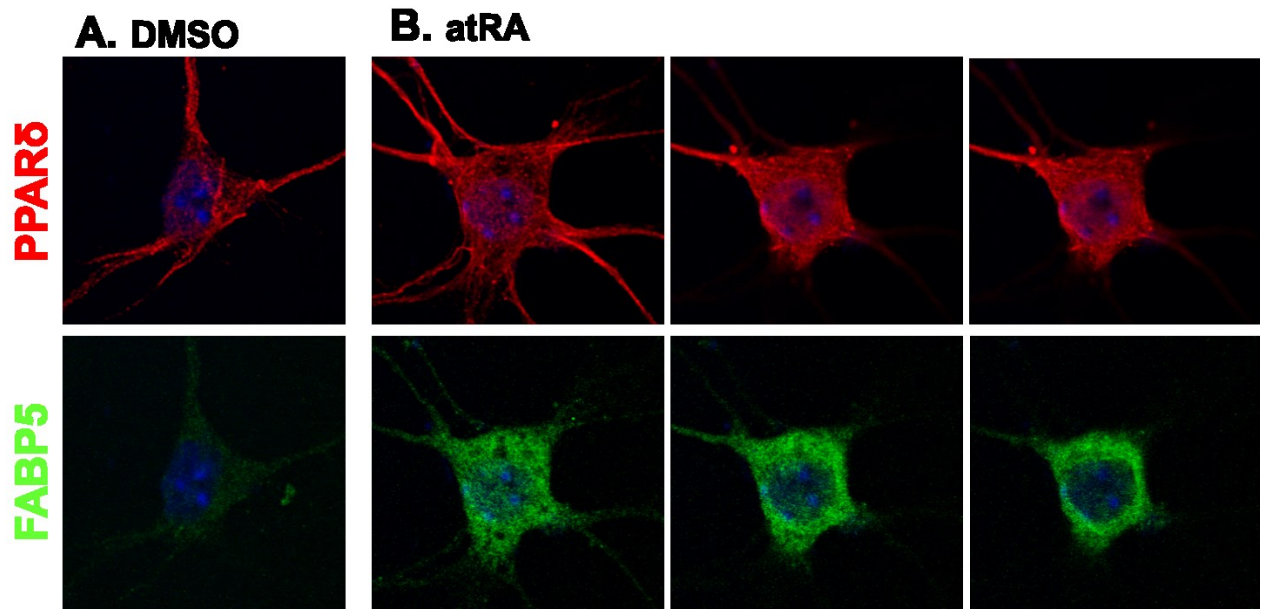

Figure 14. Immunofluorescence of PPARδ and FABP5 in primary neurons. Mature primary cultured neurons (DIC 16) were treated with DMSO vehicle (A) or 1 μM atRA (B) for 30 min, then immuno stained for PPARδ (red), FABP5 (green) and nuclei with DAPI (blue). Panels in (B) display z-stacked images through the nucleus.

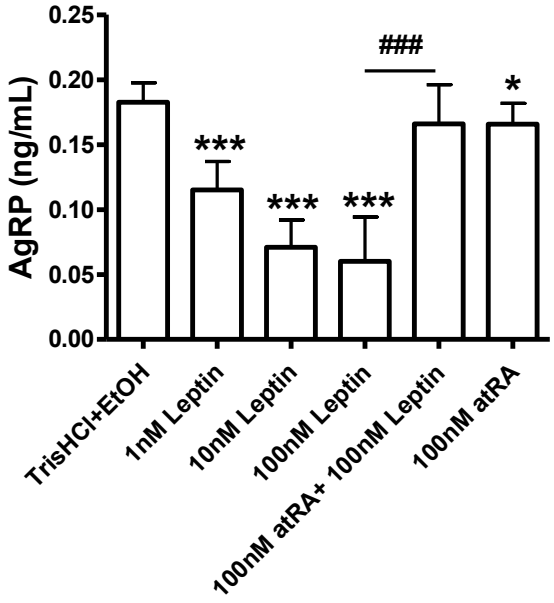

Figure 15. atRA attenuated leptin induced reduced AgRP secretion. Rat hypothalamus tissue explants were treated with vehicle, leptin, and or atRA (doses labeled) in neuropeptide secretion assay. Secreted AgRP was quantified in medium by ELISA assay. N=3-8 samples per condition. Data are means ± SE, * $P < 0.05$, *** $P < 0.005$ vs TrisHCl+EtOH vehicle; ### $P < 0.0005$.

DISCUSSION

This project set out to define a mechanism of centrally regulated energy balance by atRA in hypothalamus. While this goal was not achieved, data advances knowledge in two research areas: 1) Hypothalamus was identified as a relevant and viable region for atRA metabolism. 2) Localization of PPARδ in neuron axons supports the possibility of non-genomic function of this nuclear hormone receptor, in multiple brain regions.

I demonstrated quantitatively that atRA concentration was elevated in comparison to other brain regions measured in mouse. Initial troubleshooting concluded that small size of hypothalamus, approximately 7 mg wet tissue weight, required pooling tissue from two to three mice to raise the atRA signal optimally and minimize variability among equivalent samples. Additionally, retinoids normalized to protein, rather than tissue weight, improved accuracy. Unfortunately, I was unable to detect changes in atRA concentration during metabolic shifts *in vivo*. It is possible that atRA concentration changes differentially according to cell type, or in cellular microenvironments, which could both be undetectable in homogenate of heterogeneous tissue. Thus, evaluation of atRA in response to metabolic perturbations *in vivo* may be inadequate due to technical limitations of our current retinoid quantification assay. Alternatively, atRA may serve a housekeeping function that is not responsive to metabolic alterations tested. Finally, atRA function may be regulated independently of absolute concentration. The relative expression of atRA binding proteins determines activation of cognate receptors to atRA ligand (35), and examples of this regulation have been shown in cancer and cell differentiation (35, 184). Differential chaperoning of atRA ligand may be the relevant mechanism to steer atRA response, and regulation of, central metabolic shifts.

To characterize mechanistic response to atRA, I focused on PPARδ receptor because of its extensive role in metabolic regulation, and evidence that it responds transcriptionally to atRA ligand. Confocal imaging of immunohistochemistry in brain sections identified PPARδ in neuronal nuclei and axons. PPARδ in nucleus is expected for transcriptional regulation of target genes. However, atRA does change expression of select PPARδ target genes, nor cause nuclear import of FABP5. PPARδ in axons may be involved in anterograde transport or communication. There is evidence for local translation of mRNAs in axons, with transcripts enriched in protein translational machinery, transport, cytoskeletal components, and mitochondrial maintenance (185). Regulation of local translation by PPARδ, and atRA ligand, would be analogous to that by RARα in neuronal dendrites in hippocampus (36). It is unknown whether atRA may serve as a ligand for non-genomic function of PPARδ, or if FABP5 would serve as a chaperone in such a context. Local translation was not tested directly in this project. Apparent reduction of PPARδ signal in axons of fasted versus fed mouse hypothalamus would indicate metabolically driven turnover, and likely non-genomic function.

Reports of PPARδ functions in brain have emerged since my work on this project. In a neuroblastoma cell line, both PPARδ silencing and activation with agonist, support that PPARδ modulates neuronal differentiation (186). Specifically, PPARδ activates signal transduction pathways ERK1/2 and brain-derived neurotrophic factor (BDNF). Previous work identified MAPK (ERK) function in axon transport of neurofilaments during neurogenesis and neuronal differentiation (187). Extending research on atRA activation of PPARδ, Yu et al. found that late stage neuronal differentiation into mature neurons is mediated by transcriptional activity of PPARδ, in contrast to early commitment stage being mediated by atRA activation of RARα via CRABP2 (184). The same group identified that another ligand of PPARδ, arachidonic acid, up-regulated transcription of target genes associated with cognition in mature neurons (188). Other reports on PPARδ function in mature brain have utilized synthetic agonists to evaluate therapeutic potential. Mice treated with PPARδ agonist showed improved performance in Morris water maze test, as an indicator of increased learning and memory formation (189). Treatment with PPARδ agonist in a rat model of induced Parkinson's disease significantly improved cognitive impairments, as demonstrated by passive avoidance and Morris water maze tests (190). In a transgenic mouse model of Alzheimer's disease, treatment with PPARδ agonist reduced inflammation and amyloid burden, by increasing transcription of genes in amyloid clearance (191). While PPARδ expression is ubiquitious in brain, understanding of its function(s), with possible region specificity, remain limited.

The goal of this project was to identify function of atRA in hypothalamus that contributes to central nervous system regulation of energy balance, following the hypothesis that atRA and leptin signals intersect at mTORC1 to regulate local protein synthesis. Because a unique function of hypothalamus neurons is to secrete neuropeptides involved in feeding regulation, I targeted secretion of peptides AgRP and αMSH (processed POMC). Contrary to my expectation that atRA and leptin would cooperatively activate mTORC1, atRA desensitized orexigenic neurons to leptin. Attenuation of leptin response by atRA is predicted to interfere with satiety induced feeding reduction. Indeed, hypothalamus neuron specific deletion of leptin receptor, as well as addition of exogenous AgRP *in vivo* stimulate food intake and adiposity (192, 193). This data projects that atRA would cause animals to be hyperphagic and overweight, which is contrary to established effects of atRA on energy balance. My attempts to measure POMC, and cleaved peptide αMSH, under the same experimental conditions were unsuccessful due to detection limits and viability of the tissue explant model. Additionally, this experimental model of atRA treatment may not be relevant if atRA concentration in hypothalamus does not change in response to metabolic alterations.

This work sets a foundation for study of atRA activity in hypothalamus, and identifies localization of PPARδ in axons. These observations may or not be related to one another.

Supplemental data

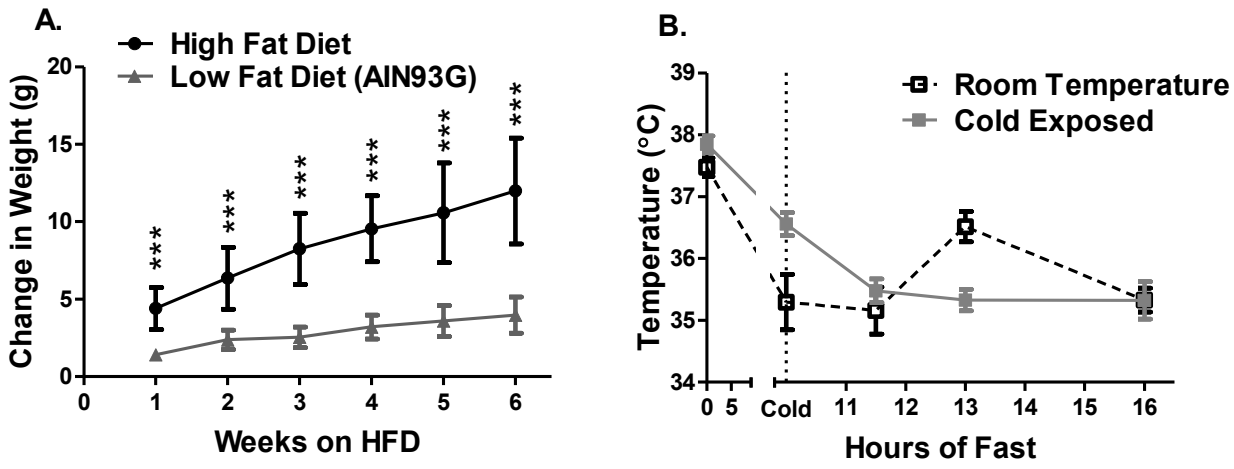

Figure S1. Body weight and temperature. (A) Body weight change in mice fed LFD or HFD for 6 wks prior to retinoid quantification in hypothalamus tissue (Ref Figure 2). Data are means ± SE, *** $P < 0.0001$. (B) Body temperature of mice during cold exposure prior to retinoid quantification in hypothalamus tissue (Ref. Figure 3). Data are means ± SE, NS difference by 2-way ANOVA.

Chapter 4

Effects of diet and strain on mouse serum and tissue retinoid concentrations

INTRODUCTION

Vitamin A (retinol) is essential for diverse physiological processes in post-natal vertebrates, including modulating energy metabolism, supporting neurogenesis and nervous system function, and sustaining the immune response (194–196). As an autacoid derived from retinol, all-*trans*-retinoic acid (atRA) regulates transcription and translation by activating nuclear hormone receptors (197–199). Retinol that exceeds demands for atRA production and for vision is stored as retinyl esters (RE), primarily in the liver, but also in many other tissues (200). atRA auto-regulates its concentrations through substrate depletion *via* enhanced RE biosynthesis by inducing lecithin:retinol acyltransferase, and also through inducing its catabolism by inducing cytochrome P-450 isozyme expression (201, 202). Excess or deficiency of atRA has adverse effects, such as abnormal fetal development and disruptions in regulation of energy balance (203, 204).

Most retinoid quantitation has been done on a few mouse strains, often fed standard laboratory chow. Standard rodent chow consists of natural sources, which vary in precise compositions, and contains copious amounts of nutrients, including vitamins (205). In contrast, semi-purified diets provide a consistent nutrient composition in amounts that meet the National Research Council recommendations for rodent nutrient intake, while avoiding delivery of copious amounts of vitamins that can confound studies of nutrient functions. The American Institute of Nutrition (AIN) has determined that the minimum amount of vitamin A necessary for rodents is 2.9 IU/g diet, and recommends an intake of 4 IU/g diet to provide a margin of safety (206, 207). Chow contains from 12 to >20 IU vitamin A/g diet, and likely provides even more depending on the carotenoid content of the natural products used to formulate the diets (208). The upper limit of vitamin A for human consumption has been recommended as no more than 3-4 times the recommended dietary allowance (RDA) (209). Vitamin A in rodent chow diet is ~5 times the recommended intake for rodents, and therefore is exceptionally copious.

The present study focused on the impact of dietary vitamin A intake on retinoid status in five strains of mice. Mice bred from dams fed standard rodent chow were weaned onto a vitamin A-sufficient diet (VAS), the AIN93G semi-purified diet with 4 IU vitamin A/g (206). After five weeks of VAS feeding, tissues of the first generation were collected and analyzed for RE, retinol and atRA concentrations. This first generation was used to breed a second generation, and the second was used to breed a third generation, while continuously being fed a VAS. Tissues and serum of the third generation were analyzed at a similar age as the first generation. The experimental design allowed for evaluation of the impacts of diet and strain on endogenous tissue retinoids.

MATERIALS AND METHODS

Mice and diets

Mice were purchased from Jackson Laboratories at weaning (first generation). Mice strain and catalog numbers are: 129S1/SvImJ (002448); C3H/HeJ (000659); BALB/cByJ (001026); AKR/J (000648); C57BL/6J (000664). First generation mice had been bred from and nursed by dams fed a chow diet (Lab Diet JL 6%, catalog 5K0Q), which contained copious amounts of vitamin A, as retinol, RE, and β-carotene (≥ 20 IU total vitamin A/g diet). Upon arrival, mice were fed an AIN93G semi-purified diet (Dyets, catalog 110700) with sufficient vitamin A (4 IU/g diet) in the form of retinyl palmitate. The VAS was maintained throughout the study for all mice (dams and pups), including during breeding, nursing, and after weaning. Mice were housed up to five per cage with littermates, and fed ad libitum for the duration of the study. Mice were euthanized in the morning, at 9-10 weeks old. This study was done in strict accordance with the recommendations in the Guide for the care and use of Laboratory Animals of the National Institutes of Health. The protocol was approved by the Animal Care and Use Committee of UC-Berkeley.

Quantification of retinoids

Retinoid concentrations were quantified in 6 to 10 male mice per group. Tissues were collected under yellow light, weighed, and frozen immediately in liquid nitrogen. Tissues were thawed on ice and hand homogenized in 0.9% saline. Retinoids were recovered by a two-step acid and base extraction (210). All materials in contact with samples were glass or stainless steel. Internal standards were used to calculate extraction efficiency of retinoids. RE and retinol were extracted and then quantified by HPLC-UV as described, with retinyl acetate as internal standard (211). atRA was extracted and quantified by LC/MS/MS as described, with 4,4- dimethyl atRA as internal standard (212, 213).

Statistics

Data are presented as mean ± standard error (SE) and were analyzed using two-tailed, unpaired student's *t* tests or linear regression analysis.

RESULTS

Serum and tissue RE concentrations

Serum RE concentrations occurred in a limited range from 0.1 to 0.24 nmol/L in the first generation mice switched to a VAS (Figure 1A). By the third generation of VAS feeding, serum RE in the C3H, AKR and 129 strains increased ~2-fold, decreased 86% in C57 mice and did not change significantly for BALB mice, with a range from 0.2 to 0.35 nmol/L for the five strains. Liver RE concentrations were greater in first-generation than in third generation mice for all but C57 strain, and spanned a wide range (~360 to 1000 nmol/g tissue). RE in the third generation of C3H, AKR and BALB mice decreased 42, 64 and 73%, respectively, relative to the first generation. In the 129 strain, the 27% decrease was not statistically significant (P = 0.3). Liver RE of C57 were unaffected by long-term VAS. The range of liver RE in the third generation varied from ~100 to 580 nmol/g tissue). Kidney RE concentrations were similar regardless of strain for first-generation mice, ranging from ~10 to 13 nmol/g, and remained the same for the VAS-fed C3H and 129 strains into the third generation. RE in kidney of the third generation mice increased 34% in AKR, and decreased 92 and 54% in C57 and BALB mice, respectively. The range for kidney RE in the third generation was broad (1 to 13.3 nmol/g tissue). Testes RE concentrations occurred in a tight range regardless of strain in first-generation mice (0.7 to 1.2 pmol/g tissue), and did not change significantly in mice fed a VAS into the third generation (0.8 to 1.5 pmol/g tissue). RE concentrations in white adipose were the lowest of the tissues assayed, ranging from ~0.17-0.3 nmol/g in first-generation mice. Long-term VAS did not significantly change white adipose RE in C3H and C57 strains, but resulted in a >60% decrease in AKR, a 1.8-fold increase in 129, and a 40% decrease in BALB. The range of RE in white adipose, 0.15 to 0.3 nmol/g tissue, was similar for third generation as first generation mice fed VAS.

Serum and tissue retinol concentrations

Serum retinol concentrations were nearly identical regardless of mouse strain in first-generation mice fed a VAS, ranging from 1.1 to 1.3 nmol/ml (Figure 1B). Serum retinol increased 18, 35, 50, and 60%, respectively, for long-term VAS-fed C3H, 129, C57 and BALB strains, but did not change in the AKR strain. A VAS broadened the range to span from 1.1 to 1.7 nmol retinol/ml. Liver retinol concentrations spanned a limited range of 3.6 to 6.9 nmol/g in first-generation mice. Long-term feeding a VAS diet increased liver retinol 25 to 100% in C3H, C57 and BALB strains, decreased retinol 55% in AKR, and did not change retinol in 129 mice. This resulted in a much broader range of liver retinol values, 2.8 to 13 nmol/g tissue, compared to the first generation. Kidney retinol concentrations spanned a limited range of 1.4 to 2.1 nmol/g in first-generation mice, and varied widely with strain in response to long-term VAS-feeding, remaining the same in the C3H and 129 strains, increasing 38 and 26% in AKR and C57 strains, respectively, and decreasing 50% in BALB. This resulted in an expanded range of ~1 to 2.5 nmol/g tissue. Testis retinol concentrations ranged from 0.3 to 0.6 nmol/g in first-generation mice, and also reacted in a strain-dependent manner to long-term VAS-feeding, resulting in no change for 129 and BALB mice, a ~20% decrease in C3H and C57 mice, a 33% increase in AKR. The range was only modestly affected,

however (0.3 to 0.8 nmol/g), in third generation mice. White adipose retinol concentrations were very close regardless of mouse strain in first-generation mice, ranging tightly from ~0.6 to 0.8 nmol/g tissue. Long-term VAS did not significantly affect white adipose retinol concentrations in C3H, 129, or BALB strains, but produced a 39% decrease in AKR, and a 38% increase in C57. The range of white adipose retinol broadened to 0.4 to 1 nmol/g.

Serum and tissue atRA concentrations

Serum atRA concentrations were similar in the five strains in the first generation, ranging from 3.8 to 5.4 pmol/ml (Figure 1C). Long-term feeding a VAS did not alter serum atRA significantly, except for BALB mice, which responded with a 68% decrease. Liver atRA concentrations decreased with long-term VAS feeding 21, 62, and 53% in C3H, AKR, and C57 strains, respectively, but did not change in 129 and BALB mice. The range of liver atRA narrowed from ~9 to 24 pmol/g tissue in first generation to ~8 to 13 pmol/g tissue with long-term VAS. Kidney atRA concentrations in first generation mice ranged from 7 to 13 pmol/g tissue. Long-term VAS caused kidney atRA to decrease from 37 to 52% for all but the BALB strain, which remained unaffected. This resulted in a reduced range of ~5 to 9 pmol/g tissue. Testis atRA concentrations ranged from 13-20 pmol/g tissue in first generation strains, *i.e.* similar to the values in liver. Long-term feeding VAS decreased testis atRA 30 to 66% for all strains except C3H, which was unaffected. The range of testis atRA reduced to ~6 to 13 pmol/g tissue—again similar to concentrations measured in liver. White adipose atRA concentrations were very similar among strains in the first generation assayed, ranging tightly from 4 to 4.8 pmol/g tissue, with an average value of 4.5 pmol/g tissue. Long-term feeding VAS did not change white adipose atRA in the C3H and C57 strains, but decreased it 69, 53 and 62% in the AKR, 129 and BALB strains, respectfully. The strain-specific response to VAS increased the range of white adipose atRA to ~1.5 to 4.2 pmol/g tissue.

atRA generally decreased in tissues of mice fed the VAS diet for three generations, with 14 of 20 tissues in the five strains showing significant decreases. atRA did not change significantly in the remaining 6 tissues, and in no case did it increase with VAS. Although the effects of reducing the amount of dietary vitamin A on tissue atRA were both strain and tissue dependent, the relative orders of atRA tissue concentrations remained the same in the first and third generations. Liver and testis had the highest concentrations, kidney had intermediate concentrations, and white adipose had the lowest concentrations.

Serum atRA values clustered in both the first and third generations (except for BALB in the third generation) and therefore were dependent on diet rather than strain. This clustering of atRA values in serum contrasts with tissue-specific variations, and indicates that serum atRA does not reflect or predict tissue atRA concentrations. Neither did serum retinol reflect tissue atRA. Further, no linear correlations were observed between retinol and atRA concentrations in serum or tissues from either generation (Figure 2). Linear regression analysis of each data set revealed none with a slope significantly different from zero.

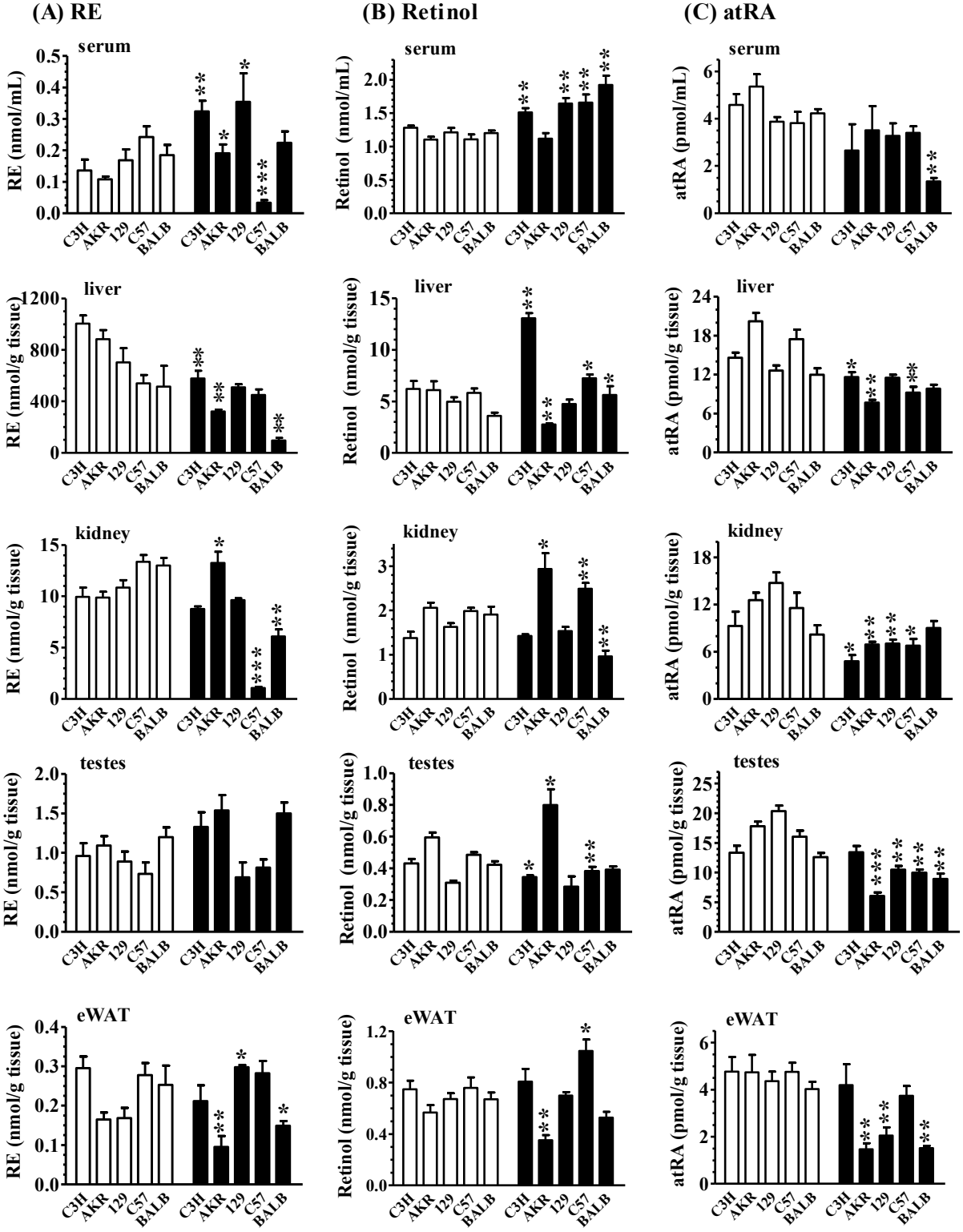
(A) RE
(B) Retinol
(C) atRA
serum
liver
kidney
testes
eWAT
RE (nmol/mL)
Retinol (nmol/mL)
atRA (pmol/mL)
RE (nmol/g tissue)
Retinol (nmol/g tissue)
atRA (pmol/g tissue)
C3H
AKR
129
C57
BALB

Figure 1. **Retinoids in serum and tissues of five mouse strains.** (A) Retinyl esters (RE), (B) Retinol and (C) all-*trans*-retinoic acid (atRA). Mice were fed a VAS after weaning from dams fed a chow diet (generation 1). Generation 1 mice were maintained and bred on the VAS, continuing into the third generation. Retinoids were quantified in male mice after week 9 of the first generation (open bars), or week 10 of the third generation (filled bars). Tissues and serum of 3 to 10 mice were assayed for each strain and generation: eWAT, epididymal white adipose tissue. Data are means ± SE: **P* < 0.05; ***P* < 0.005, ****P* < 0.001 relative to first generation values.

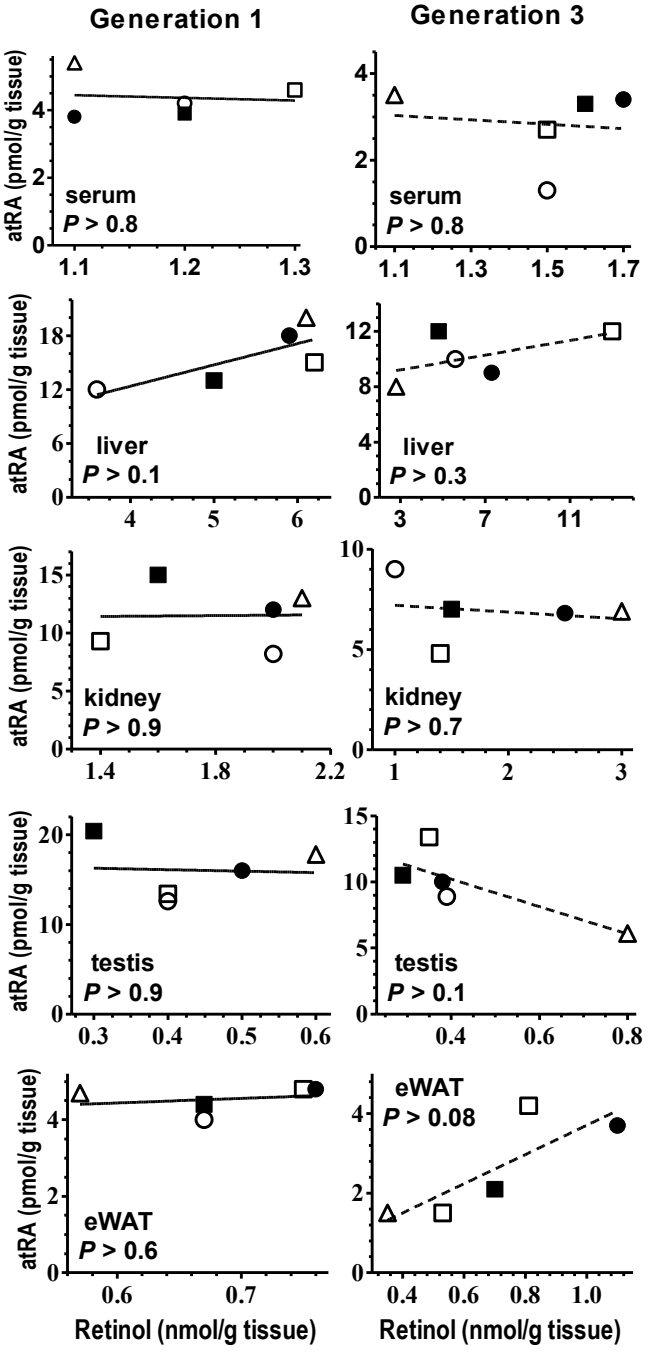

Figure 2. Relationships between retinol and atRA. Retinol (x-axis) and atRA (y-axis) values for serum and tissues from first generation (left column) and third generation (right column) fed a VAS (eWAT, epididymal white adipose tissue): □, C3H; Δ, AKR; ■, 129; ●, C57; ○, BALB. Linear regression analysis for each tissue and generation verified that none of the slopes differed significantly from zero.

DISCUSSION

Previous reports with mice fed copious vitamin A have shown that liver RE correlate directly with dietary vitamin A levels when mice are challenged with even greater dietary vitamin A, or fed a vitamin A-deficient diet (214, 215). The impact, however, of transitioning from a chow diet to a VAS had not been studied, nor had strain differences been addressed. The present study addressed these issues, and revealed that the transition of copious to sufficient dietary vitamin A affects retinoid homeostasis with strain and tissue-specificity. The decreases in atRA with a decrease in dietary vitamin A across the five strains show that retinol availability affects atRA concentrations, even with modest changes in dietary vitamin A, but the lack of correlation between retinol and atRA concentrations indicates that strain-specificity determines the exact relationships between the two. Although atRA decreased in general with a decrease in dietary retinol, sometimes greater than 60%, the magnitudes of the decreases did not adhere to quantitatively predictable patterns. This partial dependence of atRA on dietary vitamin A, and its strain and tissue-dependent variation, would have physiological consequences because relatively modest 2-fold increases in atRA concentrations can have toxic effects (203). Even in the absence of toxicity, increased atRA *via* increased dietary retinol may have profound consequences. Phenotypes resulting from ablation of genes that modulate retinoid homeostasis can be rescued by a chow diet (copious vitamin A). For example, when fed chow diet *Rbp4*-null (*Rbp4* encodes the serum retinol binding-protein) mice reproduce and grow normally, experiencing only modestly impaired vision, but when fed a VAS diet fail to thrive and reproduce (216). Similarly, *Rdh1*-null mice fed a chow diet do not display a phenotype, but when fed a VAS become ≥30% heavier than wild-type littermates, even when fed a low-fat diet (217). *Rbp2*-null (*Rbp2* encodes cellular retinol binding-protein type 2) mice nursed by dams fed a chow diet show no phenotype, but when nursed by dams fed a diet limited in vitamin A have high neonatal mortality (218). These observations are consistent with evolution of retinoid homeostasis associated-proteins enabling animals to efficiently use and thrive on limited dietary vitamin A. Copious dietary vitamin A may allow synthesis of atRA by non-physiological paths, independent of retinoid-chaperoning proteins, and thereby would obscure the functions of proteins that evolved to increase the efficiency of vitamin A use. Even with phenotypes that manifest in mice fed a diet with copious vitamin A, the higher vitamin A levels of chow diets might ameliorate the severity of the phenotype or reduce its complexity. Because atRA has multiple actions in diverse tissues, and laboratory mice are rarely challenged to the extent of mice living in the wild, the ameliorating impact of a chow diet on a knock-out would not necessarily be obvious. The combination of a protected environment and a chow diet can reasonably be expected to prevent manifestations of phenotypes, and therefore could render a gene ablation non-informative.

Surprisingly, not all strains responded to decreased dietary retinol with a decrease in liver RE. Two of the most popular strains used to ablate genes, 129 and C57, did not experience significant decreases in liver RE over three generations of feeding a VAS. This phenomenon of conserving RE, even during reduced dietary intake, likely underlies the common observation that mice are difficult to render vitamin

A deficient, if bred from dams fed a diet copious in vitamin A. Other results also were not anticipated, such as the C57 strain having a very large decrease in kidney RE during long-term VAS feeding, while liver RE resisted change. The strain-specific effect of diet on white adipose RE and the lack of correlation with liver RE also were not anticipated. Increases in serum RE and retinol with decreases in dietary vitamin A in four of five strains also were not anticipated, and perhaps reflect enhanced mobilization from liver to support extra-hepatic tissue atRA biosynthesis. The inconsistent changes in tissue retinol with decreases in dietary retinol were another unexpected outcome, and indicate that tissue retinol concentrations were more strain than diet dependent in mice fed a VAS.

Serum atRA exchanges with tissue atRA, except in testis (219). The blood-testis barrier prevents physiological amounts of circulating atRA from entering Sertoli and germ cells. Instead, retinol permeates the blood-testis barrier and supports atRA biosynthesis *in situ*. Therefore, testis atRA would most likely reveal the true nature of the relationship between tissue retinol and atRA, compared to other tissues. The amount of dietary retinol affected the steady-state concentrations of atRA in testis in a strain-specific final concentration, just as with other tissues, which reinforces strain dominance of the retinol-atRA relationship (except for the AKR strain).

Strain dependent retinoid concentrations suggests differential activity and/or expression of enzymes that catalyze retinoid homeostasis. Biosynthesis and catabolism of atRA are regulated to meet biological demand and remain within a safe range. Retinol from diet, or mobilized from RE by retinyl ester hydrolases is substrate for atRA biosynthesis (220). Two sequential reactions from retinol catalyze synthesis of atRA. Retinol dehydrogenases (Rdh) catalyze the first and rate limiting reaction that converts retinol into retinal. Retinal dehydrogenases (Raldh) catalyze the conversion of retinal into atRA (202). Various cytochromes P-450 (Cyp) catabolize atRA (201). Multiple isozymes of Rdh, Raldh and Cyp contribute to atRA biosynthesis and catabolism. These data also indicate that the concentrations of atRA are tissue autonomous, because the relative amount in each tissue differs with strain. For example, the relative order of atRA in thirds generation VAS liver was C3H ≈ 129 > BALB > C57 > AKR, but in kidney was BALB > AKR ≈ 129 ≈ C57 > C3H. This observation suggests that a comparison of retinoid metabolizing enzyme expression in tissues of various strains could provide insight into the enzymes that predominate in maintaining atRA homeostasis.

Understanding the impact of dietary vitamin A on retinol and atRA levels would be important to understanding retinoid homeostasis and to the study of animals with disruptions in retinoid homeostasis-regulating genes. This work showed that: 1) copious vitamin A, such as used in chow diets, increases tissue atRA markedly; 2) decreasing dietary retinol decreases serum and tissue atRA with strain-specific degrees; 3) neither serum retinol nor atRA reflect tissue atRA concentrations; 4) RE concentrations react to a decrease in dietary vitamin A with strain and tissue-specific effects; 5) replacing a copious vitamin A diet (chow) with a VAS for one month (generation 1) did not reduce serum and tissue atRA levels to those achieved with long-term VAS feeding (generation 3). These data quantify the impact of dietary vitamin A on endogenous retinoid concentrations, and highlight both strain and tissue-specific differences that could have

profound effects on retinoid action. Notably, elevated atRA in tissues of mice fed copious vitamin A could rescue or mask phenotypes generated by ablating retinoid homeostasis-regulating genes.

Conclusions and Discussion

RA homeostasis is intricately regulated by layers of binding protein chaperones, enzyme accessibility, as well as feed-back and feed-forward regulation of synthesis and catabolism, respectfully. Consequently, retinoid-homeostasis is maintained within a safe biological range. Perhaps more interesting, atRA synthesis and catabolism is pliable and responsive to external stimuli. Long evidenced by spatial and temporal expression of retinoid-regulating genes during development to drive patterning and cell differentiation, adequate atRA is essential and excessive atRA is teratogenic. Research in this dissertation characterizes dynamic atRA synthesis in mature animals. Application of modern techniques and protocols enabled sensitive and sophisticated quantification of endogenous retinoids. Genetically wild type and metabolically normal models, allowed for detection of regulation during acute shifts in energy status, and by dietary vitamin A. The transition between fasting and feeding defines a switch in nutritional and hormonal stimuli systemically, is physiologically relevant, and translatable to higher mammals. Surprisingly, atRA concentrations change in fasted and re-fed mice, with apparent tissue and temporal specificity. My work focused on synthesis regulation to identify a mechanism of atRA response. Research described in this dissertation, and in progress by other members of the Napoli lab, is first to characterize metabolic regulation of *Rdh* expression, and related shifts in atRA concentrations. I expect this is just “the tip of the iceberg” for integrated regulation of energy and retinoid metabolism. Generally, I observed a global increase in atRA concentration and expression of atRA synthesis genes in tissues of fasted animals, and those fed copious dietary vitamin A. Conversely, I observed a decrease in atRA and synthesis in animals that were re-fed following a fast, and those fed sufficient vitamin A. A brief summary of specific contexts is described as follows:

In liver, atRA was elevated with fasting and reduced with re-feeding after 9 and 12 hr, but not 6 hr. mRNA expression of *Rdh10*, *Rdh1*, and *Rdh5* were elevated with fasting and reduced with re-feeding after 6 hr, thus preceded the reduction in atRA, and was consistent with regulated synthesis. *Rdh10* expression was similarly reduced by oral gavage glucose and i.p. insulin, but not i.p. glucose or GLP-1 analog. The reduction in atRA concentration was likely a result of both reduced synthesis *and* increased catabolism, however only the former was addressed directly. Regulation of *Rdhs* expression was generally reduced by re-feeding in other tissues measured, including pancreas, brown adipose and kidney, but not white adipose. A global reduction in atRA synthesis is consistent with associations of atRA with reduced body weight and increased insulin sensitivity. The intriguing observation of *Rdh* regulation, with specificity by tissue and magnitude of change, warrants further research. Focus on *Rdh10* regulation in the human hepatoma (HepG2 cell) model identified that insulin suppressed transcription, dependent on PI3K, AKT, and inactivation of FOXO1. Key aspects of that mechanism were consistent for *Rdh16* expression, which emphasized biological importance of dynamically regulated atRA synthesis.

In pancreas, 9cRA was elevated with fasting and reduced with feeding and glucose (32). Pancreas expression of *Rdh5* was elevated in fasted and reduced in re-fed mice. Mechanistic characterization of the *cis*- active *Rdh5* in 832/13 beta cell model identified transcriptional repression by glucose and cAMP. Additionally, overexpression of *Rdh5* was sufficient to increase 9c-retinal and 9cRA synthesis. Elevated 9cRA in fasted pancreas is thought to prevent hypoglycemia, and dynamic regulation of 9cRA concentration allows for maximal glucose stimulated insulin secretion.

Research efforts in hypothalamus identified active atRA metabolism, and detection of PPARδ in neuron axons, which established the potential for non-genomic function. Recent advances in the nuclear hormone receptor field have uncovered multiple examples of non-genomic regulation, with common activation of MAPK signaling pathways (29). It will be interesting to see what function(s) are determined for PPARδ in hypothalamus, as well as other brain regions, and also if atRA is a ligand in such contexts.

Finally, endogenous retinoids were measured in tissues of five mouse strains in response to dietary vitamin A over three generations. Switching mice from copious vitamin A, in chow diet, to sufficient vitamin A, in AIN93G diet, generally reduced atRA in most tissues of most strains. Dietary vitamin A had strain and tissue-dependent effects on retinoid concentrations, and is expected to impact physiological processes regulated by atRA. Specifically this insight emphasized the importance of feeding animals sufficient, rather than copious, vitamin A for evaluation of regulated retinoid homeostasis, especially genetic knock out models. Furthermore, results predict strain and tissue-specific response of genes regulating biosynthesis and catabolism of atRA, according to dietary vitamin A.

Future directions of this research may include additional characterization of mechanisms regulating *Rdhs*. This should evaluate applicability of the regulatory signals identified here, to other genes and tissues. Regulation of *Rdh* expression in *vivo* by re-feeding was recapitulated by glucose and insulin, with specificity according to tissue, gene, and route of administration. Sorting out response to glucose and insulin for other tissues would predict whether the intracellular signaling through PI3K, AKT, and FOXO1, is conserved among tissues. It may also be informative to test whether macronutrients can regulate *Rdh* expression, and atRA levels. There is evidence for branch chain amino acids, specifically leucine, to activate mTORC signaling, and atRA activation of mTORC may indicate an intersected regulation of nutrient sensing and retinoid metabolism (221, 222).

In the HepG2 model, transcriptional regulation of *Rdh* expression and enzyme activity correlated directly with one another. However, specific knock down of each *Rdh* isoform is necessary to demonstrate causative relationship between a specific *Rdh* and functional synthesis of atRA. While redundancy of *Rdh* activity presents limitations, consistent regulation of the two major all-*trans*- *Rdhs*, namely *Rdh10* and *Rdh16,* emphasizes the biological importance of controlled atRA synthesis. Also unresolved is the protein expression of RDHs mediating activity. Continued research on RDH regulation should elucidate protein expression, stability, and the relationship between

regulated transcription, translation, and activity. Extensive efforts were unsuccessful to quantify a change in RDH10 protein expression under different metabolic conditions. Poor quality and specificity of RDH antibodies may contribute to inability to detect expected changes. It also may be that the amount of change in protein expression necessary to confer a change in enzymatic activity is very small, and together with low absolute expression of RDHs, is undetectable by western blot approach. Another possibility is that post-translational modification of RDH determines activity, although that would seem independent of mRNA regulation uncovered here. There is evidence that nuclear hormone receptors are modified by phosphorylation and sumoylation, introducing the possibility that other regulatory proteins in retinoid metabolism may be similarly modified (29).

In HepG2 cells, serum deprivation caused mRNA amount and stability to increase, and stabilization required protein synthesis. Following evidence that CRABP2 interacts with ELAV-like 1 RNA binding protein, HUR, we hypothesized that elevated atRA in a fasted state would bind CRABP2 to release stabilization of *RDH10* message, as another means of auto-regulation (116). But, atRA did not destabilize *Rdh10* mRNA, and the mechanism of message stabilization remains a topic for future research. HUR is in a class of RNA binding proteins that stabilize mRNAs by binding characteristic AU-rich elements (ARE) in the 3' UTR. A prediction program, AREsite (http://rna.tbi.univie.ac.at/cgi-bin/AREsite.cgi), identified three sequences for RDH10, generating a testable hypothesis for stabilization by HUR and related proteins (223). Generally it will be interesting to learn if regulation of *Rdh*, and hence atRA synthesis, is driven by transcriptional activity, or also involves regulated translation.

The timeframe of regulation prompts questions about physiological impact of dynamic atRA concentrations on metabolic fluctuations. Referencing re-feeding data *in vivo*, I detected reduced *Rdh* expression after 6 hr, and reduced atRA concentration after 9 hr, in liver. Thus, transcriptional activity driven by atRA is unlikely to mediate the metabolic shift, from glucose to production to energy storage in liver, because the time lags far behind feeding initiation. Conversely *in vitro* data models a transition from medium complete with serum, to that deprived of serum, and I detect significant increase in *Rdh* expression within 2 hr. I did not test how soon a change in synthesis may be detected, but rather designed experiment with 16 hr of serum exposure. During a fast, hepatocytes activate gluconeogenesis to generate glucose for hepatic export and hypoglycemia prevention, by increasing expression of *Pck1, G6pc* and others (224). *Pck1* is a target gene of atRA, and in a fasted state elevated atRA will increase transcription of *Pck1* and reinforce shift toward glucose production. Re-feeding, and insulin signal in particular, reduce transcription of *Pck1* by inactivating FOXO1 (105). Thus, insulin suppresses expression of both *Rdh* and *Pck1*, and the consequential reduction in atRA reinforces reduced transcription of *Pck1*. The challenge comes in reconciling the length of time for atRA to respond to energy state, initiate transcriptional regulation of a target gene (i.e. *Pck1)*, which then regulates energy storage and utilization. I propose that metabolically driven changes in atRA synthesis contribute to regulation on a longer timescale than that of meal pattern throughout a day, such as a diurnal cycle. Observations may also be interpreted as *Rdh*s, and consequently atRA

synthesis, are suppressed during the day, when circulating blood glucose and insulin are fairly stable; and are elevated during a prolonged overnight fast. Of course, atRA is one of many signals orchestrated to achieve biological homeostasis.

The small molecule atRA causes an astonishing number and variety of biological consequences. Diversity is achieved by differential receptor mediated transcriptional regulation, and also non-genomic functions. Increasing examples of MAPK activation by extra-nuclear RARs broadens the scope of atRA functions to include rapid activation of intracellular signaling pathways (29). Adaptability of atRA to metabolic signals through altered synthesis further diversifies its potential, and provides a physiological basis for metabolically driven transcriptional regulation. Tissue specific examples of transcription targets of elevated atRA in energy insufficient state include *Pck1* in liver to increase gluconeogenesis, *Ucp1* in brown adipose to produce heat, and *Pref1* in white adipose to suppress adipogenesis (39, 47, 64). Dynamic regulation of atRA enables understanding of the systemic integration between retinoid and energy metabolism.

Retinoid metabolites and synthetic analogs are used to treat cancer and skin disorders (1–3). Recognition of atRA sensitivity to metabolic conditions lends to possible therapeutic application. Suppression of RDH expression by feeding, glucose and insulin, predicts that in glucose intolerant and insulin insensitive states, the lack of cellular uptake and response to glucose and insulin would disable regulation, and lead to elevated atRA. While potency and non-specific targets of atRA pose safety concerns, extending research on *Rdh* and atRA synthesis regulation to models of metabolic dysfunction would be interesting and informative toward clinical relevance.

In summary, the research projects reported in my dissertation demonstrate original and novel integration of retinoid and energy metabolism. I have demonstrated dynamic regulation of atRA synthesis according to acute shifts in metabolic energy status and dietary vitamin A conditions. From exploring the mechanistic regulation of three major *Rdhs* in two tissue models it is evident that, despite tissue and gene autonomous impacts, there is a general trend towards reduced RA synthesis in energy sufficient state, consistent with the notion that atRA is protective against metabolic dysfunction.

References

1. **Love JM, Gudas LJ**. 1994. Vitamin A, differentiation and cancer. Curr. Opin. Cell Biol. **6**:825–831.
2. **Baldwin HE, Nighland M, Kendall C, Mays DA, Grossman R, Newburger J**. 2013. 40 years of topical tretinoin use in review. J. Drugs Dermatol. JDD **12**:638–642.
3. **Woolery-Lloyd HC, Keri J, Doig S**. 2013. Retinoids and azelaic acid to treat acne and hyperpigmentation in skin of color. J. Drugs Dermatol. JDD **12**:434–437.
4. **Niederreither K, Dollé P**. 2008. Retinoic acid in development: towards an integrated view. Nat. Rev. Genet. **9**:541–553.
5. **Napoli JL**. 2012. Physiological insights into all-trans-retinoic acid biosynthesis. Biochim. Biophys. Acta **1821**:152–167.
6. **Soprano DR, Qin P, Soprano KJ**. 2004. Retinoic acid receptors and cancers. Annu. Rev. Nutr. **24**:201–221.
7. **Murguía-Peniche T**. 2013. Vitamin D, vitamin A, maternal-perinatal considerations: old concepts, new insights, new questions. J. Pediatr. **162**:S26–30.
8. **Sommer A, Vyas KS**. 2012. A global clinical view on vitamin A and carotenoids. Am. J. Clin. Nutr. **96**:1204S–6S.
9. **Collins MD, Mao GE**. 1999. Teratology of retinoids. Annu. Rev. Pharmacol. Toxicol. **39**:399–430.
10. **Tang G**. 2010. Bioconversion of dietary provitamin A carotenoids to vitamin A in humans. Am. J. Clin. Nutr. **91**:1468S–1473S.
11. **Reboul E**. 2013. Absorption of vitamin A and carotenoids by the enterocyte: focus on transport proteins. Nutrients **5**:3563–3581.
12. **Senoo H, Yoshikawa K, Morii M, Miura M, Imai K, Mezaki Y**. 2010. Hepatic stellate cell (vitamin A-storing cell) and its relative--past, present and future. Cell Biol. Int. **34**:1247–1272.
13. **Kaji EH, Lodish HF**. 1993. Unfolding of newly made retinol-binding protein by dithiothreitol. Sensitivity to retinoids. J. Biol. Chem. **268**:22188–22194.
14. **van Bennekum AM, Wei S, Gamble MV, Vogel S, Piantedosi R, Gottesman M, Episkopou V, Blaner WS**. 2001. Biochemical basis for depressed serum retinol levels in transthyretin-deficient mice. J. Biol. Chem. **276**:1107–1113.
15. **Kawaguchi R, Yu J, Honda J, Hu J, Whitelegge J, Ping P, Wiita P, Bok D, Sun H**. 2007. A membrane receptor for retinol binding protein mediates cellular uptake of vitamin A. Science **315**:820–825.
16. **Alapatt P, Guo F, Komanetsky SM, Wang S, Cai J, Sargsyan A, Rodríguez Díaz E, Bacon BT, Aryal P, Graham TE**. 2013. Liver retinol transporter and receptor for serum retinol-binding protein (RBP4). J. Biol. Chem. **288**:1250–1265.
17. **Napoli JL**. 1999. Interactions of retinoid binding proteins and enzymes in retinoid metabolism. Biochim. Biophys. Acta **1440**:139–162.
18. **Cascella M, Bärfuss S, Stocker A**. 2013. Cis-retinoids and the chemistry of vision. Arch. Biochem. Biophys. **539**:187–195.

19. **Ross AC, Zolfaghari R**. 2011. Cytochrome P450s in the regulation of cellular retinoic acid metabolism. Annu. Rev. Nutr. **31**:65–87.
20. **Wu L, Ross AC**. 2010. Acidic retinoids synergize with vitamin A to enhance retinol uptake and STRA6, LRAT, and CYP26B1 expression in neonatal lung. J. Lipid Res. **51**:378–387.
21. **Elizondo G, Corchero J, Sterneck E, Gonzalez FJ**. 2000. Feedback inhibition of the retinaldehyde dehydrogenase gene ALDH1 by retinoic acid through retinoic acid receptor alpha and CCAAT/enhancer-binding protein beta. J. Biol. Chem. **275**:39747–39753.
22. **Ross AC**. 2003. Retinoid production and catabolism: role of diet in regulating retinol esterification and retinoic Acid oxidation. J. Nutr. **133**:291S–296S.
23. **Balmer JE, Blomhoff R**. 2002. Gene expression regulation by retinoic acid. J. Lipid Res. **43**:1773–1808.
24. **Sonoda J, Pei L, Evans RM**. 2008. Nuclear receptors: decoding metabolic disease. FEBS Lett. **582**:2–9.
25. **Petkovich M, Brand NJ, Krust A, Chambon P**. 1987. A human retinoic acid receptor which belongs to the family of nuclear receptors. Nature **330**:444–450.
26. **Brand N, Petkovich M, Krust A, Chambon P, de Thé H, Marchio A, Tiollais P, Dejean A**. 1988. Identification of a second human retinoic acid receptor. Nature **332**:850–853.
27. **Krust A, Kastner P, Petkovich M, Zelent A, Chambon P**. 1989. A third human retinoic acid receptor, hRAR-gamma. Proc. Natl. Acad. Sci. U. S. A. **86**:5310–5314.
28. **Leid M, Kastner P, Lyons R, Nakshatri H, Saunders M, Zacharewski T, Chen JY, Staub A, Garnier JM, Mader S**. 1992. Purification, cloning, and RXR identity of the HeLa cell factor with which RAR or TR heterodimerizes to bind target sequences efficiently. Cell **68**:377–395.
29. **Al Tanoury Z, Piskunov A, Rochette-Egly C**. 2013. Vitamin A and retinoid signaling: genomic and nongenomic effects. J. Lipid Res. **54**:1761–1775.
30. **Rochette-Egly C, Germain P**. 2009. Dynamic and combinatorial control of gene expression by nuclear retinoic acid receptors (RARs). Nucl. Recept. Signal. **7**:e005.
31. **Germain P, Chambon P, Eichele G, Evans RM, Lazar MA, Leid M, De Lera AR, Lotan R, Mangelsdorf DJ, Gronemeyer H**. 2006. International Union of Pharmacology. LX. Retinoic acid receptors. Pharmacol. Rev. **58**:712–725.
32. **Kane MA, Folias AE, Pingitore A, Perri M, Obrochta KM, Krois CR, Cione E, Ryu JY, Napoli JL**. 2010. Identification of 9-cis-retinoic acid as a pancreas-specific autacoid that attenuates glucose-stimulated insulin secretion. Proc. Natl. Acad. Sci. U. S. A. **107**:21884–21889.
33. **Sessler RJ, Noy N**. 2005. A ligand-activated nuclear localization signal in cellular retinoic acid binding protein-II. Mol. Cell **18**:343–353.
34. **Shaw N, Elholm M, Noy N**. 2003. Retinoic acid is a high affinity selective ligand for the peroxisome proliferator-activated receptor beta/delta. J. Biol. Chem. **278**:41589–41592.

35. **Schug TT, Berry DC, Shaw NS, Travis SN, Noy N**. 2007. Opposing effects of retinoic acid on cell growth result from alternate activation of two different nuclear receptors. Cell **129**:723–733.
36. **Chen N, Napoli JL**. 2008. All-trans-retinoic acid stimulates translation and induces spine formation in hippocampal neurons through a membrane-associated RARalpha. FASEB J. Off. Publ. Fed. Am. Soc. Exp. Biol. **22**:236–245.
37. **Piskunov A, Rochette-Egly C**. 2012. A retinoic acid receptor RARα pool present in membrane lipid rafts forms complexes with G protein αQ to activate p38MAPK. Oncogene **31**:3333–3345.
38. **Berry DC, Noy N**. 2009. All-trans-retinoic acid represses obesity and insulin resistance by activating both peroxisome proliferation-activated receptor beta/delta and retinoic acid receptor. Mol. Cell. Biol. **29**:3286–3296.
39. **Berry DC, DeSantis D, Soltanian H, Croniger CM, Noy N**. 2012. Retinoic acid upregulates preadipocyte genes to block adipogenesis and suppress diet-induced obesity. Diabetes **61**:1112–1121.
40. **Bonet ML, Oliver J, Picó C, Felipe F, Ribot J, Cinti S, Palou A**. 2000. Opposite effects of feeding a vitamin A-deficient diet and retinoic acid treatment on brown adipose tissue uncoupling protein 1 (UCP1), UCP2 and leptin expression. J. Endocrinol. **166**:511–517.
41. **Felipe F, Bonet ML, Ribot J, Palou A**. 2004. Modulation of resistin expression by retinoic acid and vitamin A status. Diabetes **53**:882–889.
42. **Felipe F, Mercader J, Ribot J, Palou A, Bonet ML**. 2005. Effects of retinoic acid administration and dietary vitamin A supplementation on leptin expression in mice: lack of correlation with changes of adipose tissue mass and food intake. Biochim. Biophys. Acta **1740**:258–265.
43. **Ribot J, Felipe F, Bonet ML, Palou A**. 2001. Changes of adiposity in response to vitamin A status correlate with changes of PPAR gamma 2 expression. Obes. Res. **9**:500–509.
44. **Bojic LA, Huff MW**. 2013. Peroxisome proliferator-activated receptor δ: a multifaceted metabolic player. Curr. Opin. Lipidol. **24**:171–177.
45. **Yang Q, Graham TE, Mody N, Preitner F, Peroni OD, Zabolotny JM, Kotani K, Quadro L, Kahn BB**. 2005. Serum retinol binding protein 4 contributes to insulin resistance in obesity and type 2 diabetes. Nature **436**:356–362.
46. **Wolf G, Wagle SR, Lane MD, Johnson BC**. 1958. Studies on the function of vitamin A in metabolism by the use of radioactive metabolic intermediates. Biol. Sci. **2**:457–468.
47. **Lucas PC, O'Brien RM, Mitchell JA, Davis CM, Imai E, Forman BM, Samuels HH, Granner DK**. 1991. A retinoic acid response element is part of a pleiotropic domain in the phosphoenolpyruvate carboxykinase gene. Proc. Natl. Acad. Sci. U. S. A. **88**:2184–2188.
48. **Scott DK, Mitchell JA, Granner DK**. 1996. Identification and charaterization of the second retinoic acid response element in the phosphoenolpyruvate carboxykinase gene promoter. J. Biol. Chem. **271**:6260–6264.
49. **Shin D-J, Odom DP, Scribner KB, Ghoshal S, McGrane MM**. 2002. Retinoid regulation of the phosphoenolpyruvate carboxykinase gene in liver. Mol. Cell. Endocrinol. **195**:39–54.

50. **Felipe F, Bonet ML, Ribot J, Palou A**. 2003. Up-regulation of muscle uncoupling protein 3 gene expression in mice following high fat diet, dietary vitamin A supplementation and acute retinoic acid-treatment. Int. J. Obes. Relat. Metab. Disord. J. Int. Assoc. Study Obes. **27**:60–69.
51. **Scarpace PJ, Matheny M, Moore RL, Kumar MV**. 2000. Modulation of uncoupling protein 2 and uncoupling protein 3: regulation by denervation, leptin and retinoic acid treatment. J. Endocrinol. **164**:331–337.
52. **Palou A, Picó C, Bonet ML**. 2003. The molecular basis of body weight control. Forum Nutr. **56**:164–168.
53. **Zhang M, Hu P, Krois CR, Kane MA, Napoli JL**. 2007. Altered vitamin A homeostasis and increased size and adiposity in the rdh1-null mouse. FASEB J. Off. Publ. Fed. Am. Soc. Exp. Biol. **21**:2886–2896.
54. **Kane MA, Folias AE, Pingitore A, Perri M, Krois CR, Ryu JY, Cione E, Napoli JL**. 2011. Crbpl modulates glucose homeostasis and pancreas 9-cis-retinoic acid concentrations. Mol. Cell. Biol. **31**:3277–3285.
55. **Fan X, Molotkov A, Manabe S-I, Donmoyer CM, Deltour L, Foglio MH, Cuenca AE, Blaner WS, Lipton SA, Duester G**. 2003. Targeted disruption of Aldh1a1 (Raldh1) provides evidence for a complex mechanism of retinoic acid synthesis in the developing retina. Mol. Cell. Biol. **23**:4637–4648.
56. **Ziouzenkova O, Orasanu G, Sharlach M, Akiyama TE, Berger JP, Viereck J, Hamilton JA, Tang G, Dolnikowski GG, Vogel S, Duester G, Plutzky J**. 2007. Retinaldehyde represses adipogenesis and diet-induced obesity. Nat. Med. **13**:695–702.
57. **Ross AC**. 2007. Vitamin A supplementation and retinoic acid treatment in the regulation of antibody responses in vivo. Vitam. Horm. **75**:197–222.
58. **Maden M**. 2007. Retinoic acid in the development, regeneration and maintenance of the nervous system. Nat. Rev. Neurosci. **8**:755–765.
59. **Pino-Lagos K, Guo Y, Noelle RJ**. 2010. Retinoic acid: a key player in immunity. BioFactors Oxf. Engl. **36**:430–436.
60. **Gudas LJ**. 2012. Emerging roles for retinoids in regeneration and differentiation in normal and disease states. Biochim. Biophys. Acta **1821**:213–221.
61. **Rhinn M, Dollé P**. 2012. Retinoic acid signalling during development. Dev. Camb. Engl. **139**:843–858.
62. **Frey SK, Vogel S**. 2011. Vitamin A metabolism and adipose tissue biology. Nutrients **3**:27–39.
63. **Berry DC, Noy N**. 2012. Signaling by vitamin A and retinol-binding protein in regulation of insulin responses and lipid homeostasis. Biochim. Biophys. Acta **1821**:168–176.
64. **Bonet ML, Ribot J, Palou A**. 2012. Lipid metabolism in mammalian tissues and its control by retinoic acid. Biochim. Biophys. Acta **1821**:177–189.
65. **Mercader J, Ribot J, Murano I, Felipe F, Cinti S, Bonet ML, Palou A**. 2006. Remodeling of white adipose tissue after retinoic acid administration in mice. Endocrinology **147**:5325–5332.
66. **Zizola CF, Frey SK, Jitngarmkusol S, Kadereit B, Yan N, Vogel S**. 2010. Cellular retinol-binding protein type I (CRBP-I) regulates adipogenesis. Mol. Cell. Biol. **30**:3412–3420.

67. **Sugiyama T, Scott DK, Wang JC, Granner DK**. 1998. Structural requirements of the glucocorticoid and retinoic acid response units in the phosphoenolpyruvate carboxykinase gene promoter. Mol. Endocrinol. Baltim. Md **12**:1487–1498.
68. **Mercader J, Palou A, Bonet ML**. 2010. Induction of uncoupling protein-1 in mouse embryonic fibroblast-derived adipocytes by retinoic acid. Obes. Silver Spring Md **18**:655–662.
69. **Noy N**. 2013. The one-two punch: Retinoic acid suppresses obesity both by promoting energy expenditure and by inhibiting adipogenesis. Adipocyte **2**:184–187.
70. **Zhang M, Chen W, Smith SM, Napoli JL**. 2001. Molecular characterization of a mouse short chain dehydrogenase/reductase active with all-trans-retinol in intact cells, mRDH1. J. Biol. Chem. **276**:44083–44090.
71. **Belyaeva OV, Johnson MP, Kedishvili NY**. 2008. Kinetic analysis of human enzyme RDH10 defines the characteristics of a physiologically relevant retinol dehydrogenase. J. Biol. Chem. **283**:20299–20308.
72. **Wu BX, Chen Y, Chen Y, Fan J, Rohrer B, Crouch RK, Ma J-X**. 2002. Cloning and characterization of a novel all-trans retinol short-chain dehydrogenase/reductase from the RPE. Invest. Ophthalmol. Vis. Sci. **43**:3365–3372.
73. **Adams MK, Belyaeva OV, Wu L, Kedishvili NY**. 2014. The retinaldehyde reductase activity of DHRS3 is reciprocally activated by Retinol Dehydrogenase 10 to control retinoid homeostasis. J. Biol. Chem.
74. **Rhinn M, Schuhbaur B, Niederreither K, Dollé P**. 2011. Involvement of retinol dehydrogenase 10 in embryonic patterning and rescue of its loss of function by maternal retinaldehyde treatment. Proc. Natl. Acad. Sci. U. S. A. **108**:16687–16692.
75. **Van den Berghe G**. 1991. The role of the liver in metabolic homeostasis: implications for inborn errors of metabolism. J. Inherit. Metab. Dis. **14**:407–420.
76. **Moore MC, Coate KC, Winnick JJ, An Z, Cherrington AD**. 2012. Regulation of hepatic glucose uptake and storage in vivo. Adv. Nutr. Bethesda Md **3**:286–294.
77. **Tobe K, Kadowaki T, Hara K, Gotoh Y, Kosako H, Matsuda S, Tamemoto H, Ueki K, Akanuma Y, Nishida E**. 1992. Sequential activation of MAP kinase activator, MAP kinases, and S6 peptide kinase in intact rat liver following insulin injection. J. Biol. Chem. **267**:21089–21097.
78. **Siddle K**. 2011. Signalling by insulin and IGF receptors: supporting acts and new players. J. Mol. Endocrinol. **47**:R1–10.
79. **Shin D-J, Joshi P, Hong S-H, Mosure K, Shin D-G, Osborne TF**. 2012. Genome-wide analysis of FoxO1 binding in hepatic chromatin: potential involvement of FoxO1 in linking retinoid signaling to hepatic gluconeogenesis. Nucleic Acids Res. **40**:11499–11509.
80. **Kane MA, Napoli JL**. 2010. Quantification of endogenous retinoids. Methods Mol. Biol. Clifton NJ **652**:1–54.
81. **Kane MA, Folias AE, Wang C, Napoli JL**. 2008. Quantitative profiling of endogenous retinoic acid in vivo and in vitro by tandem mass spectrometry. Anal. Chem. **80**:1702–1708.

82. **Kane MA, Folias AE, Napoli JL**. 2008. HPLC/UV quantitation of retinal, retinol, and retinyl esters in serum and tissues. Anal. Biochem. **378**:71–79.
83. **Heikkinen S, Argmann CA, Champy M-F, Auwerx J**. 2007. Evaluation of glucose homeostasis. Curr. Protoc. Mol. Biol. Ed. Frederick M Ausubel Al **Chapter 29**:Unit 29B.3.
84. **Zarrinpar A, Loomba R**. 2012. Review article: the emerging interplay among the gastrointestinal tract, bile acids and incretins in the pathogenesis of diabetes and non-alcoholic fatty liver disease. Aliment. Pharmacol. Ther. **36**:909–921.
85. **Eng J, Kleinman WA, Singh L, Singh G, Raufman JP**. 1992. Isolation and characterization of exendin-4, an exendin-3 analogue, from Heloderma suspectum venom. Further evidence for an exendin receptor on dispersed acini from guinea pig pancreas. J. Biol. Chem. **267**:7402–7405.
86. **Pirkmajer S, Chibalin AV**. 2011. Serum starvation: caveat emptor. Am. J. Physiol. Cell Physiol. **301**:C272–279.
87. **Sancho P, Fabregat I**. 2010. NADPH oxidase NOX1 controls autocrine growth of liver tumor cells through up-regulation of the epidermal growth factor receptor pathway. J. Biol. Chem. **285**:24815–24824.
88. **Mithieux G, Vidal H, Zitoun C, Bruni N, Daniele N, Minassian C**. 1996. Glucose-6-phosphatase mRNA and activity are increased to the same extent in kidney and liver of diabetic rats. Diabetes **45**:891–896.
89. **Nakae J, Kitamura T, Silver DL, Accili D**. 2001. The forkhead transcription factor Foxo1 (Fkhr) confers insulin sensitivity onto glucose-6-phosphatase expression. J. Clin. Invest. **108**:1359–1367.
90. **Nakae J, Park BC, Accili D**. 1999. Insulin stimulates phosphorylation of the forkhead transcription factor FKHR on serine 253 through a Wortmannin-sensitive pathway. J. Biol. Chem. **274**:15982–15985.
91. **Kido Y, Nakae J, Accili D**. 2001. Clinical review 125: The insulin receptor and its cellular targets. J. Clin. Endocrinol. Metab. **86**:972–979.
92. **Martín M, Gallego-Llamas J, Ribes V, Kedinger M, Niederreither K, Chambon P, Dollé P, Gradwohl G**. 2005. Dorsal pancreas agenesis in retinoic acid-deficient Raldh2 mutant mice. Dev. Biol. **284**:399–411.
93. **Pérez RJ, Benoit YD, Gudas LJ**. 2013. Deletion of retinoic acid receptor β (RARβ) impairs pancreatic endocrine differentiation. Exp. Cell Res. **319**:2196–2204.
94. **Chertow BS, Blaner WS, Baranetsky NG, Sivitz WI, Cordle MB, Thompson D, Meda P**. 1987. Effects of vitamin A deficiency and repletion on rat insulin secretion in vivo and in vitro from isolated islets. J. Clin. Invest. **79**:163–169.
95. **Zhao S, Li R, Li Y, Chen W, Zhang Y, Chen G**. 2012. Roles of vitamin A status and retinoids in glucose and fatty acid metabolism. Biochem. Cell Biol. Biochim. Biol. Cell. **90**:142–152.
96. **Ishida T, Chap Z, Chou J, Lewis R, Hartley C, Entman M, Field JB**. 1983. Differential effects of oral, peripheral intravenous, and intraportal glucose on hepatic glucose uptake and insulin and glucagon extraction in conscious dogs. J. Clin. Invest. **72**:590–601.

97. **Myers SR, Biggers DW, Neal DW, Cherrington AD**. 1991. Intraportal glucose delivery enhances the effects of hepatic glucose load on net hepatic glucose uptake in vivo. J. Clin. Invest. **88**:158–167.
98. **Bergman RN, Beir JR, Hourigan PM**. 1982. Intraportal glucose infusion matched to oral glucose absorption. Lack of evidence for “gut factor” involvement in hepatic glucose storage. Diabetes **31**:27–35.
99. **Ohlsson L, Kohan AB, Tso P, Ahrén B**. 2014. GLP-1 released to the mesenteric lymph duct in mice: Effects of glucose and fat. Regul. Pept.
100. **Yamamoto Y, Zolfaghari R, Ross AC**. 2000. Regulation of CYP26 (cytochrome P450RAI) mRNA expression and retinoic acid metabolism by retinoids and dietary vitamin A in liver of mice and rats. FASEB J. Off. Publ. Fed. Am. Soc. Exp. Biol. **14**:2119–2127.
101. **Ross AC, Cifelli CJ, Zolfaghari R, Li N-Q**. 2011. Multiple cytochrome P-450 genes are concomitantly regulated by vitamin A under steady-state conditions and by retinoic acid during hepatic first-pass metabolism. Physiol. Genomics **43**:57–67.
102. **Matsuura T, Ross AC**. 1993. Regulation of hepatic lecithin: retinol acyltransferase activity by retinoic acid. Arch. Biochem. Biophys. **301**:221–227.
103. **Kousteni S**. 2012. FoxO1, the transcriptional chief of staff of energy metabolism. Bone **50**:437–443.
104. **Barthel A, Schmoll D, Unterman TG**. 2005. FoxO proteins in insulin action and metabolism. Trends Endocrinol. Metab. TEM **16**:183–189.
105. **Hall RK, Yamasaki T, Kucera T, Waltner-Law M, O’Brien R, Granner DK**. 2000. Regulation of phosphoenolpyruvate carboxykinase and insulin-like growth factor-binding protein-1 gene expression by insulin. The role of winged helix/forkhead proteins. J. Biol. Chem. **275**:30169–30175.
106. **Vander Kooi BT, Streeper RS, Svitek CA, Oeser JK, Powell DR, O’Brien RM**. 2003. The three insulin response sequences in the glucose-6-phosphatase catalytic subunit gene promoter are functionally distinct. J. Biol. Chem. **278**:11782–11793.
107. **Matsumoto M, Pocai A, Rossetti L, Depinho RA, Accili D**. 2007. Impaired regulation of hepatic glucose production in mice lacking the forkhead transcription factor Foxo1 in liver. Cell Metab. **6**:208–216.
108. **Nakae J, Biggs WH 3rd, Kitamura T, Cavenee WK, Wright CVE, Arden KC, Accili D**. 2002. Regulation of insulin action and pancreatic beta-cell function by mutated alleles of the gene encoding forkhead transcription factor Foxo1. Nat. Genet. **32**:245–253.
109. **Haeusler RA, Han S, Accili D**. 2010. Hepatic FoxO1 ablation exacerbates lipid abnormalities during hyperglycemia. J. Biol. Chem. **285**:26861–26868.
110. **Matsuzaki H, Daitoku H, Hatta M, Tanaka K, Fukamizu A**. 2003. Insulin-induced phosphorylation of FKHR (Foxo1) targets to proteasomal degradation. Proc. Natl. Acad. Sci. U. S. A. **100**:11285–11290.
111. **Schwer B, Verdin E**. 2008. Conserved metabolic regulatory functions of sirtuins. Cell Metab. **7**:104–112.

112. **Dong XC, Copps KD, Guo S, Li Y, Kollipara R, DePinho RA, White MF**. 2008. Inactivation of hepatic Foxo1 by insulin signaling is required for adaptive nutrient homeostasis and endocrine growth regulation. Cell Metab. **8**:65–76.
113. **Kubota N, Kubota T, Itoh S, Kumagai H, Kozono H, Takamoto I, Mineyama T, Ogata H, Tokuyama K, Ohsugi M, Sasako T, Moroi M, Sugi K, Kakuta S, Iwakura Y, Noda T, Ohnishi S, Nagai R, Tobe K, Terauchi Y, Ueki K, Kadowaki T**. 2008. Dynamic functional relay between insulin receptor substrate 1 and 2 in hepatic insulin signaling during fasting and feeding. Cell Metab. **8**:49–64.
114. **Rossi E, Picozzi P, Bodega B, Lavazza C, Carlo-Stella C, Marozzi A, Ginelli E**. 2007. Forced expression of RDH10 gene retards growth of HepG2 cells. Cancer Biol. Ther. **6**:238–244.
115. **Spasic M, Friedel CC, Schott J, Kreth J, Leppek K, Hofmann S, Ozgur S, Stoecklin G**. 2012. Genome-wide assessment of AU-rich elements by the AREScore algorithm. PLoS Genet. **8**:e1002433.
116. **Vreeland AC, Yu S, Levi L, de Barros Rossetto D, Noy N**. 2014. Transcript stabilization by the RNA-binding protein HuR is regulated by cellular retinoic acid-binding protein 2. Mol. Cell. Biol.
117. **Lin HV, Accili D**. 2011. Hormonal regulation of hepatic glucose production in health and disease. Cell Metab. **14**:9–19.
118. **Vogelstein B, Papadopoulos N, Velculescu VE, Zhou S, Diaz LA, Kinzler KW**. 2013. Cancer genome landscapes. Science **339**:1546–1558.
119. **Chakravarti N, Lotan R, Diwan AH, Warneke CL, Johnson MM, Prieto VG**. 2007. Decreased expression of retinoid receptors in melanoma: entailment in tumorigenesis and prognosis. Clin. Cancer Res. Off. J. Am. Assoc. Cancer Res. **13**:4817–4824.
120. **Tanabe K, Utsunomiya H, Tamura M, Niikura H, Takano T, Yoshinaga K, Nagase S, Suzuki T, Ito K, Matsumoto M, Hayashi S, Yaegashi N**. 2008. Expression of retinoic acid receptors in human endometrial carcinoma. Cancer Sci. **99**:267–271.
121. **Calmon MF, Rodrigues RV, Kaneto CM, Moura RP, Silva SD, Mota LDC, Pinheiro DG, Torres C, de Carvalho AF, Cury PM, Nunes FD, Nishimoto IN, Soares FA, da Silva AMA, Kowalski LP, Brentani H, Zanelli CF, Silva WA, Rahal P, Tajara EH, Carraro DM, Camargo AA, Valentini SR**. 2009. Epigenetic silencing of CRABP2 and MX1 in head and neck tumors. Neoplasia N. Y. N **11**:1329–1339.
122. **Campos B, Warta R, Chaisaingmongkol J, Geiselhart L, Popanda O, Hartmann C, von Deimling A, Unterberg A, Plass C, Schmezer P, Herold-Mende C**. 2012. Epigenetically mediated downregulation of the differentiation-promoting chaperon protein CRABP2 in astrocytic gliomas. Int. J. Cancer J. Int. Cancer **131**:1963–1968.
123. **Mira-Y-Lopez R, Zheng WL, Kuppumbatti YS, Rexer B, Jing Y, Ong DE**. 2000. Retinol conversion to retinoic acid is impaired in breast cancer cell lines relative to normal cells. J. Cell. Physiol. **185**:302–309.
124. **Pierzchalski K, Yu J, Norman V, Kane MA**. 2013. Crbpl regulates mammary retinoic acid homeostasis and the mammary microenvironment. FASEB J. Off. Publ. Fed. Am. Soc. Exp. Biol. **27**:1904–1916.

125. **Simon A, Hellman U, Wernstedt C, Eriksson U**. 1995. The retinal pigment epithelial-specific 11-cis retinol dehydrogenase belongs to the family of short chain alcohol dehydrogenases. J. Biol. Chem. **270**:1107–1112.
126. **Simon A, Lagercrantz J, Bajalica-Lagercrantz S, Eriksson U**. 1996. Primary structure of human 11-cis retinol dehydrogenase and organization and chromosomal localization of the corresponding gene. Genomics **36**:424–430.
127. **Mertz JR, Shang E, Piantedosi R, Wei S, Wolgemuth DJ, Blaner WS**. 1997. Identification and characterization of a stereospecific human enzyme that catalyzes 9-cis-retinol oxidation. A possible role in 9-cis-retinoic acid formation. J. Biol. Chem. **272**:11744–11749.
128. **Romert A, Tuvendal P, Simon A, Dencker L, Eriksson U**. 1998. The identification of a 9-cis retinol dehydrogenase in the mouse embryo reveals a pathway for synthesis of 9-cis retinoic acid. Proc. Natl. Acad. Sci. U. S. A. **95**:4404–4409.
129. **Yamamoto H, Simon A, Eriksson U, Harris E, Berson EL, Dryja TP**. 1999. Mutations in the gene encoding 11-cis retinol dehydrogenase cause delayed dark adaptation and fundus albipunctatus. Nat. Genet. **22**:188–191.
130. **Kim TS, Maeda A, Maeda T, Heinlein C, Kedishvili N, Palczewski K, Nelson PS**. 2005. Delayed dark adaptation in 11-cis-retinol dehydrogenase-deficient mice: a role of RDH11 in visual processes in vivo. J. Biol. Chem. **280**:8694–8704.
131. **Wang J, Chai X, Eriksson U, Napoli JL**. 1999. Activity of human 11-cis-retinol dehydrogenase (Rdh5) with steroids and retinoids and expression of its mRNA in extra-ocular human tissue. Biochem. J. **338 (Pt 1)**:23–27.
132. **Eberhard D, Lammert E**. 2009. The pancreatic beta-cell in the islet and organ community. Curr. Opin. Genet. Dev. **19**:469–475.
133. **Hohmeier HE, Mulder H, Chen G, Henkel-Rieger R, Prentki M, Newgard CB**. 2000. Isolation of INS-1-derived cell lines with robust ATP-sensitive K+ channel-dependent and -independent glucose-stimulated insulin secretion. Diabetes **49**:424–430.
134. **Miyazaki J, Araki K, Yamato E, Ikegami H, Asano T, Shibasaki Y, Oka Y, Yamamura K**. 1990. Establishment of a pancreatic beta cell line that retains glucose-inducible insulin secretion: special reference to expression of glucose transporter isoforms. Endocrinology **127**:126–132.
135. **Holz GG, Heart E, Leech CA**. 2008. Synchronizing Ca2+ and cAMP oscillations in pancreatic beta-cells: a role for glucose metabolism and GLP-1 receptors? Focus on “regulation of cAMP dynamics by Ca2+ and G protein-coupled receptors in the pancreatic beta-cell: a computational approach”. Am. J. Physiol. Cell Physiol. **294**:C4–6.
136. **Inada A, Yamada Y, Someya Y, Kubota A, Yasuda K, Ihara Y, Kagimoto S, Kuroe A, Tsuda K, Seino Y**. 1998. Transcriptional repressors are increased in pancreatic islets of type 2 diabetic rats. Biochem. Biophys. Res. Commun. **253**:712–718.
137. **Glauser DA, Brun T, Gauthier BR, Schlegel W**. 2007. Transcriptional response of pancreatic beta cells to metabolic stimulation: large scale identification of immediate-early and secondary response genes. BMC Mol. Biol. **8**:54.

138. **Kawaguchi M, Minami K, Nagashima K, Seino S**. 2006. Essential role of ubiquitin-proteasome system in normal regulation of insulin secretion. J. Biol. Chem. **281**:13015–13020.
139. **Schuit FC, Huypens P, Heimberg H, Pipeleers DG**. 2001. Glucose sensing in pancreatic beta-cells: a model for the study of other glucose-regulated cells in gut, pancreas, and hypothalamus. Diabetes **50**:1–11.
140. **Tsui S, Dai W, Lu L**. 2014. CCCTC-binding factor mediates effects of glucose on beta cell survival. Cell Prolif. **47**:28–37.
141. **Filhoulaud G, Guilmeau S, Dentin R, Girard J, Postic C**. 2013. Novel insights into ChREBP regulation and function. Trends Endocrinol. Metab. TEM **24**:257–268.
142. **Noordeen NA, Meur G, Rutter GA, Leclerc I**. 2012. Glucose-induced nuclear shuttling of ChREBP is mediated by sorcin and Ca(2+) ions in pancreatic β-cells. Diabetes **61**:574–585.
143. **Boergesen M, Poulsen L la C, Schmidt SF, Frigerio F, Maechler P, Mandrup S**. 2011. ChREBP mediates glucose repression of peroxisome proliferator-activated receptor alpha expression in pancreatic beta-cells. J. Biol. Chem. **286**:13214–13225.
144. **Noordeen NA, Khera TK, Sun G, Longbottom ER, Pullen TJ, da Silva Xavier G, Rutter GA, Leclerc I**. 2010. Carbohydrate-responsive element-binding protein (ChREBP) is a negative regulator of ARNT/HIF-1beta gene expression in pancreatic islet beta-cells. Diabetes **59**:153–160.
145. **Zhang H, Li W, Wang Q, Wang X, Li F, Zhang C, Wu L, Long H, Liu Y, Li X, Luo M, Li G, Ning G**. 2012. Glucose-mediated repression of menin promotes pancreatic β-cell proliferation. Endocrinology **153**:602–611.
146. **Molina CA, Foulkes NS, Lalli E, Sassone-Corsi P**. 1993. Inducibility and negative autoregulation of CREM: an alternative promoter directs the expression of ICER, an early response repressor. Cell **75**:875–886.
147. **Kulkarni RN, Brüning JC, Winnay JN, Postic C, Magnuson MA, Kahn CR**. 1999. Tissue-specific knockout of the insulin receptor in pancreatic beta cells creates an insulin secretory defect similar to that in type 2 diabetes. Cell **96**:329–339.
148. **Shearer KD, Stoney PN, Nanescu SE, Helfer G, Barrett P, Ross AW, Morgan PJ, McCaffery P**. 2012. Photoperiodic expression of two RALDH enzymes and the regulation of cell proliferation by retinoic acid in the rat hypothalamus. J. Neurochem. **122**:789–799.
149. **Shearer KD, Goodman TH, Ross AW, Reilly L, Morgan PJ, McCaffery PJ**. 2010. Photoperiodic regulation of retinoic acid signaling in the hypothalamus. J. Neurochem. **112**:246–257.
150. **Ross AW, Webster CA, Mercer JG, Moar KM, Ebling FJ, Schuhler S, Barrett P, Morgan PJ**. 2004. Photoperiodic regulation of hypothalamic retinoid signaling: association of retinoid X receptor gamma with body weight. Endocrinology **145**:13–20.
151. **Ransom J, Morgan PJ, McCaffery PJ, Stoney PN**. 2014. The rhythm of retinoids in the brain. J. Neurochem. **129**:366–376.

152. **Zetterström RH, Lindqvist E, Mata de Urquiza A, Tomac A, Eriksson U, Perlmann T, Olson L**. 1999. Role of retinoids in the CNS: differential expression of retinoid binding proteins and receptors and evidence for presence of retinoic acid. Eur. J. Neurosci. **11**:407–416.
153. **Krezel W, Kastner P, Chambon P**. 1999. Differential expression of retinoid receptors in the adult mouse central nervous system. Neuroscience **89**:1291–1300.
154. **Faouzi M, Leshan R, Björnholm M, Hennessey T, Jones J, Münzberg H**. 2007. Differential accessibility of circulating leptin to individual hypothalamic sites. Endocrinology **148**:5414–5423.
155. **Collin M, Bäckberg M, Ovesjö M-L, Fisone G, Edwards RH, Fujiyama F, Meister B**. 2003. Plasma membrane and vesicular glutamate transporter mRNAs/proteins in hypothalamic neurons that regulate body weight. Eur. J. Neurosci. **18**:1265–1278.
156. **Cowley MA, Smart JL, Rubinstein M, Cerdán MG, Diano S, Horvath TL, Cone RD, Low MJ**. 2001. Leptin activates anorexigenic POMC neurons through a neural network in the arcuate nucleus. Nature **411**:480–484.
157. **Wang C, Kane MA, Napoli JL**. 2011. Multiple retinol and retinal dehydrogenases catalyze all-trans-retinoic acid biosynthesis in astrocytes. J. Biol. Chem. **286**:6542–6553.
158. **Chambon P**. 1996. A decade of molecular biology of retinoic acid receptors. FASEB J. Off. Publ. Fed. Am. Soc. Exp. Biol. **10**:940–954.
159. **DiRenzo J, Söderstrom M, Kurokawa R, Ogliastro MH, Ricote M, Ingrey S, Hörlein A, Rosenfeld MG, Glass CK**. 1997. Peroxisome proliferator-activated receptors and retinoic acid receptors differentially control the interactions of retinoid X receptor heterodimers with ligands, coactivators, and corepressors. Mol. Cell. Biol. **17**:2166–2176.
160. **Rochette-Egly C, Germain P**. 2009. Dynamic and combinatorial control of gene expression by nuclear retinoic acid receptors (RARs). Nucl. Recept. Signal. **7**:e005.
161. **Chen N, Onisko B, Napoli JL**. 2008. The nuclear transcription factor RARalpha associates with neuronal RNA granules and suppresses translation. J. Biol. Chem. **283**:20841–20847.
162. **Ali FY, Davidson SJ, Moraes LA, Traves SL, Paul-Clark M, Bishop-Bailey D, Warner TD, Mitchell JA**. 2006. Role of nuclear receptor signaling in platelets: antithrombotic effects of PPARbeta. FASEB J. Off. Publ. Fed. Am. Soc. Exp. Biol. **20**:326–328.
163. **Ali FY, Hall MG, Desvergne B, Warner TD, Mitchell JA**. 2009. PPARbeta/delta agonists modulate platelet function via a mechanism involving PPAR receptors and specific association/repression of PKCalpha--brief report. Arterioscler. Thromb. Vasc. Biol. **29**:1871–1873.
164. **Michalik L, Auwerx J, Berger JP, Chatterjee VK, Glass CK, Gonzalez FJ, Grimaldi PA, Kadowaki T, Lazar MA, O'Rahilly S, Palmer CNA, Plutzky J, Reddy JK, Spiegelman BM, Staels B, Wahli W**. 2006. International Union of Pharmacology. LXI. Peroxisome proliferator-activated receptors. Pharmacol. Rev. **58**:726–741.

165. **Peters JM, Lee SS, Li W, Ward JM, Gavrilova O, Everett C, Reitman ML, Hudson LD, Gonzalez FJ**. 2000. Growth, adipose, brain, and skin alterations resulting from targeted disruption of the mouse peroxisome proliferator-activated receptor beta(delta). Mol. Cell. Biol. **20**:5119–5128.
166. **Barak Y, Liao D, He W, Ong ES, Nelson MC, Olefsky JM, Boland R, Evans RM**. 2002. Effects of peroxisome proliferator-activated receptor delta on placentation, adiposity, and colorectal cancer. Proc. Natl. Acad. Sci. U. S. A. **99**:303–308.
167. **Wang Y-X, Zhang C-L, Yu RT, Cho HK, Nelson MC, Bayuga-Ocampo CR, Ham J, Kang H, Evans RM**. 2004. Regulation of muscle fiber type and running endurance by PPARdelta. PLoS Biol. **2**:e294.
168. **Hall MG, Quignodon L, Desvergne B**. 2008. Peroxisome Proliferator-Activated Receptor beta/delta in the Brain: Facts and Hypothesis. PPAR Res. **2008**:780452.
169. **Girroir EE, Hollingshead HE, He P, Zhu B, Perdew GH, Peters JM**. 2008. Quantitative expression patterns of peroxisome proliferator-activated receptor-beta/delta (PPARbeta/delta) protein in mice. Biochem. Biophys. Res. Commun. **371**:456–461.
170. **Moreno S, Farioli-Vecchioli S, Cerù MP**. 2004. Immunolocalization of peroxisome proliferator-activated receptors and retinoid X receptors in the adult rat CNS. Neuroscience **123**:131–145.
171. **Higashiyama H, Billin AN, Okamoto Y, Kinoshita M, Asano S**. 2007. Expression profiling of peroxisome proliferator-activated receptor-delta (PPAR-delta) in mouse tissues using tissue microarray. Histochem. Cell Biol. **127**:485–494.
172. **Basu-Modak S, Braissant O, Escher P, Desvergne B, Honegger P, Wahli W**. 1999. Peroxisome proliferator-activated receptor beta regulates acyl-CoA synthetase 2 in reaggregated rat brain cell cultures. J. Biol. Chem. **274**:35881–35888.
173. **Saladin R, De Vos P, Guerre-Millo M, Leturque A, Girard J, Staels B, Auwerx J**. 1995. Transient increase in obese gene expression after food intake or insulin administration. Nature **377**:527–529.
174. **Niswender KD, Morton GJ, Stearns WH, Rhodes CJ, Myers MG Jr, Schwartz MW**. 2001. Intracellular signalling. Key enzyme in leptin-induced anorexia. Nature **413**:794–795.
175. **Cota D, Proulx K, Smith KAB, Kozma SC, Thomas G, Woods SC, Seeley RJ**. 2006. Hypothalamic mTOR signaling regulates food intake. Science **312**:927–930.
176. **Gao Q, Horvath TL**. 2007. Neurobiology of feeding and energy expenditure. Annu. Rev. Neurosci. **30**:367–398.
177. **Breen TL, Conwell IM, Wardlaw SL**. 2005. Effects of fasting, leptin, and insulin on AGRP and POMC peptide release in the hypothalamus. Brain Res. **1032**:141–148.
178. **Pritchard LE, White A**. 2005. Agouti-related protein: more than a melanocortin-4 receptor antagonist? Peptides **26**:1759–1770.
179. **Swiech L, Perycz M, Malik A, Jaworski J**. 2008. Role of mTOR in physiology and pathology of the nervous system. Biochim. Biophys. Acta **1784**:116–132.

180. **Bergonzelli GE, Pralong FP, Glauser M, Cavadas C, Grouzmann E, Gaillard RC**. 2001. Interplay between galanin and leptin in the hypothalamic control of feeding via corticotropin-releasing hormone and neuropeptide Y. Diabetes **50**:2666–2672.
181. **MacLean DB, Luo L-G**. 2004. Increased ATP content/production in the hypothalamus may be a signal for energy-sensing of satiety: studies of the anorectic mechanism of a plant steroidal glycoside. Brain Res. **1020**:1–11.
182. **Hallett PJ, Collins TL, Standaert DG, Dunah AW**. 2008. Biochemical fractionation of brain tissue for studies of receptor distribution and trafficking. Curr. Protoc. Neurosci. Editor. Board Jacqueline N Crawley Al **Chapter 1**:Unit 1.16.
183. **Mullen RJ, Buck CR, Smith AM**. 1992. NeuN, a neuronal specific nuclear protein in vertebrates. Dev. Camb. Engl. **116**:201–211.
184. **Yu S, Levi L, Siegel R, Noy N**. 2012. Retinoic acid induces neurogenesis by activating both retinoic acid receptors (RARs) and peroxisome proliferator-activated receptor β/δ (PPARβ/δ). J. Biol. Chem. **287**:42195–42205.
185. **Taylor AM, Berchtold NC, Perreau VM, Tu CH, Li Jeon N, Cotman CW**. 2009. Axonal mRNA in uninjured and regenerating cortical mammalian axons. J. Neurosci. Off. J. Soc. Neurosci. **29**:4697–4707.
186. **D'Angelo B, Benedetti E, Di Loreto S, Cristiano L, Laurenti G, Cerù MP, Cimini A**. 2011. Signal transduction pathways involved in PPARβ/δ-induced neuronal differentiation. J. Cell. Physiol. **226**:2170–2180.
187. **Chan WK-H, Dickerson A, Ortiz D, Pimenta AF, Moran CM, Motil J, Snyder SJ, Malik K, Pant HC, Shea TB**. 2004. Mitogen-activated protein kinase regulates neurofilament axonal transport. J. Cell Sci. **117**:4629–4642.
188. **Yu S, Levi L, Casadesus G, Kunos G, Noy N**. 2014. Fatty acid-binding protein 5 (FABP5) regulates cognitive function both by decreasing anandamide levels and by activating the nuclear receptor PPARβ/δ in the brain. J. Biol. Chem.
189. **Kobilo T, Yuan C, van Praag H**. 2011. Endurance factors improve hippocampal neurogenesis and spatial memory in mice. Learn. Mem. Cold Spring Harb. N **18**:103–107.
190. **Das NR, Gangwal RP, Damre MV, Sangamwar AT, Sharma SS**. 2014. A PPAR-β/δ Agonist is Neuroprotective and Decreases Cognitive Impairment in a Rodent Model of Parkinson's Disease. Curr. Neurovasc. Res.
191. **Kalinin S, Richardson JC, Feinstein DL**. 2009. A PPARdelta agonist reduces amyloid burden and brain inflammation in a transgenic mouse model of Alzheimer's disease. Curr. Alzheimer Res. **6**:431–437.
192. **McMinn JE, Liu S-M, Liu H, Dragatsis I, Dietrich P, Ludwig T, Boozer CN, Chua SC Jr**. 2005. Neuronal deletion of Lepr elicits diabesity in mice without affecting cold tolerance or fertility. Am. J. Physiol. Endocrinol. Metab. **289**:E403–411.
193. **Hagan MM, Rushing PA, Pritchard LM, Schwartz MW, Strack AM, Van Der Ploeg LH, Woods SC, Seeley RJ**. 2000. Long-term orexigenic effects of AgRP-(83---132) involve mechanisms other than melanocortin receptor blockade. Am. J. Physiol. Regul. Integr. Comp. Physiol. **279**:R47–52.
194. **Maden M**. 2007. Retinoic acid in the development, regeneration and maintenance of the nervous system. Nat. Rev. Neurosci. **8**:755–765.

195. **Pino-Lagos K, Guo Y, Noelle RJ**. 2010. Retinoic acid: a key player in immunity. BioFactors Oxf. Engl. **36**:430–436.
196. **Gudas LJ, Wagner JA**. 2011. Retinoids regulate stem cell differentiation. J. Cell. Physiol. **226**:322–330.
197. **Germain P, Chambon P, Eichele G, Evans RM, Lazar MA, Leid M, De Lera AR, Lotan R, Mangelsdorf DJ, Gronemeyer H**. 2006. International Union of Pharmacology. LX. Retinoic acid receptors. Pharmacol. Rev. **58**:712–725.
198. **Rochette-Egly C, Germain P**. 2009. Dynamic and combinatorial control of gene expression by nuclear retinoic acid receptors (RARs). Nucl. Recept. Signal. **7**:e005.
199. **Rhinn M, Dollé P**. 2012. Retinoic acid signalling during development. Dev. Camb. Engl. **139**:843–858.
200. **Senoo H, Yoshikawa K, Morii M, Miura M, Imai K, Mezaki Y**. 2010. Hepatic stellate cell (vitamin A-storing cell) and its relative--past, present and future. Cell Biol. Int. **34**:1247–1272.
201. **Ross AC, Cifelli CJ, Zolfaghari R, Li N-Q**. 2011. Multiple cytochrome P-450 genes are concomitantly regulated by vitamin A under steady-state conditions and by retinoic acid during hepatic first-pass metabolism. Physiol. Genomics **43**:57–67.
202. **Napoli JL**. 2012. Physiological insights into all-trans-retinoic acid biosynthesis. Biochim. Biophys. Acta **1821**:152–167.
203. **Nau H**. 2001. Teratogenicity of isotretinoin revisited: species variation and the role of all-trans-retinoic acid. J. Am. Acad. Dermatol. **45**:S183–187.
204. **Penniston KL, Tanumihardjo SA**. 2006. The acute and chronic toxic effects of vitamin A. Am. J. Clin. Nutr. **83**:191–201.
205. **Savenije, B., Strubbe, J. and Ritshes-Hoitinga, M.** 2010. Nutrition, feeding and animal welfare., p. 183–193. *In* The Care and Management of Laboratory and Other Research AnimalsEight.
206. **Reeves PG, Nielsen FH, Fahey GC Jr**. 1993. AIN-93 purified diets for laboratory rodents: final report of the American Institute of Nutrition ad hoc writing committee on the reformulation of the AIN-76A rodent diet. J. Nutr. **123**:1939–1951.
207. **Reeves PG**. 1997. Components of the AIN-93 diets as improvements in the AIN-76A diet. J. Nutr. **127**:838S–841S.
208. **Subcommittee on Laboratory Animal Nutrition, Committee on Nutriltion, Board on Agriculture and National Research Council**. 1995. Nutrient Requirements of Laboratory AnimalsFourth, revised.
209. DRI Tables | Food and Nutrition Information Center.
210. **Napoli JL**. 1986. Quantification of physiological levels of retinoic acid. Methods Enzymol. **123**:112–124.
211. **Kane MA, Folias AE, Napoli JL**. 2008. HPLC/UV quantitation of retinal, retinol, and retinyl esters in serum and tissues. Anal. Biochem. **378**:71–79.
212. **Kane MA, Chen N, Sparks S, Napoli JL**. 2005. Quantification of endogenous retinoic acid in limited biological samples by LC/MS/MS. Biochem. J. **388**:363–369.

213. **Kane MA, Folias AE, Wang C, Napoli JL**. 2008. Quantitative profiling of endogenous retinoic acid in vivo and in vitro by tandem mass spectrometry. Anal. Chem. **80**:1702–1708.
214. **Batten ML, Imanishi Y, Maeda T, Tu DC, Moise AR, Bronson D, Possin D, Van Gelder RN, Baehr W, Palczewski K**. 2004. Lecithin-retinol acyltransferase is essential for accumulation of all-trans-retinyl esters in the eye and in the liver. J. Biol. Chem. **279**:10422–10432.
215. **Liu L, Tang X-H, Gudas LJ**. 2008. Homeostasis of retinol in lecithin: retinol acyltransferase gene knockout mice fed a high retinol diet. Biochem. Pharmacol. **75**:2316–2324.
216. **Quadro L, Blaner WS, Salchow DJ, Vogel S, Piantedosi R, Gouras P, Freeman S, Cosma MP, Colantuoni V, Gottesman ME**. 1999. Impaired retinal function and vitamin A availability in mice lacking retinol-binding protein. EMBO J. **18**:4633–4644.
217. **Zhang M, Hu P, Krois CR, Kane MA, Napoli JL**. 2007. Altered vitamin A homeostasis and increased size and adiposity in the rdh1-null mouse. FASEB J. Off. Publ. Fed. Am. Soc. Exp. Biol. **21**:2886–2896.
218. **E X, Zhang L, Lu J, Tso P, Blaner WS, Levin MS, Li E**. 2002. Increased neonatal mortality in mice lacking cellular retinol-binding protein II. J. Biol. Chem. **277**:36617–36623.
219. **Hogarth CA, Griswold MD**. 2013. Retinoic acid regulation of male meiosis. Curr. Opin. Endocrinol. Diabetes Obes. **20**:217–223.
220. **Schreiber R, Taschler U, Preiss-Landl K, Wongsiriroj N, Zimmermann R, Lass A**. 2012. Retinyl ester hydrolases and their roles in vitamin A homeostasis. Biochim. Biophys. Acta **1821**:113–123.
221. **Jewell JL, Russell RC, Guan K-L**. 2013. Amino acid signalling upstream of mTOR. Nat. Rev. Mol. Cell Biol. **14**:133–139.
222. **Lal L, Li Y, Smith J, Sassano A, Uddin S, Parmar S, Tallman MS, Minucci S, Hay N, Platanias LC**. 2005. Activation of the p70 S6 kinase by all-trans-retinoic acid in acute promyelocytic leukemia cells. Blood **105**:1669–1677.
223. **Gruber AR, Fallmann J, Kratochvill F, Kovarik P, Hofacker IL**. 2011. AREsite: a database for the comprehensive investigation of AU-rich elements. Nucleic Acids Res. **39**:D66–69.
224. **Anne M, Larsen and Matthew Hauswald**. 2014. Normal Functional Biology of the Liver, p. 23–51. *In* Diseases of the Liver in Children.